



---

MSU Graduate Theses

---

Summer 2020

## Field Measurements of Bed-Load Transport Distances Using Painted Sediment Tracers in an Urban Stream in the Missouri Ozarks


Kristen E. Breckenridge

*Missouri State University*, Breckenridge518@live.missouristate.edu

As with any intellectual project, the content and views expressed in this thesis may be considered objectionable by some readers. However, this student-scholar's work has been judged to have academic value by the student's thesis committee members trained in the discipline. The content and views expressed in this thesis are those of the student-scholar and are not endorsed by Missouri State University, its Graduate College, or its employees.

---

Follow this and additional works at: <https://bearworks.missouristate.edu/theses>

 Part of the [Environmental Monitoring Commons](#), [Geology Commons](#), [Geomorphology Commons](#), [Hydrology Commons](#), [Sedimentology Commons](#), and the [Water Resource Management Commons](#)

### Recommended Citation

Breckenridge, Kristen E., "Field Measurements of Bed-Load Transport Distances Using Painted Sediment Tracers in an Urban Stream in the Missouri Ozarks" (2020). *MSU Graduate Theses*. 3544.  
<https://bearworks.missouristate.edu/theses/3544>

This article or document was made available through BearWorks, the institutional repository of Missouri State University. The work contained in it may be protected by copyright and require permission of the copyright holder for reuse or redistribution.

For more information, please contact [BearWorks@library.missouristate.edu](mailto: BearWorks@library.missouristate.edu).

**FIELD MEASUREMENTS OF BED-LOAD TRANSPORT DISTANCE USING PAINTED  
SEDIMENT TRACERS IN AN URBAN STREAM IN THE MISSOURI OZARKS**

A Master's Thesis

Presented to

The Graduate College of  
Missouri State University

In Partial Fulfillment

Of the Requirements for the Degree  
Master of Science, Geospatial Science

By

Kristen E. Breckenridge

May 2020



# **FIELD MEASUREMENTS OF BED-LOAD TRANSPORT DISTANCE USING PAINTED SEDIMENT TRACERS IN AN URBAN STREAM IN THE MISSOURI OZARKS**

Geography, Geology, and Planning

Missouri State University, May 2020

Kristen E. Breckenridge

## **ABSTRACT**

Predictions of bed-load mobility and transport in stream channels are useful for restoration and management purposes. This study uses native gravel tracers to determine transport distances for bed-load in an urban stream in the Ozark Highlands. The objectives of this project are to: (i) determine downstream transport distances of painted tracers of different sizes over a range of flow conditions; (ii) evaluate the influence of channel morphology and thalweg location on transport; and (iii) compare field results to those predicted by mobility equations. The study site is located on South Creek, which drains Springfield, Missouri. The study reach is 132 m long and averages 5.8 m wide with a confining bank height of 1.5 m. A USGS discharge gage (#07052120, drainage area = 27.2 km<sup>2</sup>) is located 80 m above the study reach. Painted tracers of four sizes were released at pool, glide, and riffle locations along the channel bed with intermediate diameters based on pebble count survey results as follows: D<sub>50</sub>, 16-22.6 mm; D<sub>75</sub>, 22.6-32 mm; D<sub>84</sub>, 32-45 mm; and D<sub>90</sub>, 45-64 mm. As expected, higher flows resulted in a higher percent and larger distance of tracer movement. After a 7-year recurrence interval flood, 71% of tracers were either carried out of the study reach or buried in bar deposits. However, no tracers were found downstream with some later found after other flow events, suggesting that the tracers were most likely buried in bar deposits either within the study reach or beyond it. Overall, the riffle location and mid-channel deployment points produced the highest percentage of sediment mobility. Annual transport distances were estimated as follows: D<sub>50</sub>, 306 m; D<sub>75</sub>, 170 m; D<sub>84</sub>, 87 m; and D<sub>90</sub>, 39 m. Observed mobility trends validated the use of Shield's and Wolman's equations for the estimation of bed-load mobility and transport.

**KEYWORDS:** Fluvial geomorphology, bed-load mobility, sediment transport, tracer experiments, urban streams

**FIELD MEASUREMENTS OF BED-LOAD TRANSPORT DISTANCE USING PAINTED  
SEDIMENT TRACERS IN AN URBAN STREAM IN THE MISSOURI OZARKS**

By

Kristen E. Breckenridge

A Master's Thesis  
Submitted to the Graduate School  
Of Missouri State University  
In Partial Fulfillment of the Requirements  
For the Degree of Master of Science, Geospatial Sciences

May 2020

Approved:

Robert T. Pavlowsky, Ph. D., Thesis Committee Chair

Charles Rovey, Ph.D., Committee Member

Xiaomin Qiu, Ph.D., Committee Member

Julie Masterson, Ph.D., Dean of Graduate Collage

## ACKNOWLEDGMENTS

There have been many professors, family members, friends, and students that have helped me achieve my master's degree through support encouragement, and their never-ending supply of opinions and suggestions. I would like to thank my advisors including Dr. Robert T. Pavlowsky for his guidance through out the entire thesis process, Dr. Charles Rovey for his help in understanding sediment transport, and Dr. Xiaomin Qui for all her work with me to conquer GIS. Marc Owen with the Ozarks Environmental Water Resource Institute also deserves a special thank you for all his help and technical assistance. I also want like to thank Missouri State University for the teaching assistantship and Ozarks Environmental Water Resource Institute (OEWRI) for a summer research assistantship.

In addition, I would like to send a special thank you to Dr. Peter Davis from Pacific Lutheran University where I attended my undergraduate program in geosciences. With out Dr. Davis's endless computer help, I would have surely given up before reaching this major achievement.

Finally, I would like to thank my parents who supported me in everyway and never doubted I could achieve my goals. And to my two incredible sons, thank you so much for putting up with many nights of TV dinners; with out your love and support I never could have gone back to school and accomplished so much.

## TABLE OF CONTENTS

Introduction	Page 1
Study Area	Page 8
Location	Page 8
Geology and Soils	Page 8
Climate	Page 12
South Creek USGS Continuous Flow Monitoring Station	Page 15
Methods	Page 18
Assessment of Channel Reach Morphology	Page 18
Longitudinal Profile Surveys	Page 18
Cross-Section Surveys	Page 20
Channel Substrate	Page 21
Bed-Load Tracer Experiments	Page 22
Preparation	Page 23
Tracer Properties	Page 23
Tracer Deployment	Page 25
Data Analysis	Page 27
Channel Discharge Analysis using Hydraflow	Page 27
Bed-Load Equations	Page 27
Flood Analysis using PeakFQ	Page 28
Results And Discussion	Page 30
Study Reach Morphology	Page 30
Longitudinal Profile	Page 30
Channel Cross-Sections	Page 32
Channel Substrate	Page 33
Particle Density and Shape	Page 35
Channel Hydraulics and Sediment Mobility	Page 36
Gage Site Analysis	Page 36
Flood Events in the Study Reach	Page 37
Sediment Mobility	Page 40
Boundary Shear Stress	Page 40
Critical Shear Stress	Page 41
Tracer Experiments	Page 42
Sampled Flow Events	Page 42
Tracer and Transport Distances	Page 43
Event Transport Distances	Page 43
Average Travel Distance	Page 50
Missing Tracers	Page 50
Effect of Channel Location on Transport	Page 53
Tracer Transport at Discharges Above Bankfull	Page 55

## TABLE OF CONTENTS CONTINUED

Annual Transport Distances	Page 56
Conclusions	Page 63
Literature Cited	Page 66
Appendices	Page 70
Appendix A-Individual Tracer Characteristics	Page 70
Appendix B-Deployment Times	Page 78
Appendix C-Tracer Movement	Page 79
Appendix D-Percent of Tracer Movement per Event	Page 87
Appendix E-Data for Cross-Sections and Boundary Shear Stress vs. Water Depth and Discharge	Page 94
Appendix F-Longitudinal Profile and Cross-Section Data	Page 95
Appendix G-Pebble Count Data	Page 101
Appendix H-Flow Event Data from Gage #07052120 South Creek near Springfield, MO	Page 102

## LIST OF TABLES

Table 3.1 Shield's parameter for different particle sizes	Page 29
Table 4.1 Hydraflow results for cross-sections at bankfull	Page 32
Table 4.2 Percentile size distribution (bedrock and roots excluded)	Page 35
Table 4.3 $D_{50}$ , $D_{75}$ , $D_{84}$ , and $D_{90}$ for cross-sections	Page 35
Table 4.4 Average density and shape per pebble size	Page 36
Table 4.5 Dates and discharges of flow events at pool cross-section	Page 39
Table 4.6 Boundary shear stress ( $N/m^2$ ) at cross-sections vs. stage	Page 41
Table 4.7 Critical shear stress and discharge for each grain size class	Page 41
Table 4.8 Magnitude, recurrence interval, and duration of flow events from USGS gage #07052120	Page 45
Table 4.9 Tracer transport results.	Page 46
Table 4.10 Comparison of average distance traveled above critical discharge	Page 51
Table 4.11 Missing/found tracers for event #1 September 1, 2012	Page 52
Table 4.12 Missing/found tracers for event #2 September 7, 2012	Page 52
Table 4.13 Missing/found tracers for event #3 September 15, 2012	Page 52
Table 4.14 Missing/found tracers for event #4 October 14, 2012	Page 52
Table 4.15 Missing/found tracers for event #5 October 23, 2012	Page 53
Table 4.16 Missing/found tracers for event #6 January 29, 2013	Page 53
Table 4.17 Initial movement at cross-sections for September 1, 2012 event, R.I. <1	Page 54
Table 4.18 Initial movement at cross-sections for September 7, 2012 event, R.I. <1	Page 54
Table 4.19 Initial movement at cross-sections for September 15, 2012 event, R.I. 1.3	Page 55
Table 4.20 Initial movement at cross-sections for October 14, 2012 event, R.I. 6.7	Page 55
Table 4.21 Initial movement at cross-sections for January 29, 2013 event, R.I. 1.2	Page 55
Table 4.22 Comparison of distance traveled between events with a R.I. of >1 to 1.3 years and a bankfull event with a R.I. of 6.7 years	Page 57
Table 4.23 Comparison of maximum distance traveled between an event with a R.I. of >1 to 1.3 years and a bankfull event of a R.I. of 6.7 years	Page 57
Table 4.24 Comparison of recovery rate between events with a R.I. of >1 to 1.3 years and a bankfull event with a R.I. of 6.7 years	Page 57
Table 4.25 Comparison of initial movement within channel units between events with a R.I. of >1 to 1.3 years and a bankfull event with a R.I. of 6.7 years	Page 60
Table 4.26 Comparison of initial movement within deployment sites between events with a R.I. of >1 to 1.3 years and a bankfull event with a R.I. of 6.7 years	Page 60

## LIST OF TABLES

Table 4.27 Average/Maximum distance traveled above critical shear stress	Page 61
Table 4.28 Tracer transport in a year with 11.3% run off	Page 62

## LIST OF FIGURES

Figure 1.1 Three modes of sediment transport	Page 3
Figure 2.1 Study area located west of Springfield Missouri	Page 9
Figure 2.2 Study reach location	Page 10
Figure 2.3 Current land use within the Wilson Creek Watershed	Page 11
Figure 2.4 Geology of the James River Water Basin	Page 13
Figure 2.5 Study reach in the South Creek looking downstream	Page 14
Figure 2.6 Study reach in South Creek looking upstream	Page 14
Figure 2.7 USGS Gages within the Wilson Creek Watershed	Page 16
Figure 2.8 Average monthly discharge, years 1998-2014	Page 17
Figure 2.9 Annual Peak gage discharge	Page 17
Figure 3.1 Longitudinal profile	Page 19
Figure 3.2 Downstream edge of the upstream low-water bridge	Page 19
Figure 3.3 Cross-section measurements	Page 20
Figure 3.4 Gravelometer	Page 22
Figure 3.5 Blue tracer at 100% rough, green tracer at 100% smooth	Page 24
Figure 3.6 Power's index chart	Page 24
Figure 3.7 Axis dimensions for pebble size measurements (cm)	Page 24
Figure 3.8 Cross-sections and deployment sites	Page 26
Figure 3.9 Taking a measurement from deployment site to tracer position after flow event	Page 26
Figure 4.1 Longitudinal profile taken on March 7, 2013	Page 31
Figure 4.2 Longitudinal profile comparison	Page 31
Figure 4.3 Comparisons of Cross Sections	Page 33
Figure 4.4 Pebble count results for study reach (352 Pebbles)	Page 34
Figure 4.5 Gage #07052120 rating curve for discharge and channel area	Page 37
Figure 4.6 Hydraulic geometry relations at gage #07052120	Page 38
Figure 4.7 Flood-frequency curve	Page 38
Figure 4.8 Flow events at pool cross-section	Page 39
Figure 4.9 Time in hours of individual events vs. discharge	Page 40
Figure 4.10 Eight sampled flow events	Page 42
Figure 4.11 Average travel distance vs recurrence interval (Recurrence intervals of 0.5-1.3 years)	Page 58
Figure 4.12 Average travel distance vs recurrence interval (Recurrence interval of 6.7 years only)	Page 58
Figure 4.13 Maximum distance traveled vs recurrence interval (Recurrence intervals of 0.5-1.3 years)	Page 59
Figure 4.14 Maximum distance traveled vs recurrence interval (Recurrence interval of 6.7 years only)	Page 59
Figure 4.15 Average percent recovered vs recurrence interval	Page 60



## INTRODUCTION

Rivers have political, social, economic and physical relevance, whether as a resource or hazard (Knighton, 1998). Their drainage networks are a fundamental part of our environment that provides for water supply, navigation, power generation, and recreation. The unidirectional flow of water in river channels creates a renewable water resource, filtration system for unwanted substances, and valuable source of energy. Channels function as the primary conduit of the discharge of water and sediment within the drainage network. Natural stream channels tend towards equilibrium, or a natural balanced condition, that is most stable under prevailing discharge and sediment conditions (Charlton, 2008). Stability indicates a balance between flow energy and sediment transport where reach inputs roughly equal outputs, minimum amounts of geomorphic energy is expended, and channel form varies little (Allan and Castillo, 2007). When the amount of sediment introduced into a stream is larger than the flow velocity needed to transport the imposed load, excessive deposition or aggradation can occur, forcing the channel into an unstable state. When the flow velocity and transport capacity exceeds sediment input, erosion occurs, and this again can cause channel instability (Lane, 1955).

Natural or human-induced disturbances of the soil and vegetation characteristics in the watershed and water and sediment discharge in the channel can cause stream channel instability (Jacobson and Pugh, 1992, Leopold, 1992). For example, channel instability can result from changes in runoff, sediment supply, strength or roughness of bank materials, and patterns of flow within the channel (Jacobson and Pugh, 1992). Even in relatively undisturbed rivers, channel instability can be caused by climate and geological factors that trigger mass wasting and internal geomorphic adjustments including changes in erosion and deposition (Jacobson and Pugh, 1992).

Investigations of fluvial sediment and bed load transport can provide valuable insight into

how channel stability is maintained and the rates at which sediment transport and bed-form adjustments can occur in stream channels (Carling and Orr, 2000). In fact, bed-load studies are common in the field of fluvial geomorphology including studies to determine sediment mobility, erosion, transport, loading rates, and channel sediment budgets (van Rijn, 1984; Wilcock, 1997; Hassan *et al*, 1992; Church and Hassan, 1992).

Sediment is considered the largest contaminant of surface water by weight and volume and was identified by the United States Environmental Protection Agency as the number one problem threatening America's waterways (Koltun *et al*, 1997). Bed sediment has generally been defined as "solid bits and pieces of material (fragments of rocks and minerals) produced by weathering, transported by various agents like wind, ice, running water, and mass movement, and either deposited or precipitated in layers on, at, or near the Earth's surface normally as loose, unconsolidated material" (Prothero and Schwab, 2004). When particles move along a bed surface by rolling, sliding, or saltation it is called bed-load transport (van Rijn, 1984) (Figure 1.1). Sediment load is the amount of sediment carried by a stream in mass per unit time such as kg/day or Mg/year (Reynolds *et al*, 2010). Sediment transport is initiated when bed sediment particles first begin to move under hydraulic forces and become entrained by the flow. Entrainment of sediment occurs when the forces exerted by the flowing water overcome particle inertia or the tendency to remain in place (Malmaeus and Hassan, 2002). The mobility of bed material in gravel and cobble bed rivers can be evaluated by the ratio between the force or shear stress imposed on the bed by the flowing water and the critical shear stress required to overcome the force of gravity on the sediment and initiate movement (Pohl, 2004). If the channel shear stress exceeds the critical shear stress, particle entrainment is assumed to occur, and entrainment and bed erosion begins. Given all else equal, sediments of smaller diameter require lower flow

velocities to initiate movement and be transported by traction, saltation, and suspension (Figure 1.1)(van Rijn, 1984). In theory, after the bed-shear velocity barely exceeds the critical shear stress, movement is initiated, and particles will roll and or slide staying in continuous contact with the bed (traction) (van Rijn, 1984). As bed-shear velocity increases, more particles will be transported by bouncing or jumping (saltation) (van Rijn, 1984). When flow rates increase even further, upward turbulent forces can exceed the submerged weight of the particles and particles may be transported within the water column (suspension) (van Rijn, 1984).

Bed load transport rate is variable both across the channel and downstream. Commonly, all or most of bed-load transport occurs within a narrow zone of the total width of channel, in the thalweg or along the main flow line of channel (Lisle *et al*, 2000). Therefore, many equally spaced transverse sampling stations may be necessary to ensure that zones of both maximum and minimum transport are adequately sampled in field transport studies (Emmett, 1981). Lisle *et al*. (2000) found that sediment-rich channels had wide zones of full mobility on the channel bed and sediment-poor channels had more bed areas of partial mobility. However, both types had

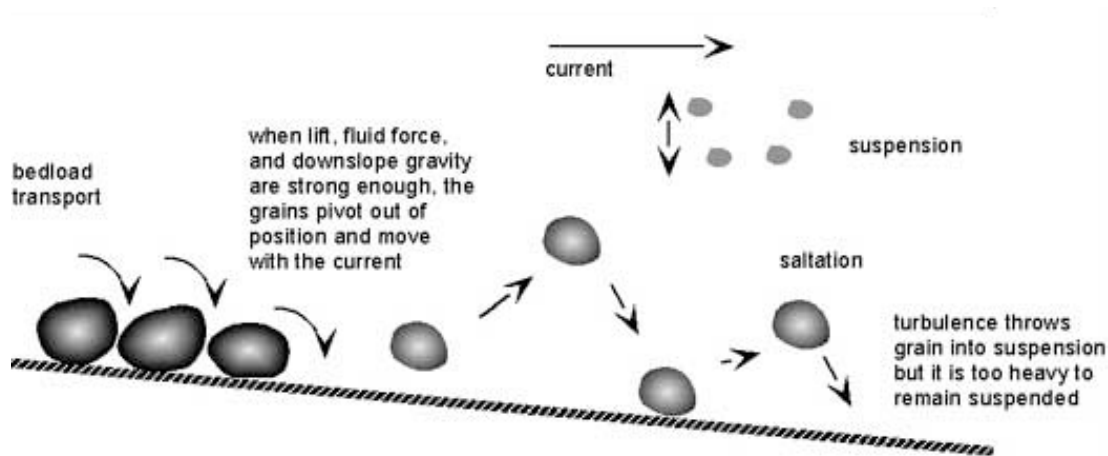


**Figure 1.1** Three modes of sediment transport (van Rijn, 1984).

significant areas on the channel bed that were essentially immobile. Therefore, downstream

transport of coarse sediment is a highly sporadic process with individual particles being stored from seconds to centuries (Bunte and Macdonald, 1995). Bed sediments can be stored within a stream when depositional “fill” rates exceed scour rate (Laronne and Duncan, 1989). Armoring of the bed can reduce the availability of finer sediment for transport in the channel (Laronne and Duncan, 1989). Armoring develops when only small particles become entrained during frequent low magnitude flow events (Charlton, 2008). Fine sediment is selectively removed from the bed, as a result a layer of coarse sediment is formed that armors and protects the finer material beneath from entrainment by relatively higher flows (Charlton, 2008).

Measuring bed load transport in the stream itself is difficult since the sediment being measured is contained within the streambed, that itself is deformed and variable in texture by location and through time within the channel (Hassan and Bradley, 2017). One method of bed sediment transport measurement involves the release of marked or tagged particles into streams in order to obtain general information on the mobility of sediment by monitoring the distance of downstream movement by flow events (Hassan and Ergenzinger, 2003; Leopold and Emmett, 1976; Vazquez-Tarrio and Menendez-Duarte, 2014). The use of these sediment tracers can produce valuable information on rate and direction of sediment transportation, volume and size distribution of mobile sediment, particle entrainment, sediment sources and depositional rates, periods of rest and movement of particles, impact of particle sedimentological environment on distance of movement, step length of individual particles, downstream fining, depth of active layer, residence time, flow competence, relations between distance of movement and flow strength, virtual rate of sediment movement (Wilcock, 1997, Bunte and Ergenzinger, 1989, Hassan and Ergenzinger, 2003; Vazquez-Tarrio *et al*, 2019). Interestingly, Henry Albert Einstein (1937) may have been the first to use tracers in a controlled hydraulic flume. However,

Takayama (1965) and Leopold et al. (1966) were pioneers in using painted tracers to study sediment transport under field conditions in natural streams (Hassan and Ergenzinger, 2003).

Tracer "seeding" occurs when individual particles are marked in some way, placed in the stream, and their location is monitored prior to and after a flow event (Knapp, 2002). By visually recording where a particle was originally placed and where it ends up in the stream after a flow event, the distance that a particle has traveled can be calculated. It is assumed that there is a direct link between the start and end points of the sediment particle. However, not all tracers may be recovered due to burial or human removal (Hassan and Ergenzinger, 2003). Recovery rates for streambed tracer studies typically range from 20 to 50 percent under field conditions (Hassan *et al*, 1984, Hassan and Church, 1992, Vazquez-Tarrio and Menendez-Tarrio, 2014). Another limitation to seeding is caused by the disruption of the bed while placing the tracer particles. The seeded particles may move more easily than natural bed material, and yield an over prediction of bed load transport (Knapp, 2002). This can be caused by unstable placement, with more exposure to flow energy while natural bed material may have to overcome armoring or other types of debris before transportation may occur.

Rivers in the Ozark Highlands of Missouri and Arkansas, are known to be affected by excessive bed-load transport and gravel bar deposition (Martin and Pavlowsky, 2011). Several studies have been conducted within the Ozark region to understand historical gravel bar dynamics. McKenney and Jacobson (1996) used repeat cross sections to monitor rates of channel change and bed sediment distribution in riffle-pool sequences. Jacobson and Pugh (1992) emphasized the role of land use changes in increasing gravel supply and deposition as a cause of long-term channel disturbances. McKenney et al. (1995) found that vegetation patterns on channel banks will affect gravel transport with denser vegetation causing more deposition.

Historical disturbances in watershed conditions in the Ozarks region have also led to observable changes in channel form (Martin and Pavlowsky, 2011). In addition, human activities have caused migrating sand and gravel sediment waves within distinct disturbance reaches in Ozark rivers (Jacobson and Gran, 1999). Further, coarse tailing sediment (2-6 mm) has resulted in both contamination and sedimentation problems in Big River (Pavlowsky *et al*, 2017). McKenney and Jacobson (1996) reported that continued bed sediment monitoring could help to understand changes in river habitat in response to long-term aggradation and degradation patterns in the Ozarks. While research on the role of land use and climate on gravel bar behavior over the past 100 years has been completed, no studies have focused on understanding the bed load transport rates and time of travel of bed particles in Ozark streams.

While the primary controls on bed sediment entrainment and transport are understood to be bed slope, sediment size distribution, flow velocity, and flow depth, the field behavior of bed-load transport in streams is still poorly understood (Malmaeus and Hassan, 2002). In general, flood events provide the hydraulic force needed to move bed sediment and higher flows tend to increase bed load transport rates (Vazquez-Tarrio *et al*, 2019). Seasonal influences and patterns of floods are believed to influence bed load transport, but very little work has been done to quantify these effects (Sidle, 1988). Further, there is still a large inconsistency between data collected in the field and the results of theoretical and empirical models (Hassan and Ergenzinger, 2003). For example, the sample size needed to represent the movement of sediment in a stream channel is still not known (Hassan and Ergenzinger, 2003).

The purpose of this study is to compare the results of the field tracer data in an urban stream in Springfield, Missouri located in the Ozark Plateau region to bed load mobility results from Shields mobility analysis (Shields, 1936) and Wolman's equations on boundary and critical

shear stress (Wolman, 1954). The findings of this study will be used to validate bed-load model results and evaluate gravel sediment transport distances in Ozark streams. The objectives of this project are to (i) determine downstream transport distances of painted tracers of different sizes over a range of flow conditions; (ii) evaluate the influence of channel form and thalweg location on transport; and (iii) compare field results to those predicted by mobility equations. Bed load transport is an important process due to its direct influence on channel morphology (Allen and Castillo, 2007), ecology (Knapp, 2002), fish habitat (Sidle, 1988), and maintenance of dynamic equilibrium of the stream system overall (Sidle, 1988). Therefore, benefits of this project will include better sediment and geomorphic understanding of channel processes in Ozark streams, and provide information to assist in restoration and habitat improvement projects.

## STUDY AREA

This study monitored bed load transport distances in a 180 m reach of South Creek in Southwest Missouri. South Creek is located in Springfield, the third largest city in Missouri, and is an example of a typical urban stream (Figure 2.1). A USGS discharge gage (#07052120, drainage area = 27.2 km<sup>2</sup>) is located 80 m above the study reach (Figure 2.2).

### Location

The South Creek study area is located within the James River Watershed, just outside of the Springfield city limits (Figure 2.1). Portions of South Creek within the Springfield city limits have been channelized and the majority of the South Creek watershed is heavily urbanized (Figure 2.3). South Creek drains into Wilson Creek, which flows into the James River. The South Creek is an ephemeral stream and flows only during rainfall or snow melt periods.

### Geology and Soils

Stream valleys in the Ozarks are incised into uplifted Paleozoic sedimentary rocks, which form gently rolling uplands. Lithologies are predominantly cherty carbonate rocks that supply the low-gradient stream with chert-rich gravel bed load (Jacobson and Pugh, 1992). Karst drainage systems are common in the Ozarks. Losing stream channels that are dry most of the year are common, whereas other parts of the drainage network are supplied with substantial base flow from springs (Jacobson and Gran, 1999). Streams with drainage areas less than 25 km<sup>2</sup> tend to be ephemeral unless spring flows maintain base flow locally. Juxtaposed stable and



# South Creek Study Area

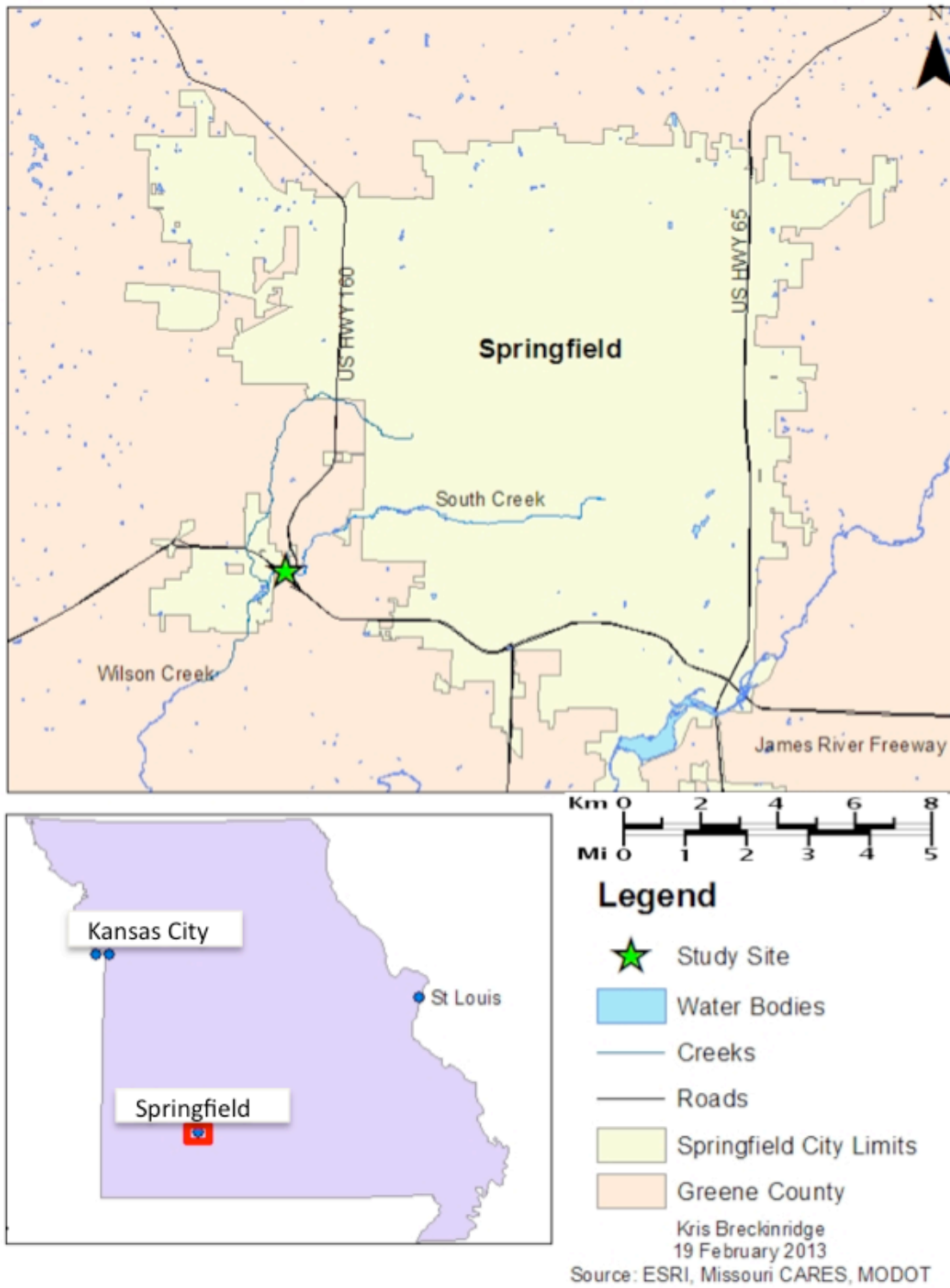
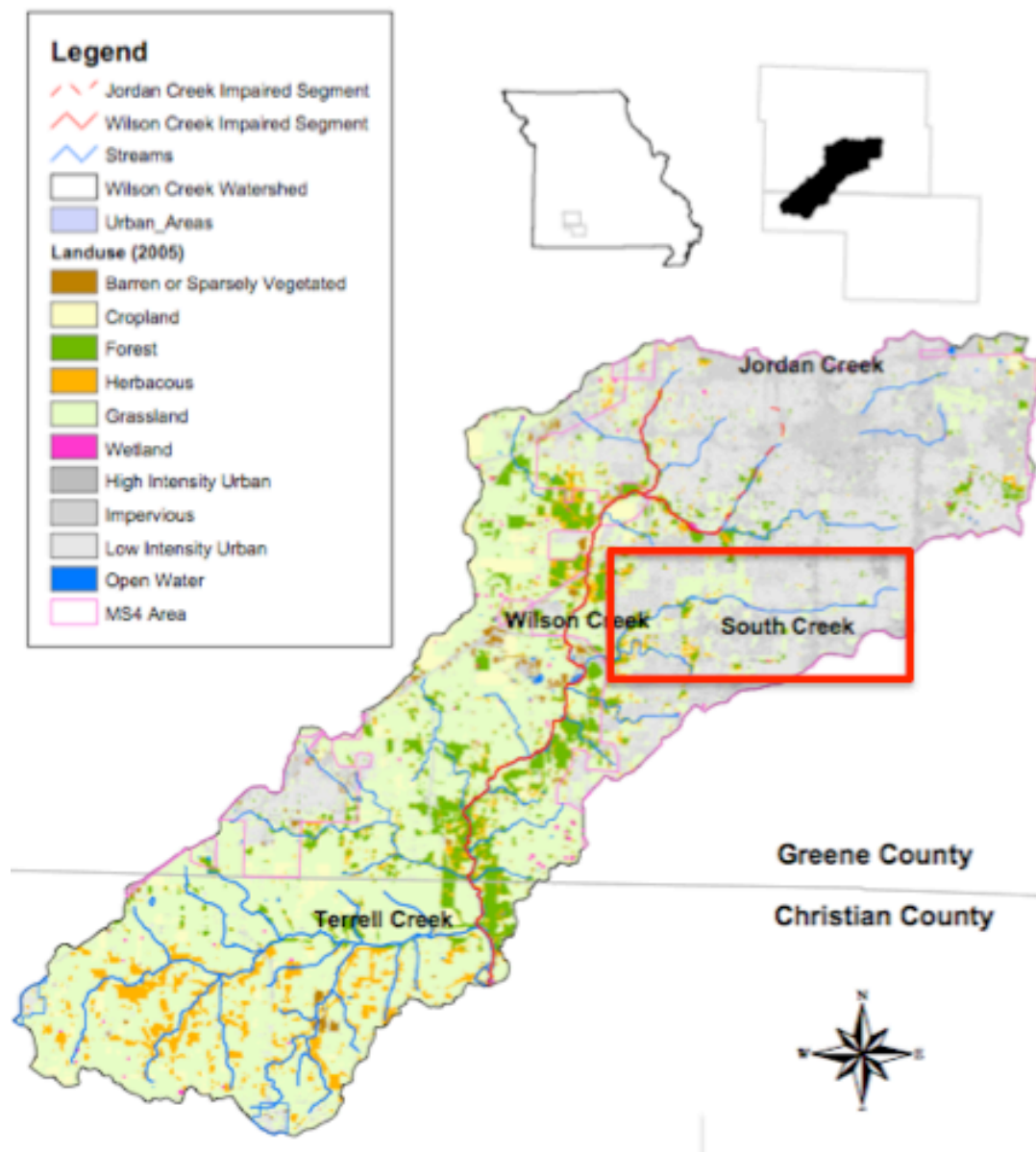


Figure 2.1 Study area located west of Springfield Missouri.



**Figure 2.2** Study reach location. The study reach is located in the red box.



**Figure 2.3** Current land use within the Wilson Creek Watershed (TMDL for Wilson and Jordan Creek, 2011). Red box shows South Creek area.

disturbance (bed load deposition) reaches characterize the channel patterns of the Ozark streams indicating that bed load transport is a process in developing the fluvial systems in the Ozarks (Jacobson and Gran, 1999; McKenney *et al.*, 1995; Martin and Pavlowsky, 2011).

The South Creek watershed lies within the Springfield Plateau of the Ozark Highlands (Missouri Department of Conservation, April 14, 2019). This plateau consists of undulating to rolling plains. Elevations range from about 900 to 1,500 ft (274 to 457 m) above sea level. Limestone underlies most of the watershed (Figure 2.4) (Missouri Department of Conservation, April 14, 2019). The streambed of the study reach is covered by chert gravel and cobble with local patches of exposed bedrock, trees along bank, and tree cover over most of the area (Figure 2.5 and Figure 2.6)

## **Climate**

The climate is one of hot summers and moderately cool winters. The average temperature for Springfield is 56.1 degrees °F (13.4 degrees °C), average high temperature 67 degrees °F (19.4 degrees °C), and average low temperature of 45.3 degrees °F (7.4 degrees °C). The average annual runoff of the basin is 30.5 cm with the average annual precipitation being 116 cm. Springfield receives the most rainfall in the months of April through June and receives the least amount of precipitation in the months of December through February (Missouri Department of Conservation, 2012).

This study was completed during 2012, which was the second warmest, and the 10<sup>th</sup> driest year on record for Springfield. As of 2012 the average mean temperature was 59.5 degrees °F (15.3 degrees °C), the highest temperature 106 degrees °F (41.4 degrees °C), average high

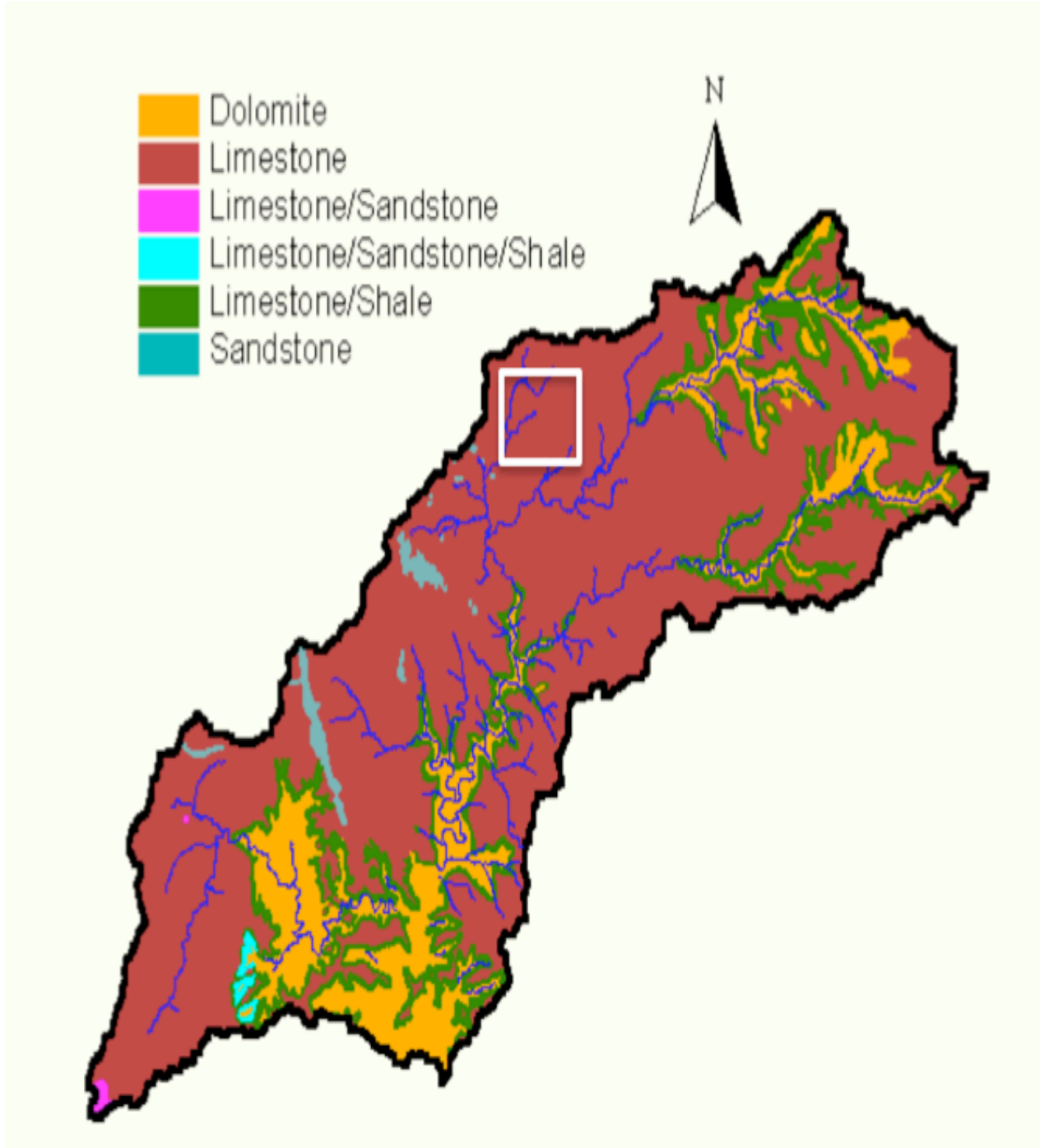


**Figure 2.4** Geology of the James River Water Basin (Missouri Department of Conservation). White box shows South Creek area.





**Figure 2.5** Study reach in the South Creek looking downstream.



**Figure 2.6** Study reach in South Creek looking upstream.

temperature 71 degrees °F (21.7 degrees °C), low temperature 10 degrees °F (-12.2 degrees °C), and an average low temperature of 48.1 degrees °F (8.9 degrees °C) (National Weather Service, 2013). The total precipitation was 78.6 cm (National Weather Service, 2013).

### **South Creek USGS Continuous Flow Monitoring Station**

The USGS discharge gage (South Creek near Springfield Mo, #07052120) on South Creek is located at latitude 37° 09'13.1" and longitude 93° 21'46.0" (NAD83) at an elevation of 1,146.46 ft above sea level (NAVD88) (USGS Water Data, May 10, 2012) (Figure 2.7). The gage has been recording stream flow since June of 1998, with 14 years of record at the time of this study. Average monthly discharge for the gage ranged from 0.06 m<sup>3</sup>/s to 0.24 m<sup>3</sup>/s (Figure 2.8). Annual peak discharge has ranged from 8 m<sup>3</sup>/s to 81 m<sup>3</sup>/s since 1998 (Figure 2.9).



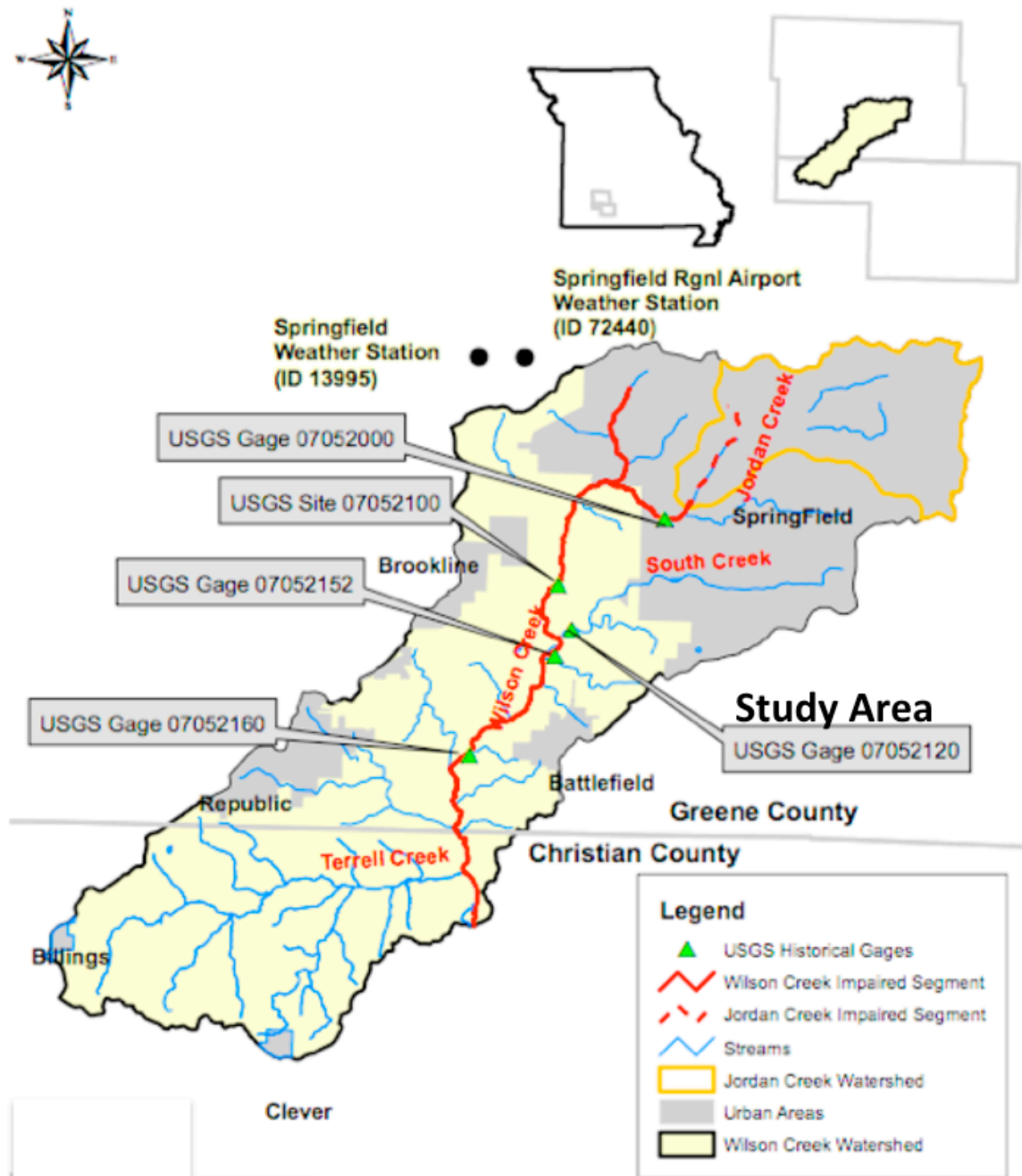


**Figure 2.7** USGS Gages within the Wilson Creek Watershed (TMDL for Wilson and Jordan Creek, 2011).



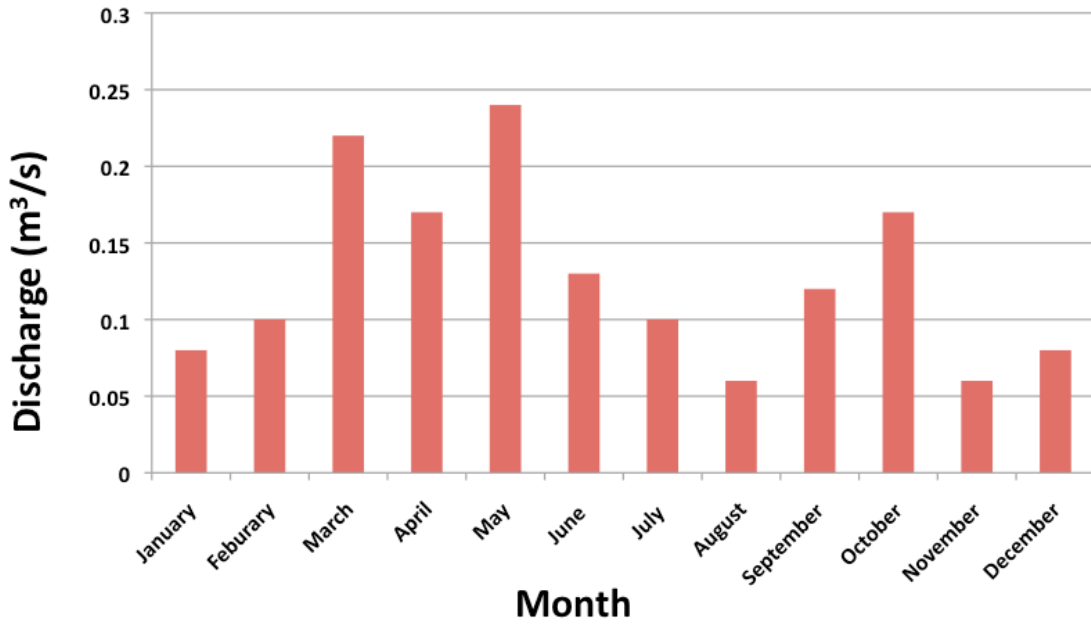


Figure 2.8 Average monthly discharge, years 1998-2014 (USGS Water Data, May 10, 2012).

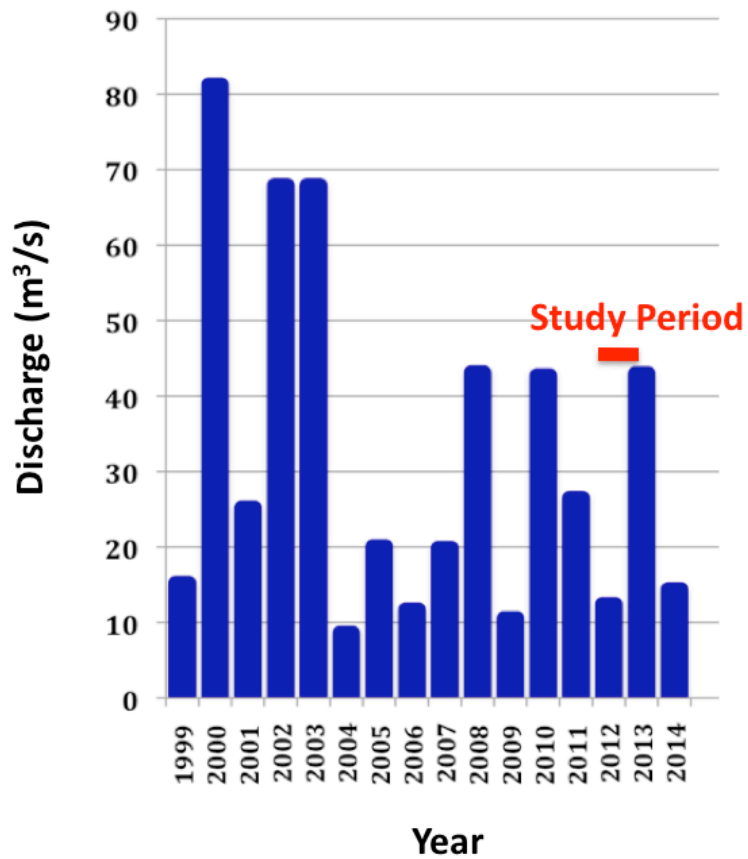
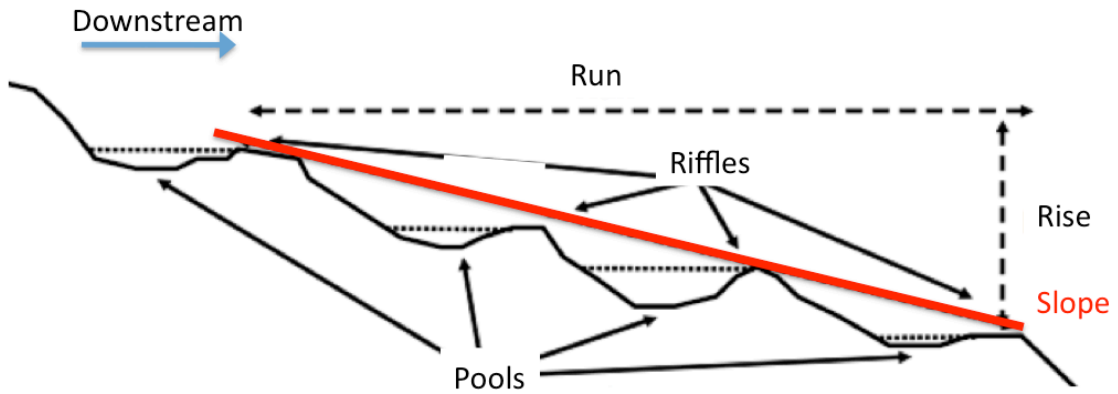


Figure 2.9 Annual Peak gage discharge (USGS Water Data, May 10, 2012).

## METHODS

### Assessment of Channel Reach Morphology

**Longitudinal Profile Surveys.** The longitudinal profile was used to determine channel gradient, slope values, and locate channel units, including riffles, glides, and pools (Figure 3.1). A riffle is an area where the bed dips steeply downstream from the riffle crest (highest point in the riffle), the glide is the area where the channel bed slopes upward to meet the riffle crest, and a pool is the deepest area between riffle crests (Panfil and Jacobson, 2001). Slope was calculated by dividing the distance measured (length of study area) by the change in elevation from beginning of the measured section to the end of the measured section (rise/run). The slope used for this study was the slope calculated only using the riffle crests, riffle crests being the highest points within the length of the study area (Figure 3.1). Equipment used in measuring the cross-section included a surveying auto-level, tripod, stadia rod, and 100-meter measuring tape. The down stream edge of the upstream low-water bridge was located at the tapeline 0 m (Figure 3.2). Survey ground points collected upstream of 0 m were recorded as negative numbers while channel distances downstream from 0 m were recorded as positive numbers. Rod readings were measured to the nearest 100<sup>th</sup> of a meter at ground points located at 2 meter intervals and/or where topographic breaks in the slope occurred.



**Figure 3.1** Longitudinal profile. Red line shows the riffle slope (Modified from Horton, 2003).



**Figure 3.2** Downstream edge of the upstream low-water bridge Location 0 m on tapeline (April, 2012).

**Cross-Section Surveys.** Based on the results of the longitudinal profile, channel cross-sections were surveyed at 40 m from the 0 m point at the bridge (riffle), 60 m (pool), and at 85 m (glide). Surveyed cross-sections provided information on channel width, depth, and slope (Figure 3.3). Equipment used in surveying the cross-section consisted of a tripod stand, auto-level, stadia rod, and 100-meter measuring tape. A measuring tape was placed across the channel units to be surveyed, pulled tight, and staked at both sides to prevent movement or slippage. Rod reading measurements were determined to the nearest 100<sup>th</sup> of a meter at ground points starting from the top of the left bank at all topographic breads in slope, typically at less than 2 m.

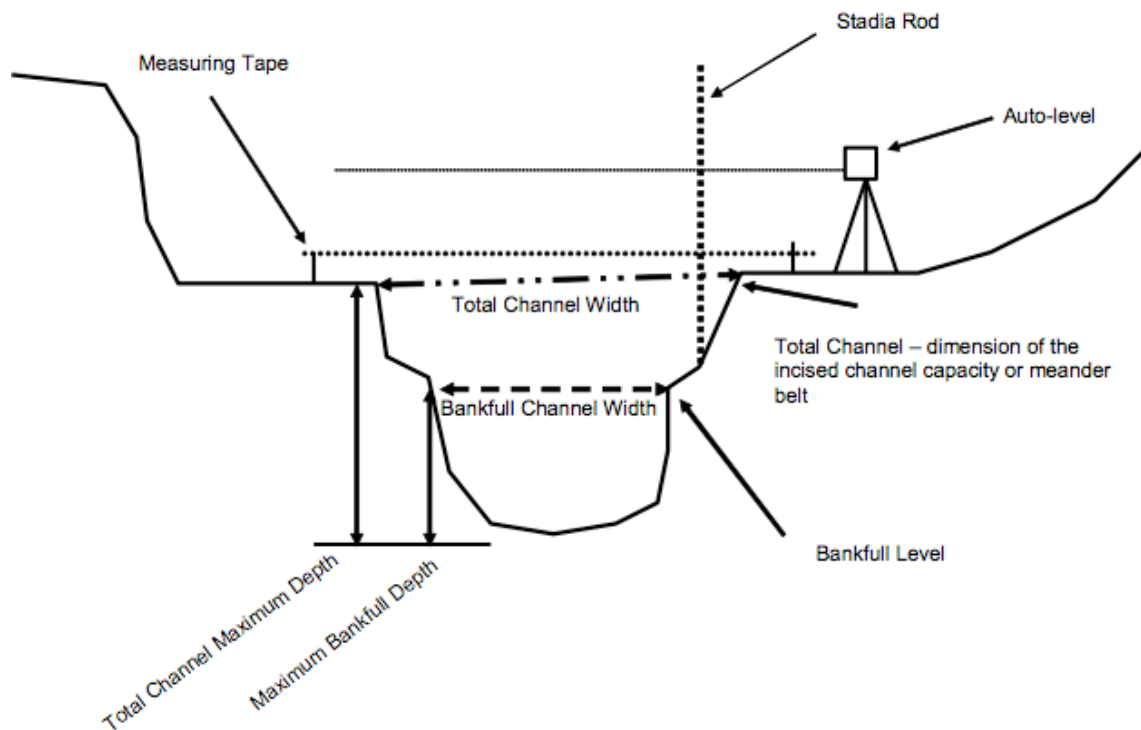


**Figure 3.3** Cross-section measurements (Horton, 2003).

**Channel Substrate.** Pebble counting methods were used to quantify the size distribution of sediment in the active channel. Information on sediment size is required to obtain sediment size distributions for sediment mobility equations and to select size classes of tracers. Sediment size was determined by the length of the intermediate B-axis measured using a gravelometer (Figure 3.4).

A gravelometer is a hand-held sieving device used to sort particles in the field into size classes of  $\frac{1}{2}$  phi intervals. The gravelometer is made up of square holes of common sieve sizes, usually 2 mm to 160 mm (Figure 3.4). The size intervals include particles that are larger than the listed size but smaller than the next largest sieve in the sequence. Data was plotted by size class and frequency to determine distributions. Two methods of sediment size sampling were used: one to evaluate the overall size distribution in the reach and another to evaluate bed texture associated with specific channel units including riffle, pool, and glide.

A channel grid method (Rosgen, 1994) based on the Wolman pebble count (Wolman, 1954) was used to evaluate channel sediment size. Rosgen pebble counts were taken from stream transects located at intervals of every three meters starting at 18 m and concluding at 99 m on the tapeline. Pebble counts were not taken at transects located between 0-18 m due to the large woody debris and large scour immediately downstream of the bridge. At each transect a tape measure was placed across the channel. Pebbles were sampled starting at the left bank toe, measuring tape reading zero, and then at every 0.5 m across to the right bank toe (channel unit grid method). The toe-to-toe sampling transect used here differs from a Rosgen sample transect which collects samples from bank top to bank top.

The second sediment size sample focused on the specific channel units. Accordingly 30 pebble counts were collected within the cross-section of the riffle, glide, and pool cross-sections

by blind touch and size was recorded using a gravelometer.



**Figure 3.4** Gravelometer (Wildlife Supply Company, 2012).

### **Bed-Load Tracer Experiments**

The primary goal of this study was to determine the mobility and travel distance of the bed surface layer, so painted tracers were selected over other tracing techniques. The study reach was ephemeral and dry between storm flows thus making tracer deployment and collection easier. Pebble count data (from the entire study area) were used to determine sizes ( $D_{50}$ ,  $D_{75}$ ,  $D_{84}$ , and  $D_{90}$ ) for tracer particles so that they closely represent the sediments naturally occurring on the bed. The B axis of each pebble was measured with a gravelometer to separate into the four size groups for tracer testing: 16 mm up to 22.6 mm ( $D_{50}$ ), 22.6 mm up to 32 mm ( $D_{75}$ ), 32 mm up to 45 mm ( $D_{84}$ ), and 45 mm up to 64 mm ( $D_{90}$ ). These sizes are within the coarse to very coarse gravel size range (Rosgen, 1994)

**Preparation.** Tracer pebbles were measured along all 3 axes, observed for texture and shape, weighed, volume calculated, and particle density determined (Appendix A). Each of the four size groups are represented by a different color Glo Spray fluorescent spray paint: D<sub>50</sub> was painted orange; D<sub>75</sub>, green; D<sub>84</sub>, yellow; and D<sub>90</sub>, blue. Every pebble was painted with two coats of paint (yellow received three coats) corresponding to their group and labeled with a number as an identifier, the tracers were then sprayed with two coats of enamel gloss paint.

**Tracer Properties.** All properties were determined in the laboratory after the pebbles had been sized, painted, and numbered. Texture was determined using personal observation of the percent of smoothness and roughness each pebble possessed (Figure 3.5). Each pebble was compared to the shapes and descriptions in the Power's index chart to determine the shape (Figure 3.6). A Sartorius scale was used to weigh the 16 mm pebbles and rounded to the nearest 0.10 g; the 22.6 mm, 32 mm, and the 45 mm pebbles were weighed using an Acculab scale rounded to the nearest 0.10 g. The Sartorius scale was used only on the 16 mm pebbles due to the larger pebbles being too heavy to measure on the scale. Volume was determined for each pebble by placing them in a graduated beaker with water and calculating the difference in the particle volume of water in milliliters (ml) before the pebble was submerged and after the pebble was submerged. Particle density ( $\text{g}/\text{cm}^3$ ) was then calculated by dividing the mass (weight) by the volume change.

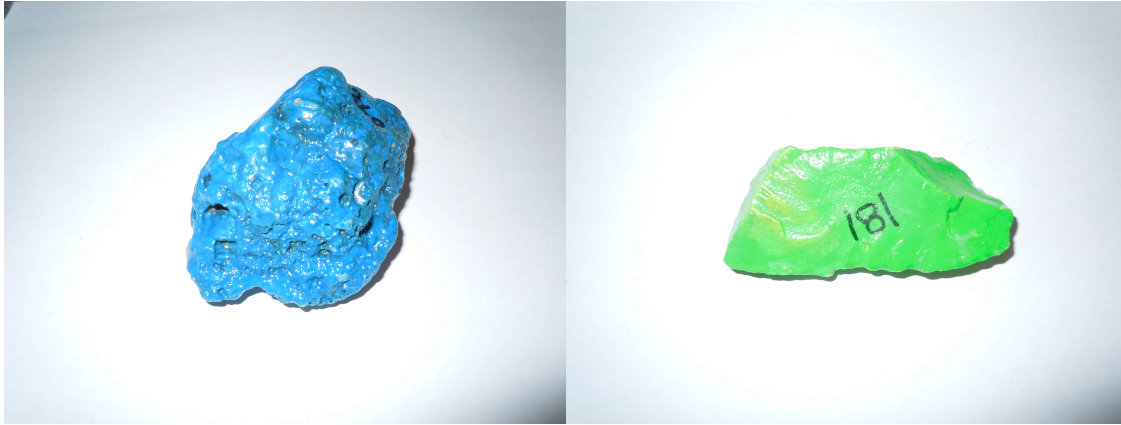


**Figure 3.5** Blue tracer at 100% rough, green tracer at 100% smooth.

Very angular	Angular	Sub-angular	Sub-rounded	Rounded	Very rounded
Every edge and every point is sharp. There are no smooth parts to the pebble.	One or two points and edges are smooth but most aspects of the pebble are sharp.	The pebble is irregular in shape and has one or two sharp points or edges. The rest of the pebble is smooth.	There are no sharp points or edges on the pebble but it is irregular in shape.	The pebble is almost perfectly smooth but there are one or two irregularities.	The pebble is perfectly smooth.

**Figure 3.6** Power's index chart (earthstudies.co.uk, March 2013).



**Figure 3.7** Axis dimensions for pebble size measurements (cm).



The A, B, and C axis were measured on each tracer (pebble) using a caliber to the nearest millimeter (Figure 3.7). The a-axis is the largest dimension, the b-axis is the intermediate, and the c-axis is the smallest axis. The diameter of a sphere with the same volume and thus corresponding to sieve size is defined as the nominal diameter (USDA Forest Service, May 2012). The b-axis is an adequate predictor of nominal diameter since most streambed particles are approximate ellipsoids, making it possible to use the b-axis alone to determine particle size frequency distribution (USDA Forest Service, May 2012).

**Tracer Deployment.** Nine deployment sites were set up within the study reach. Each riffle, pool, and glide cross-section contained three evenly spaced deployment sites (Figure 3.8). The riffle cross-section at 40 m from the bridge was 6 meters wide with deployment site 40L at 1.5 m from the left bank, site 40C at 3.0 m, and site 40R at 4.5 m. The pool cross-section at 60 m from the bridge was 6.7 m wide containing deployment site 60L at 1.7 m from the left bank, site 60C at 3.4 m, and site 60R at 5.1 m. At 85 m from the bridge the glide cross-section contained deployment site 85L at 1.2 m from the left bank, site 85C at 2.4 m, and site 85R at 3.6 m. All deployment sites were marked with pink spray paint.

Tracers were placed in the stream just prior to a predicted heavy rain with their deployment sites recorded (Appendix B and C). After the water receded, the stream channel bed was visually searched to find and record the location of as many tracers as possible (Appendix D). Displacement lengths of tracers were measured in the field using a measuring tape. Measurements were taken from the deployment site to where the tracer was found after the flow event (Figure 3.9).

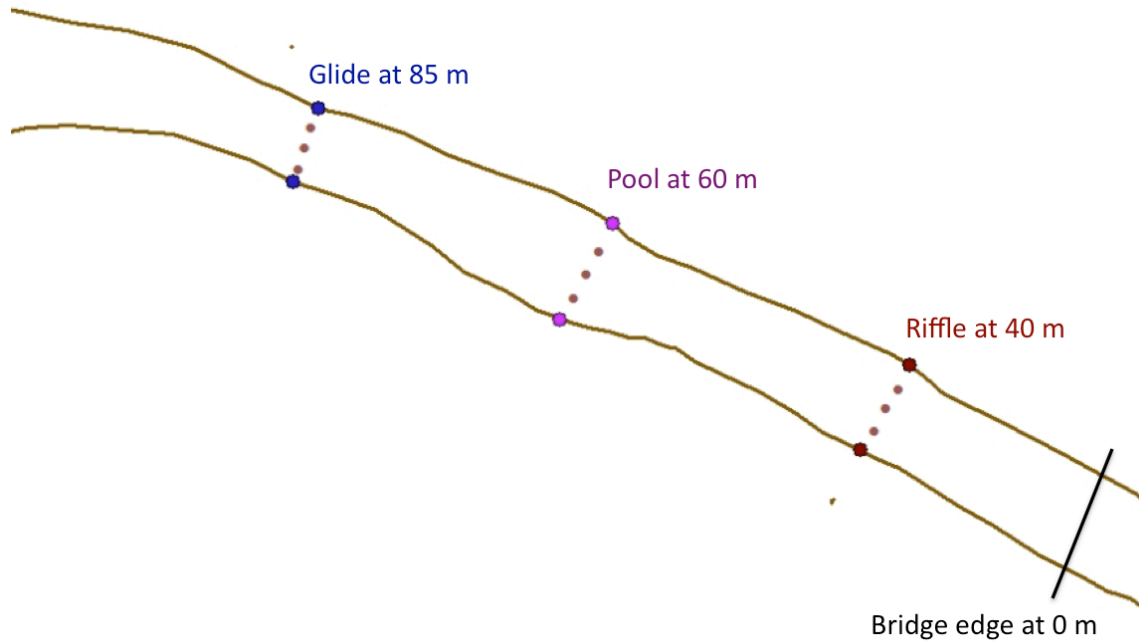


**Figure 3.8** Cross-sections and deployment sites.



**Figure 3.9** Taking a measurement from deployment site to tracer position after flow event.

## Data Analysis

**Channel Discharge Analysis using Hydraflow.** Hydraflow express software provides tools for calculating various hydraulic and hydrologic values. The user provides data on cross section elevations and distances, manning's N, stream slope, and channel depth (Intelisolve, 2006). Hydraflow express software was used to calculate the mean depth, bankfull width, terrace width, bench widths, total channel capacity width, hydraulic radius, and total channel capacity mean depth (Appendix E).

**Bed-Load Equations.** Shields developed an equation for the amount of boundary shear stress needed to initiate particle entrainment (Shields, 1936).

Boundary shear stress. Shields equation of boundary shear stress was used to quantify the shear stress exerted by the driving forces (water) acting on a particle during any specific flow (Equation 1)(U.S. Department of Agriculture, 2008).

$$\tau = \gamma RS \quad (1)$$

where:  $\tau$ =shear stress ( $\text{N/m}^2$ ),

$\gamma$ =specific weight of water ( $1000 \text{ kg/m}^3$ ),

R=hydraulic radius (m), and

S=channel slope (m/m).

Critical shear stress equation (Mobility equation). Critical shear stress is the relationship of forces (water) and resisting particle movement (tracers) at the moment of entrainment. By calculating the critical shear stress the force needed to move a particle can be calculated. Critical shear stress was calculated using a modified Shield's critical shear stress equation where the relationship between the particle size of interest ( $D_i$ ) and the median percentile  $D_{50}$  is the basis

for the equation (Equation 2)(U.S. Department of Agriculture, 2008).

$$\tau_{ci} = \tau_{D50}(\lambda_s - \lambda)D_i^{0.3}D_{50}^{0.7} \quad (2)$$

where:  $\tau_{ci}$  is the critical shear stress at which the sediment particle of interest begins to move ( $\text{N/m}^2$ ).

$\tau_{D50}$  is the dimensionless Shields parameter for  $D_{50}$  particle size (this value was obtained from table 3.1).

$\lambda_s$  is the the specific weight of the sediment particle ( $\text{kg/m}^3$ ).

$\lambda$  is the specific weight of the water ( $1000 \text{ kg/m}^3$ ).

$D_{50}$  is the diameter (m) of the median or 50<sup>th</sup> percentile particle size of the channel.

$D_i$  is the diameter (m) of the particle size of interest.

The critical shear stress units used in Table 3.1 were converted from  $\text{lbs/ft}^2$  to  $\text{N/m}^2$  by using the conversion of  $1 \text{ lb/ft}^2 = 47.880172 \text{ N/m}^2$ .

Wolman's Equation. The Wolman equation uses the boundary shear stress calculated from the Shield's equation to calculate what diameter of pebbles will move at a certain critical shear stress (Equation 3).

$$D = 78(\tau_{ci})^{1.042} \quad (3)$$

where: D is the diameter of grain (mm)

$\tau_{ci}$  is the critical shear stress ( $\text{N/m}^2$ )

**Flood Analysis using PeakFQ.** Flood recurrence figures were determined for annual maximum flood peak record for the South Creek gage (#07052120). The PeakFQ software used in this study provides estimates of instantaneous annual maximum peak flows for a range of recurrence intervals (USGS Water Resources, 2013). Flood peaks are estimated for these recurrence intervals: 1.5, 2, 2.33, 5, 10, 25, 50, 100, 200, and 500 years (annual exceedance probabilities of 0.6667, 0.50, 0.4292, 0.20, 0.10, 0.04, 0.02, 0.01, 0.005, and 0.002, respectively).

**Table 3.1** Shield's parameter for different particle sizes (U.S. Department of Agriculture, 2008).

<i>Particle size classification</i>	<i>Particle size, D (mm)</i>	<i>Angle of repose, <math>\phi</math> (degrees)</i>	<i>Shield's parameter, <math>\tau^*</math></i>	<i>Critical shear stress, <math>\tau_c</math> (lb/ft<sup>2</sup>)</i>
<i>very large boulders</i>	<i>&gt; 2,048</i>	<i>42</i>	<i>0.054</i>	<i>37.37</i>
<i>large boulders</i>	<i>1,024-2,048</i>	<i>42</i>	<i>0.054</i>	<i>18.68</i>
<i>medium boulders</i>	<i>512-1,024</i>	<i>42</i>	<i>0.054</i>	<i>9.34</i>
<i>small boulders</i>	<i>256-512</i>	<i>42</i>	<i>0.054</i>	<i>4.67</i>
<i>large cobbles</i>	<i>128-256</i>	<i>42</i>	<i>0.054</i>	<i>2.34</i>
<i>small cobbles</i>	<i>64-128</i>	<i>41</i>	<i>0.052</i>	<i>1.13</i>
<i>very coarse gravels</i>	<i>32-64</i>	<i>40</i>	<i>0.050</i>	<i>0.54</i>
<i>coarse gravels</i>	<i>16-32</i>	<i>38</i>	<i>0.047</i>	<i>0.25</i>
<i>medium gravels</i>	<i>8-16</i>	<i>36</i>	<i>0.044</i>	<i>0.12</i>
<i>fine gravels</i>	<i>4-8</i>	<i>35</i>	<i>0.042</i>	<i>0.057</i>
<i>very fine gravels</i>	<i>2-4</i>	<i>33</i>	<i>0.039</i>	<i>0.026</i>

## RESULTS AND DISCUSSION

### Study Reach Morphology

**Longitudinal Profile.** Two longitudinal profiles were surveyed during the study period. The April 2012 longitudinal profile was 137 meters long while the March 2013 longitudinal profile was 183 meters. The 2013 profile was longer to include an additional riffle downstream. The channel survey on March 7, 2013 produced a reach slope, calculated using a trend line through all points (bridge elevation and scour immediately downstream of bridge not included in the trend line) of 0.0044, with a riffle-to-riffle slope, calculated using a trend line through only riffle points of 0.0032 (Figure 4.1). The riffle-to-riffle slope of 0.0032 was used in the hydraflow software and the boundary shear stress equation (Equation 1). Riffle-spacing between the three riffles in the study reach ranged from 55 m to 65 m. A comparison of the two longitudinal profiles shows that the 2012 longitudinal had deeper scour pools at tapeline distances of 35 m to 39.5 m and 97.5 m to 101 m (Figure 4.2). Additional bed deposition was observed at tapeline intervals 4.6 m to 20 m, 25.0 m to 34 m, 50 m to 98 m, and 118.7 m to 121 m (Figure 4.2). The deposition in the 2013 longitudinal profile in the lower portion of the channel reach accounts for the higher slope in the profile. However, some of the differences in longitudinal profiles may be due to human error or change in the location of the thalweg within the channel due to scour by floods (Appendix F). All in all, the longitudinal profile comparison shows both profiles being similar with minor differences between surveys.

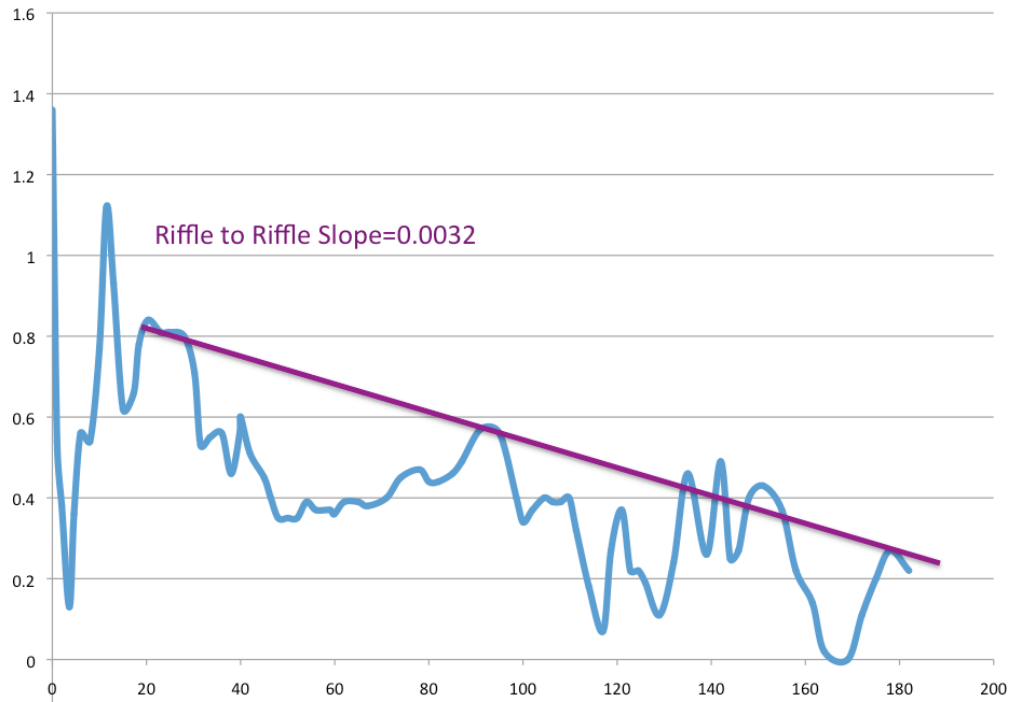


**Figure 4.1** Longitudinal profile taken on March 7, 2013.

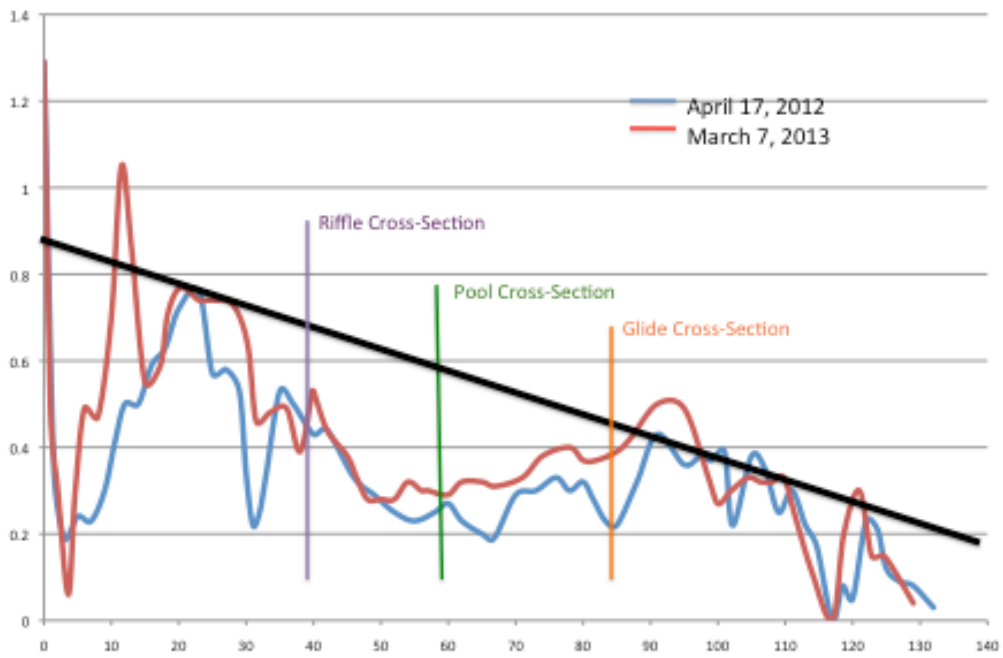


**Figure 4.2** Longitudinal profile comparison.

**Channel Cross-Sections.** Based on the April 17, 2012 longitudinal profile, the cross-section transect for the riffle was placed at 40 m, the pool cross-section at 60 m, and the glide cross-section at 85 m downstream from the bridge (Figure 3.7, 4.2). Using the hydraflow software at bankfull, and the 2013 riffle slope of 0.0032, the width, depth, wetted perimeter, hydraulic radius, area, velocity, and discharge was calculated for the riffle, glide, pool, and gage cross-sections (Table 4.1) (Appendix F).

When the right bank bankfull is aligned for all four cross-sections it is apparent that the riffle cross-section has the smallest area (Figure 4.3), and therefore a lower bankfull discharge is calculated since the same slope was used for all 3 cross-sections in the study reach (Table 4.1) (Appendix F). However, water surface slope becomes more uniform during higher flows as increased flow depth fills in bed topography (Table 4.1) (Allan and Castillo, 2007).

**Table 4.1** Hydraflow results for cross-sections at bankfull.

<b>Cross-Section</b>	<b>Survey Points Used</b>	<b>Width (m)</b>	<b>Mean Depth (m)</b>	<b>Wetted Perimeter (m)</b>	<b>Hydraulic Radius (m)</b>	<b>Area (m<sup>2</sup>)</b>	<b>Velocity (m/s)</b>	<b>Discharge (m<sup>3</sup>/s)</b>	<b>RI (years)</b>
Riffle (40 m)	15	7.82	0.95	8.73	0.71	6.25	1.27	7.97	1.07
Pool (60 m)	15	11.47	1.46	12.53	0.93	11.65	1.52	17.68	1.6
Glide (85 m)	20	11.03	1.4	11.81	0.83	9.85	1.41	13.91	1.35
Gage 7052120 (-80m)	14	9.21	1.9	10.9	0.94	11.55	1.66	19.12	1.8



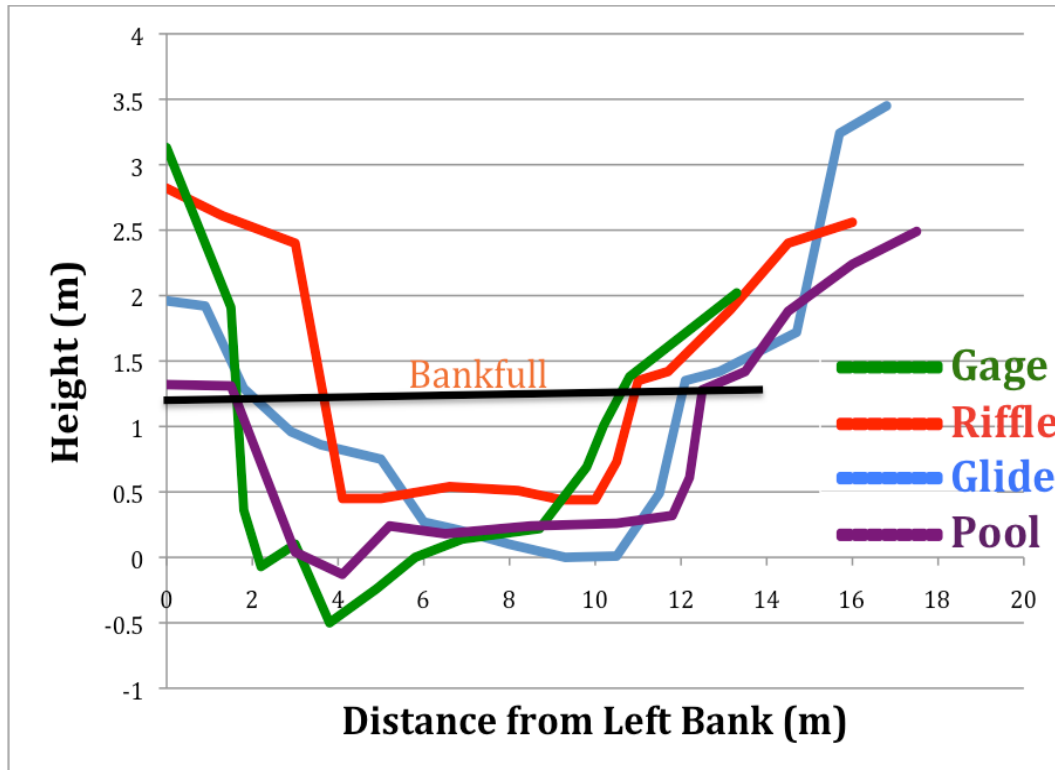


**Figure 4.3** Comparisons of Cross Sections.

**Channel Substrate.** Three hundred and fifty two pebbles were sized from the entire study reach (Figure 4.4), and 30 pebbles from each riffle, glide, and pool channel unit areas (Appendix G). Particle size distributions were determined for the reach and each channel unit for the  $D_{50}$ ,  $D_{75}$ ,  $D_{84}$ , and  $D_{90}$  were determined, excluding the bedrock and roots samples (Table 4.2, Figure 4.4, and Appendix G).

The general size of bed deposits was medium to coarse gravel, with <12% fines (<2 mm) and <10% cobble and boulder sizes (>90 mm). When comparing the results of the channel units (n=30) the overall size distributions are similar, medium to coarse gravel. However the riffle unit is slightly coarser (medium gravel) as expected given the higher bed slope. The glide and pool units consisted of fine to medium gravel.

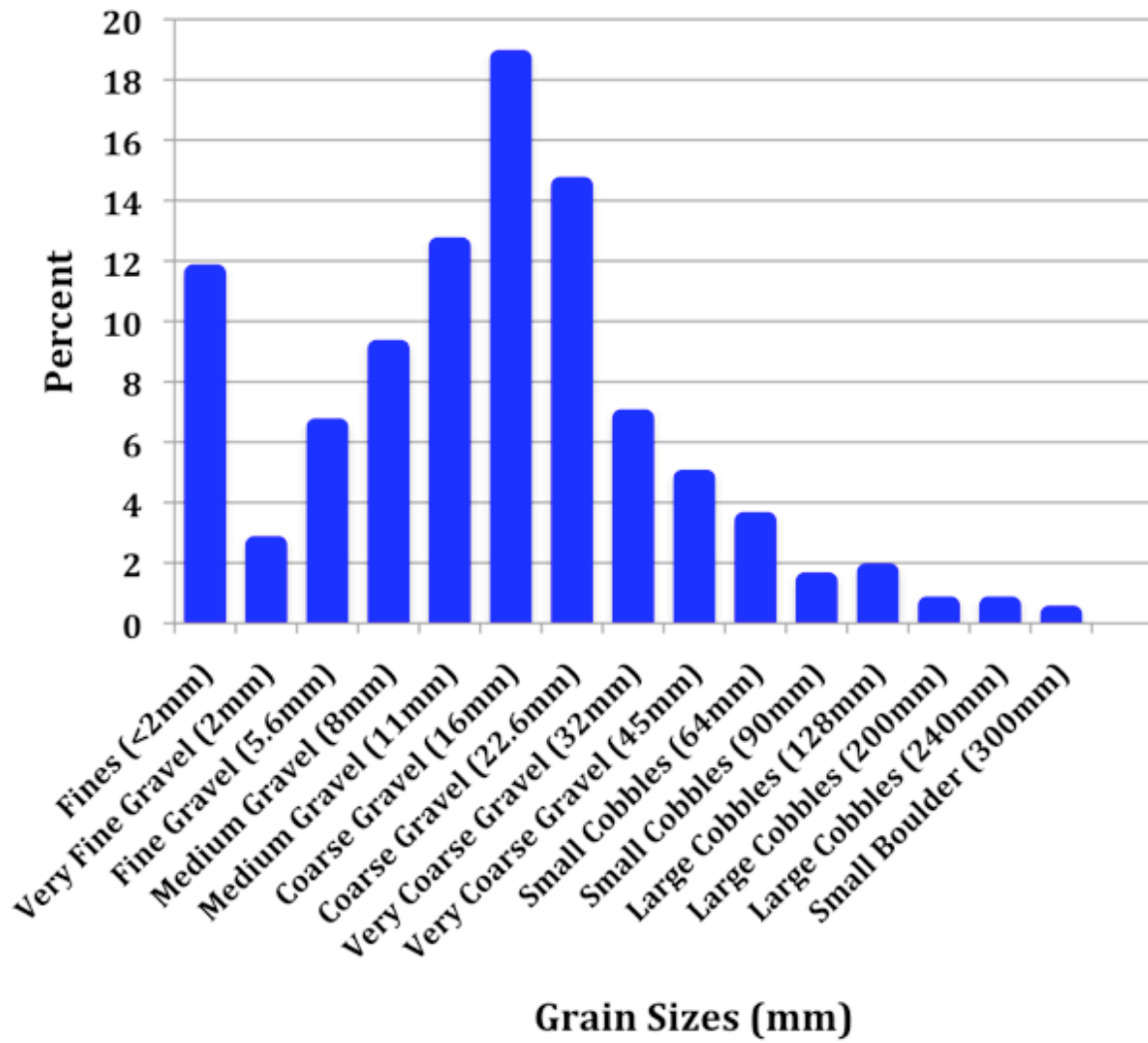


**Figure 4.4** Pebble count results for study reach (352 Pebbles).

**Table 4.2** Percentile size distribution (bedrock and roots excluded).

Percentile	Size (mm)	Size Description	Size (phi)
0	0	Fine Sands	2
10	<2 – 5.5	Very Fine to Fine Gravels	-1
16	5.6 – 7.9	Fine Gravels	-2.5
25	8 – 15.9	Medium Gravels	-3
50	16 – 22.5	Coarse Gravels	-4
75	22.6 – 31.9	Coarse Gravels	-4.5
84	32 – 44.9	Very Coarse Gravels	-5
90	45 – 63.9	Very Coarse Gravels	-5.5
95	64 – 199.9	Small to Large Cobbles	-6
100	200	Large Cobbles	-7.5

**Table 4.3** D<sub>50</sub>, D<sub>75</sub>, D<sub>84</sub>, and D<sub>90</sub> for cross-sections.

Cross-Section	Sample size (n)	50% (D <sub>50</sub> ) (mm)	75% (D <sub>75</sub> ) (mm)	84% (D <sub>84</sub> ) (mm)	90% (D <sub>90</sub> ) (mm)	Average of Max Sizes (mm)	Bedrock (%)	Fines <2mm (%)
Riffle (40m)	30	11	22.6	22.6	32	215 n=5	0	6.6
Pool (60m)	30	8	16	22.6	32	175 n=5	0	6.6
Glide (85m)	30	8	16	22.6	32	195 n=5	0	10
Entire Reach	352	16	22.6	32	45	165 n=42	4.3	11.6

**Particle Density and Shape.** Table 4.4 shows the average density for each pebble and for all pebble sizes combined and average shape. The lithology of the majority of particles is chert which has been reported to have a density of 2.52 g/cm<sup>3</sup> (odp.tamu.edu/publications/199\_IR/chap\_13/c13\_10.htm). In this study, particle density for the entire sample averaged 2.26 g/cm<sup>3</sup> (n=379). The density of chert bed material from this study reach is about 10% less than “pure” chert, probably due to weathering increasing pore and fracture space.

**Table 4.4** Average density and shape per pebble size.

<b>Pebble Size</b>	<b>Number of sizes Pebbles (n)</b>	<b>Shape Class</b>	<b>Average Density (g/cm<sup>3</sup>)</b>
16 mm	100	Sub-rounded 18% Sub-angular 59% Very angular 22%	2.29
22.6 mm	100	Sub-rounded 10% Sub-angular 78% Very angular 12%	2.17
32 mm	100	Sub-rounded 19% Sub-angular 75% Very angular 6%	2.29
45 mm	79	Sub-rounded 6% Sub-angular 85% Very angular 9%	2.30
All Pebble Sizes	379	Sub-rounded 14% Sub-angular 74% Very angular 12%	2.26

### **Channel Hydraulics and Sediment Mobility**

**Gage Site Analysis.** No stage data were collected within the study reach during flow events so flow data and hydraulic values were determined from the upstream gage site to calculate discharge within the study reach. In general, the study reach and gage site are similar in channel form (Figure 4.3 and Table 4.1). However, different tracer release points within the

study reach included different local conditions of slope, velocity, and sediment mobility. Three of the four variables, channel width, channel velocity, and stage have a good relationship with  $R^2$  values between 0.81 and 0.87, while the  $R^2$  for hydraulic radius is 0.64 (Figure 4.5 and 4.6). These hydraulic calibrations are used to determine flow characteristics for the study reach.

**Flood Events in the Study Reach.** The recurrence interval is the average return period, in years, for a flood of given magnitude. Using the annual peak discharge series, recurrence intervals for South Creek gage, with 15 years of record, were calculated using PeakFQ for each high flow or flood event sampled for this study (Figure 4.7). Figure 4.8 shows the relationship among stages for the different flow events sampled (Table 4.5)(Appendix H). Peak discharge for each event ranged from 2 to 43  $m^3/s$  and duration ranged form 7 to 15 hours for the events sampled in the study (Figure 4.9).

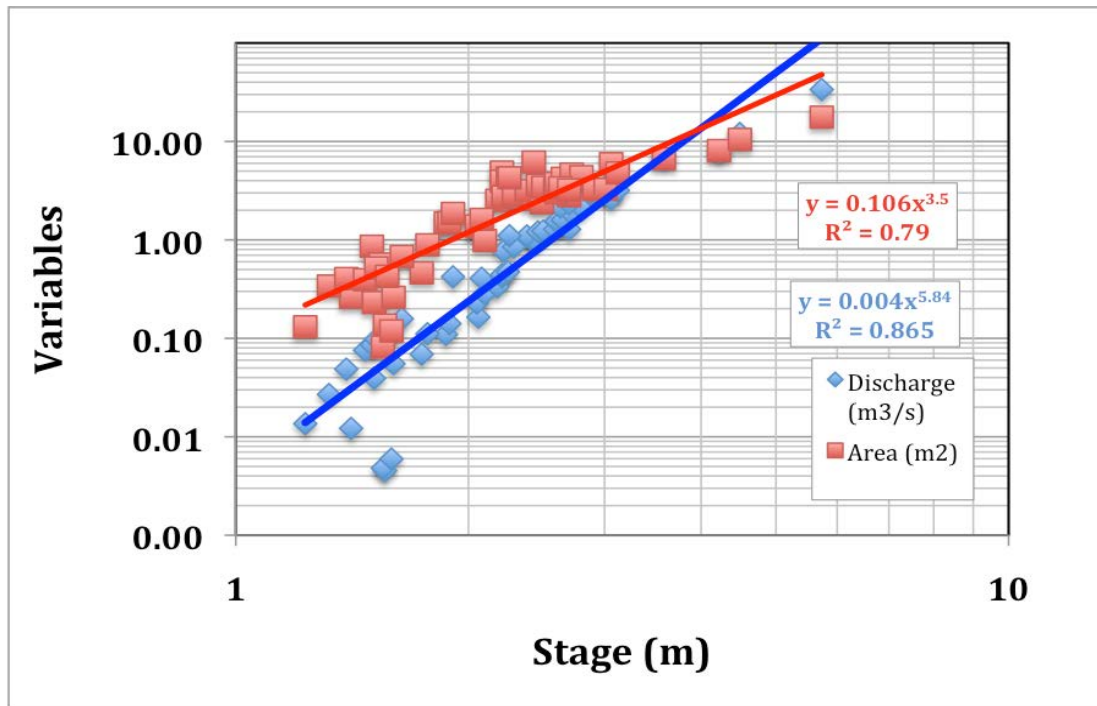


**Figure 4.5** Gage #07052120 rating curve for discharge and channel area.

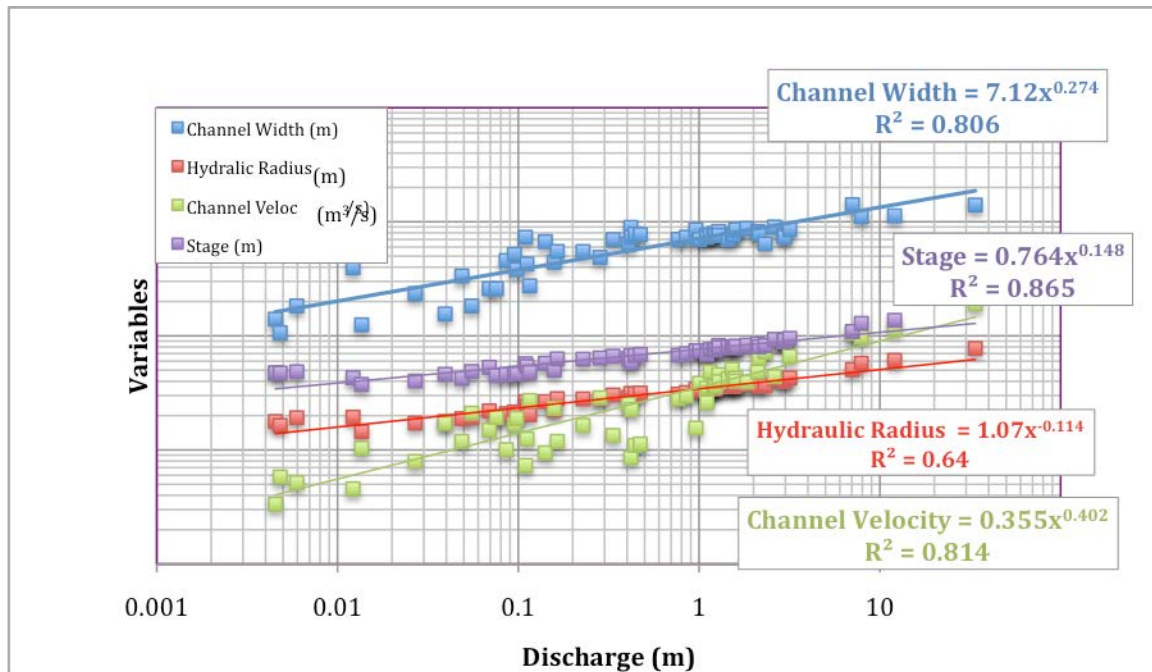


Figure 4.6 Hydraulic geometry relations at gage #07052120.

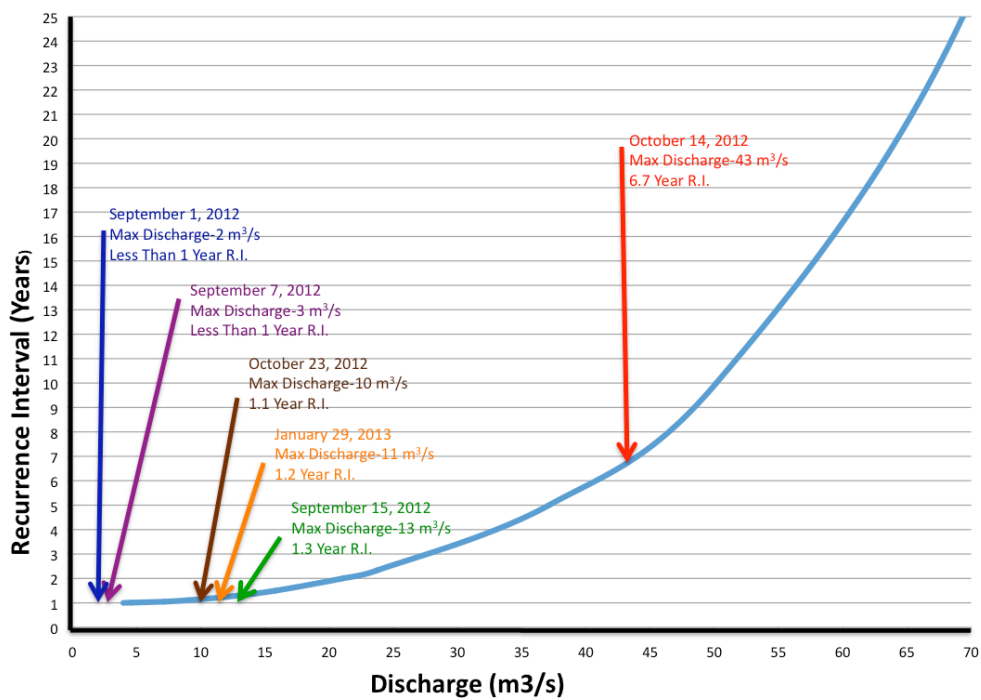
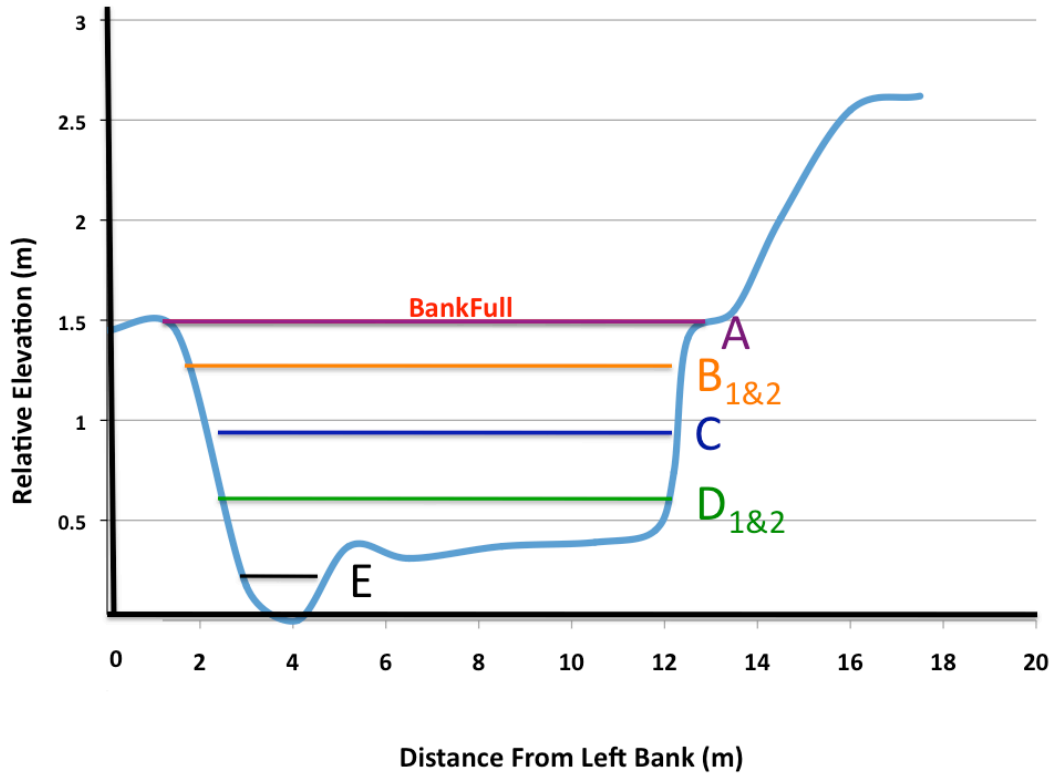


Figure 4.7 Flood-frequency curve.



**Figure 4.8** Flow events at pool cross-section (Letters correspond to flow events described in Table 4.5).

**Table 4.5** Dates and discharges of flow events at pool cross-section.

Letter Corresponding to Figure 4.9	Date	Peak Discharge (m <sup>3</sup> /s)	Shear Stress at Peak Discharge (N/m <sup>2</sup> )
A	October 14, 2012	43.1	4.3
B	September 15, 2012	12.5	2.5
B	January 29, 2013	10.5	2.3
C	October 23, 2012	9.5	2.2
D	September 7, 2012	2.5	1.1
D	September 1, 2012	2.1	0.9
E	January 11, 2013	0.05	0.1

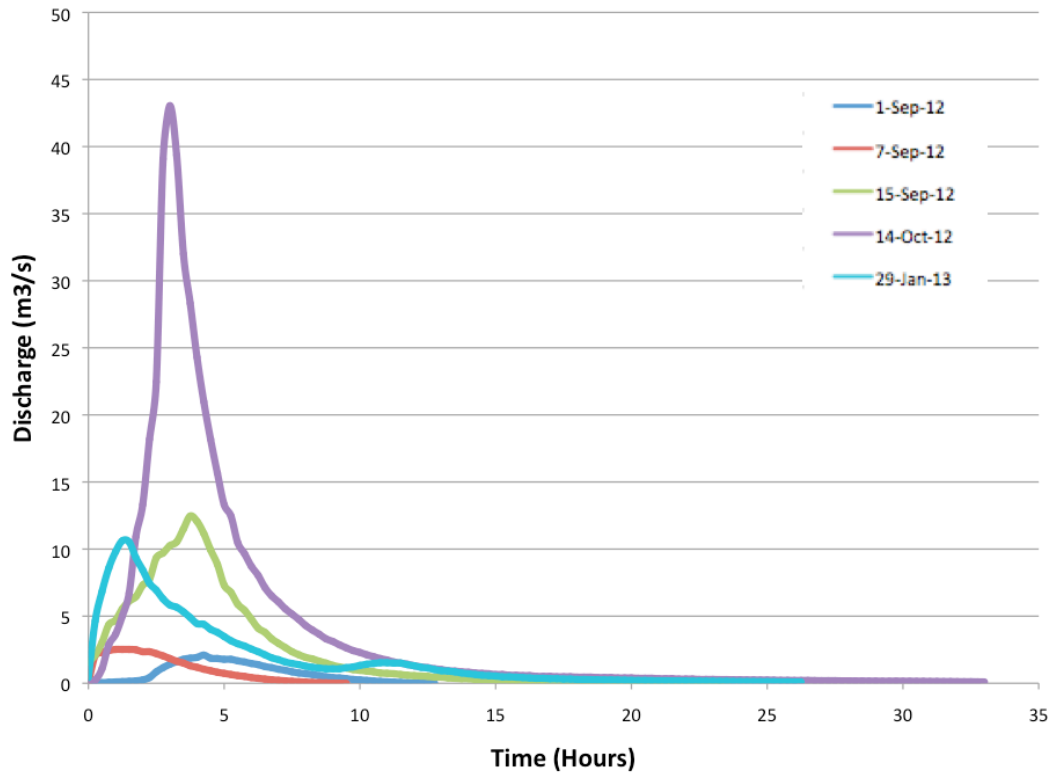


**Figure 4.9** Time in hours of individual events vs. discharge.

### Sediment Mobility

**Boundary Shear Stress.** The comparison of boundary shear stress between the three cross-sections shows that between depth of 0.25 m and 1.00 m the riffle and glide cross-sections have similar values while the pool's boundary shear stress is significantly lower (Table 4.6). As the stage increases to between 1.25 m and 1.5 m the boundary shear stress values of all three channel units become more similar in value. In contrast to pools, riffles have a higher slope, tend to be shallower, and have higher velocities than pools during low flows. The water surface slope becomes more uniform between riffles and pools at high flows. Pools remain deeper and velocities increase more in pools than in riffles, resulting in changes in the distribution of forces on the streambed. See appendix E for the calculated boundary shear stress for cross-sections and boundary shear stress vs. water depth and discharge.



**Table 4.6** Boundary shear stress ( $\text{N/m}^2$ ) at cross-sections vs. stage.

Stage (m)	Rifle Cross-Section	Pool Cross-Section	Glide Cross-Section
0.25	6.04	2.68	5.45
0.50	11.68	4.04	10.69
0.75	17.11	11.07	16.58
1.00	20.02	16.52	18.49
1.25	23.40	21.45	23.29
1.5	26.60	23.03	26.23

**Critical Shear Stress.** Critical shear stress was calculated (Equations 1 and 2) using the average density for a given grain size using the pool cross-section due to during high flows pools remain deeper and velocities increase more than the other cross-sections (Table 4.7). Critical shear stress values were evaluated by Hydraflow software to determine the corresponding critical discharge for each size tracer. The Wolman's equation (Equation 3) was used to calculate the diameter of pebble that will move at a certain discharge (Table 4.7). In theory at the pool cross-section, the October 14, September 15, January 23, and the October 23 events could mobilize the  $D_{50}$ ,  $D_{75}$ ,  $D_{84}$ , and  $D_{90}$ . The September 7 and September 1 flow events could mobilize the  $D_{50}$ ,  $D_{75}$ , and  $D_{84}$ , while the January 11 flow event with a peak discharge of 0.05 could not mobilize the  $D_{50}$ .

**Table 4.7** Critical shear stress and discharge for each grain size class.

Grain Size (mm)	Critical Shear Stress Using Average Density For Each Grain Size	Discharge At Critical Shear Stress For Average Density For Each Grain Size
16 mm- $D_{50}$	9.50 $\text{N/m}^2$	0.5 $\text{m}^3/\text{s}$
22.6 mm- $D_{75}$	9.55 $\text{N/m}^2$	0.85 $\text{m}^3/\text{s}$
32 mm- $D_{84}$	12.44 $\text{N/m}^2$	1.5 $\text{m}^3/\text{s}$
45 mm- $D_{90}$	13.89 $\text{N/m}^2$	2.75 $\text{m}^3/\text{s}$

## Tracer Experiments

**Sampled Flow Events.** Eight flow events were sampled between September 1, 2012 and January 11, 2013 (Figure 4.10). Peak discharge, recurrence interval, duration of flow, and duration of flow above critical discharge for each size tracer are shown in Table 4.8. For the eight flow events evaluated in this study the recurrence interval ranged from less than 1 year to 6.7 years (Figure 4.7). Only the October 14 event with a discharge of  $43.1 \text{ m}^3/\text{s}$  went above the bankfull. The January 11, 2013 event (peak discharge of  $0.05 \text{ m}^3/\text{s}$ ) did not move any tracers (A in Figure 4.10). The February 25, 2013 event was excluded from the study due to a large number of tracers being disturbed by humans (B in Figure 4.10). However, the few tracers that had not been moved by humans showed some movement (Appendix C)

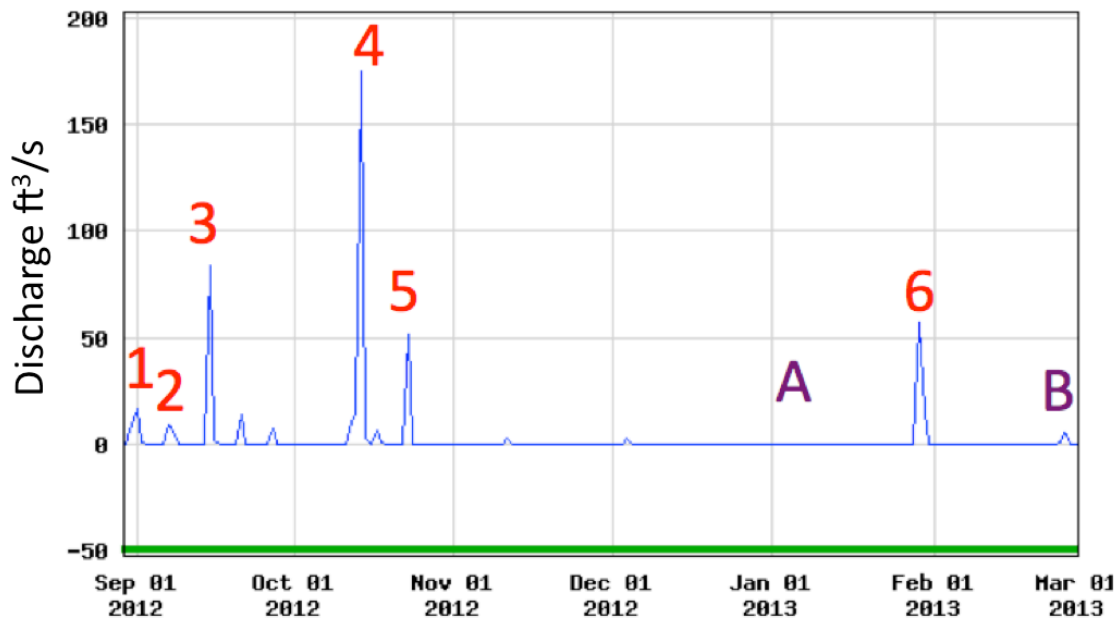


**Figure 4.10** Eight sampled flow events.

**Tracer and Transport Distances.** For each flow event, the number of tracers without movement, with movement, and not found (missing) at each deployment site were recorded and transport distances measured (Appendix D). Distance traveled was calculated by measuring how far a tracer had traveled from its original deployment location. The average distances traveled by size class per event were calculated by adding all the distances traveled by each tracer within each size class and then dividing by the total number of tracers within that size. Tracers that showed no movement were given a zero for distance traveled and were included in the total number of tracers. Missing tracers were not included in the total number. Using the duration of flow above critical discharge for each tracer size (Table 4.8) and the average distance traveled per tracer size per event (Appendix D), the average distance traveled per hour above critical discharge per size per event was calculated (Table 4.9).

**Event Transport Distances.** Results for the six flow events are summarized per event and include the peak discharge and flow duration per event, the calculated flow in hours and average distance traveled per hour above critical discharge for each tracer size (Table 4.8). The average and maximum distance for the entire flow event per tracer size and recovery rate are also reported (Table 4.9).

Event one had a peak discharge of  $2.1 \text{ m}^3/\text{s}$  and flow duration of 12.25 hrs. The  $D_{50}$  had flow above the calculated critical discharge of 6 hrs with an average distance traveled of 0.02 m/hr (Tables 4.8 and 4.9). The average distance traveled during the entire flow event was 0.1 m, the maximum distance traveled was 0.9 m, with a recovery rate of 96% (Appendix D). The  $D_{75}$  had flow above the calculated critical discharge of 5 hrs with an average distance traveled of 0.02 m/hr. The average distance traveled during the entire flow event was 0.1 m, the maximum distance traveled was 1.0 m, with a recovery rate of 100%. The  $D_{84}$  had flow above the

calculated critical discharge of 2.5 hrs with an average distance traveled of 0.04 m/hr. The average distance traveled for the entire flow event was 0.10 m, the maximum distance traveled was 0.8 m, with a recovery rate of 100% The  $D_{90}$  had no time above its critical discharge but seven tracers moved an average of 0.4 m during this event with a maximum distance of 1.0 m. These calculations include tracers with movement and tracers that showed no movement. The average distance traveled above critical shear stress for the  $D_{90}$  was not included in Table 4.9 due to movement of tracers when the calculated shear stress determined there should be no movement at the discharge recorded for flow.

Table 4.9 shows comparisons between average distance traveled, which include tracers that showed no movement and average distances, which did not include tracers with no movement. In comparing the average travel distances, travel distances tend to decrease with larger grain size. When the average distance traveled per hour above critical discharge was calculated the order reversed with the  $D_{84}$  traveled the farthest, then the  $D_{75}$ , and the  $D_{50}$ , again the  $D_{90}$  was not included in the calculation.

Event 2 had a peak discharge of  $2.5 \text{ m}^3/\text{s}$  and flow duration of 9.25 hrs. The  $D_{50}$  had flow above the calculated critical discharge of 5.5 hrs, with an average distance traveled of 0.03 m/hr. The average distance traveled during the entire flow event was 0.2 m, the maximum distance traveled was 1.3 m, with a recovery rate of 94%. The  $D_{75}$  had flow above the calculated critical discharge of 4.25 hrs with an average distance traveled of 0.03 m/hr. The average distance traveled during the entire flow event was 0.1 m, the maximum distance traveled was 0.9, with a recovery rate of 96%. The  $D_{84}$  had flow above the calculated critical discharge of 3.25 hrs with an average distance traveled of 0.04 m/hr. The average distance traveled for the entire flow event was 0.1 m, the maximum distance traveled was 1.3 m, with a recovery rate of 100% The  $D_{90}$

again had no time above it's critical discharge but seven tracers moved an average of 0.2 m during this event with a maximum distance of 1.0 m.

These calculations, excluding the average distance traveled for the D<sub>90</sub>, include tracers with movement and tracers that showed no movement. In comparing the average travel distances, travel distances tend to decrease with larger grain size. When the average distance

**Table 4.8** Magnitude, recurrence interval, and duration of flow events from USGS gage #07052120.

Number	Sampled Events Date	Flood Peak		Flow (Hours)	Duration Flow Above Critical Discharge (Hours)
		Discharge (m <sup>3</sup> /s)	Recurrence (Year)		
1	Sept 1, 2012	2.1	< 1	12.75	D <sub>50</sub> - 6 D <sub>75</sub> - 5 D <sub>84</sub> - 2.5 D <sub>90</sub> - 0
2	Sept 7, 2012	2.5	< 1	9.5	D <sub>50</sub> - 5.5 D <sub>75</sub> - 4.25 D <sub>84</sub> - 3.25 D <sub>90</sub> - 0
3	Sept 15, 2012	12.5	1.3	23.5	D <sub>50</sub> - 12.25 D <sub>75</sub> - 10.5 D <sub>84</sub> - 8.75 D <sub>90</sub> - 6.5
4	Oct 14, 2012	43.1	6.7	49.5	D <sub>50</sub> - 16.5 D <sub>75</sub> - 13.25 D <sub>84</sub> - 10.75 D <sub>90</sub> - 8.5
5	Oct 23, 2012	9.52	1.1	24.5	D <sub>50</sub> - 8.75 D <sub>75</sub> - 7.5 D <sub>84</sub> - 6.25 D <sub>90</sub> - 5
A	Jan 11, 2012	0.05	<1	1.25	No Movement
6	Jan 29, 2013	10.6	1.2	45.25	D <sub>50</sub> - 14.75 D <sub>75</sub> - 13.25 D <sub>84</sub> - 7 D <sub>90</sub> - 5.5
B	Feb 25, 2013	0.6	<1	23.25	Tracers Disturbed Some Movement

**Table 4.9** Tracer transport results. Red values indicate movement of tracers where according to the critical stress calculated, no movement should have occurred.

Event #	Grain Size (mm)	Number of Tracers Deployed	Percent Recovery	Duration of Flow Above Critical Discharge (hr)	Maximum Distance Traveled (m)	Maximum Distance Traveled per Hour Above Critical Discharge (m/hr)	Average Distance Traveled (m)	Average Distance Traveled per Hour Above Critical Discharge (m/hr)
1	16	28	96	6	0.9	0.2	0.1	0.02
	22.6	27	100	5	1.0	0.2	0.1	0.02
	32	27	100	2.5	0.8	0.3	0.1	0.04
	45	27	100	0	1.0		0.1	0.04
2	16	28	93	5.5	1.3	0.2	0.2	0.03
	22.6	27	96	4.25	0.9	0.2	0.1	0.03
	32	27	100	3.25	1.3	0.4	0.1	0.04
	45	27	100	0	1.0		0.1	0.04
3	16	27	78	12.25	4.0	0.3	1.0	0.1
	22.6	26	92	10.5	21.7	2.1	1.7	0.2
	32	27	100	8.75	7.7	0.9	0.1	0.1
	45	27	100	6.5	7.5	1.2	1.1	0.2
4	16	28	25	16.5	81.0	4.9	63.6	3.9
	22.6	30	20	13.25	82.6	6.2	42.8	3.2
	32	33	24	10.75	94.6	8.8	60.3	5.6
	45	33	49	8.5	108.6	12.8	35.1	4.1
5	16	7	86	8.75	9.8	1.1	1.7	0.2
	22.6	7	86	7.5	1.5	0.2	0.6	0.0
	32	8	75	6.25	14.2	2.3	2.8	0.4
	45	16	88	5	0.8	0.2	0.1	0.02
6	16	43	33	14.75	9.5	0.6	3.0	0.2
	22.6	40	55	13.25	25.0	1.9	3.7	0.2
	32	43	61	7	23.3	3.3	1.8	0.2
	45	48	75	5.5	7.1	1.3	1.4	0.2

traveled per hour above critical discharge was calculated the  $D_{50}$  traveled the farthest, then the  $D_{75}$ , and the  $D_{84}$ , again the  $D_{90}$  was not included in the calculation.

Event 3 had a peak discharge of  $12.5 \text{ m}^3/\text{s}$  and flow duration of 22.5 hrs. The  $D_{50}$  had flow above the calculated critical discharge of 12.25 hrs, with an average distance traveled of 0.01 m/hr. The average distance traveled during the entire flow event was 0.9 m, the maximum distance traveled was 4.0 m, with a recovery rate of 78%. The  $D_{75}$  had flow above the calculated critical discharge of 10.5 hours with an average distance traveled of 0.2 m/hr. The average distance traveled during the entire flow event was 1.7 m, the maximum distance traveled was 21.7 m, with a recovery rate of 82%. The  $D_{84}$  had flow above the calculated critical discharge of 8.75 hrs with an average distance traveled of 0.1 m/hr. The average distance traveled for the entire flow event was 1.2 m, the maximum distance traveled was 7.7 m, with a recovery rate of 100%. The  $D_{90}$  had flow above the calculated critical discharge of 6.5 hrs with an average distance traveled of 0.2 m/hr. The average distance traveled for the entire flow event was 1.2 m, the maximum distance traveled was 7.5 m, with a recovery rate of 100%. These calculations include tracers with movement and tracers that showed no movement.

In comparing the average travel distances, the  $D_{75}$  traveled the farthest distance, then the  $D_{90}$ ,  $D_{50}$ , and the  $D_{84}$ . When the average distance traveled per hour above critical discharge was calculated the  $D_{90}$  traveled the farthest, then the  $D_{75}$ ,  $D_{84}$ , and the  $D_{50}$ .

Event 4 had a peak discharge of  $43.1 \text{ m}^3/\text{s}$  and flow duration of 46.75 hrs. The  $D_{50}$  had flow above the calculated critical discharge of 16.5 hrs, with an average distance traveled of 3.9 m/hr. The average distance traveled during the entire flow event was 63.6 m, the maximum distance traveled was 81.0 m, with a recovery rate of 21%. The  $D_{75}$  had flow above the calculated critical discharge of 13.25 hrs with an average distance traveled of 3.2 m/hr. The

average distance traveled during the entire flow event was 42.8 m, the maximum distance traveled was 82.6 m, with a recovery rate of 19%. The  $D_{84}$  had flow above the calculated critical discharge of 10.75 hrs with an average distance traveled of 5.6 m/hrs. The average distance traveled for the entire flow event was 60.3 m, the maximum distance traveled was 94.6 m, with a recovery rate of 22%. The  $D_{90}$  had flow above the calculated critical discharge of 8.5 hrs with an average distance traveled of 4.1 m/hr. The average distance traveled for the entire flow event was 35.1 m, the maximum distance traveled was 108.6 m, with a recovery rate of 48%. These calculations include tracers with movement and tracers that showed no movement.

In comparing the average travel distances, the  $D_{75}$  traveled the farthest distance, then the  $D_{90}$ ,  $D_{50}$ , and the  $D_{84}$ . When the average distance traveled per hour above critical discharge was calculated the  $D_{84}$  traveled the farthest, then the  $D_{90}$ ,  $D_{50}$ , and the  $D_{75}$ .

Event 5 had a peak discharge of  $9.5 \text{ m}^3/\text{s}$  and flow duration of 10.25 hrs. The  $D_{50}$  had flow above the calculated critical discharge of 8.75 hrs, with an average distance traveled of 0.2 m/hr. The average distance traveled during the entire flow event was 1.7 m, the maximum distance traveled was 9.8 m, with a recovery rate of 86%. The  $D_{75}$  had flow above the calculated critical discharge of 7.5 hrs with an average distance traveled of 0.03 m/hr. The average distance traveled during the entire flow event was 0.2 m, the maximum distance traveled was 1.5 m, with a recovery rate of 100%. The  $D_{84}$  had flow above the calculated critical discharge of 6.25 hrs with an average distance traveled of 0.4 m/hr. The average distance traveled for the entire flow event was 2.2 m, the maximum distance traveled was 14.2 m, with a recovery rate of 75%. The  $D_{90}$  had flow above the calculated critical discharge of 5 hrs with an average distance traveled of 0.02 m/hr. The average distance traveled for the entire flow event was 0.1 m, the maximum distance traveled was 0.8 m, with a recovery rate of 87%. These calculations include tracers with



movement and tracers that showed no movement.

In comparing the average travel distances, the  $D_{75}$  traveled the farthest distance, then the  $D_{90}$ ,  $D_{50}$ , and the  $D_{84}$ . When the average distance traveled per hour above critical discharge was calculated the  $D_{84}$  traveled the farthest, then the  $D_{50}$ ,  $D_{75}$ , and the  $D_{90}$ .

Event 6 had a peak discharge of  $10.6 \text{ m}^3/\text{s}$  and flow duration of 31.75 hrs. The  $D_{50}$  had flow above the calculated critical discharge of 14.75 hrs, with an average distance traveled of 0.2 m/hr. The average distance traveled during the entire flow event was 3.0 m, the maximum distance traveled was 9.5 m, with a recovery rate of 33%. The  $D_{75}$  had flow above the calculated critical discharge of 13.25 hrs with an average distance traveled of 0.2 m/hr. The average distance traveled during the entire flow event was 2.5 m, the maximum distance traveled was 25.0 m, with a recovery rate of 56%. The  $D_{84}$  had flow above the calculated critical discharge of 7 hrs with an average distance traveled of 0.2 m/hr. The average distance traveled for the entire flow event was 1.7 m, the maximum distance traveled was 23.3 m, with a recovery rate of 59%. The  $D_{90}$  had flow above the calculated critical discharge of 5.5 hrs with an average distance traveled of 0.2 m/hr. The average distance traveled for the entire flow event was 1.1 m, the maximum distance traveled was 7.1 m, with a recovery rate of 74%. While this flow event only had a peak discharge of  $10.6 \text{ m}^3/\text{s}$  the low recovery rate could be due to the flow lasting 45.25 hrs. These calculations include tracers with movement and tracers that showed no movement.

In comparing the average travel distances, the  $D_{50}$  traveled the farthest distance, then the  $D_{75}$ ,  $D_{84}$ , and the  $D_{90}$ . When the average distance traveled per hour above critical discharge was calculated all four-grain sizes traveled a distance of 0.2 m/hr.

An event occurring on January 11, 2013 with a peak discharge of  $0.048 \text{ m}^3/\text{s}$  and flow duration of 1.25 hrs produced no movement. A flow event on February 25, 2013 with a peak

discharge of 0.6 m<sup>3</sup>/s and duration of 23.5 hrs showed some tracer movement but was not included in the calculations due to tracers being disturbed by humans.

**Average Travel Distance.** Transport distances were averaged two ways: for only tracers which showed movement, and all tracers recovered including those that showed no movement. As expected the average distance traveled where only tracers with movement were calculated was higher than averages calculated to include tracers with no movement (Table 4.10). The higher the maximum discharge, the higher the average distance traveled per hour above critical discharge. In two of the six events the D<sub>90</sub> traveled a larger average distance than the smaller tracers. This may have occurred because of the smaller tracers being buried, while the larger tracers are harder to bury and easier to see. The two events, which moved the largest tracer size the farthest average distance, October 14, 2012 and January 29, 2013, also had the longest duration of flow (Figure 4.9). During events 1 and 2 the D<sub>90</sub> showed movement when according to the critical shear stress calculated for the D<sub>90</sub>, no movement should have occurred (red in Table 4.10). This could be due to the slope used in calculating the shear stress. On several occasions tracers showed movement in the upstream direction. This could be occurring due to the initial “pulses” or first flush turbulences entering the study area in the upstream flow direction.

**Missing Tracers.** Recovery of tracers during less than bankfull events (RI of < 1 to 1.3 years) averaged between 56% to 99%, while the recovery rate of the one bankfull event (RI of 6.7 years) was 31%. Several tracers that were not recovered during events and later found within the study area suggests that tracers are more likely to become buried rather than traveling out of the study area. The distance traveled per hour for tracers found that were previously missing was calculated by taking the number of hours above critical discharge that had occurred since the

event the tracer went missing and dividing data by the distance the tracer had traveled from its last know site (Tables 4.11 thru 4.16).

**Table 4.10** Comparison of average distance traveled above critical discharge. Red values indicate movement of tracers where according to the critical stress calculated, no movement should have occurred.

Event	Grain Size (mm)	Flow above Critical Discharge (Hours)	Average Distance Traveled (m) Only Tracers w/Mvmt	Average Distance Traveled per Hour above Critical Discharge (m/H) Only Tracers w/Mvmt	Average Distance Traveled (m) Tracers w/Mvmt & w/o Mvmt	Average Distance Traveled per Hour above Critical Discharge (m/H) Tracers w/Mvmt & w/o Mvmt
1	16	6	0.4	0.1	0.1	0.02
	22.6	5	0.4	0.7	0.1	0.02
	32	2.5	0.4	0.2	0.1	0.04
	45	0	0.4		0.1	
2	16	5.5	0.4	0.1	0.2	0.03
	22.6	4.25	0.4	1.0	0.1	0.03
	32	3.25	0.4	0.1	0.1	0.04
	45	0	0.2		0.1	
3	16	12.25	1.2	0.1	0.9	0.1
	22.6	10.5	2.2	0.2	1.7	0.2
	32	8.75	2.3	0.3	1.2	0.1
	45	6.5	2.3	0.4	1.2	0.2
4	16	16.5	63.6	3.9	13.1	3.9
	22.6	13.25	42.8	3.2	8.3	3.2
	32	10.75	60.3	5.6	14.6	5.6
	45	8.5	35.1	4.1	17	4.1
5	16	8.75	3.4	0.4	1.7	0.2
	22.6	7.5	0.4	.0	0.2	0.03
	32	6.25	2.9	0.5	2.2	0.4
	45	5	0.2	0.0	0.1	0.02
6	16	14.75	3.8	0.3	3.0	0.2
	22.6	13.25	3.4	0.3	2.5	0.2
	32	7	2.0	0.3	1.7	0.2
	45	5.5	1.6	0.3	1.1	0.2

**Table 4.11** Missing/found tracers for event #1 September 1, 2012.

Grain Size	Number of New Tracers Missing	Number of Tracers still Missing	Number of Missing Tracers Found	Hours above Critical Discharge (hr)	Distance Tracers Traveled (m)	Average Distance Traveled per tracer per Hour (m/hr)
16 mm	1	0	0			
22.6 mm	0	0	0			
32 mm	0	0	0			
45 mm	0	0	0			

**Table 4.12** Missing/found tracers for event #2 September 7, 2012.

Grain Size	Number of New Tracers Missing	Number of Tracers still Missing	Number of Missing Tracers Found	Hours above Critical Discharge (hr)	Distance Tracers Traveled (m)	Average Distance Traveled per tracer per Hour (m/hr)
16 mm	1	1	0			
22.6 mm	1	0	0			
32 mm	0	0	0			
45 mm	0	0	0			

**Table 4.13** Missing/found tracers for event #3 September 15, 2012.

Grain Size	Number of New Tracers Missing	Number of Tracers still Missing	Number of Missing Tracers Found	Hours above Critical Discharge (hr)	Distance Tracers Traveled (m)	Average Distance Traveled per tracer per Hour (m/hr)
16 mm	5	1	1	17.8	5.1	0.29
22.6 mm	2	0	1	14.8	3.1	0.21
32 mm	0	0	0			
45 mm	0	0	0			

**Table 4.14** Missing/found tracers for event #4 October 14, 2012.

Grain Size	Number of New Tracers Missing	Number of Tracers still Missing	Number of Missing Tracers Found	Hours above Critical Discharge (hr)	Distance Tracers Traveled (m)	Average Distance Traveled per tracer per Hour (m/hr)
16 mm	21	6	0			
22.6 mm	24	1	1	23.8	41.8	1.76
32 mm	25	0	0			
45 mm	17	0	0			

**Table 4.15** Missing/found tracers for event #5 October 23, 2012.

Grain Size	Number of New Tracers Missing	Number of Tracers still Missing	Number of Missing Tracers Found	Hours above Critical Discharge (hr)	Distance Tracers Traveled (m)	Average Distance Traveled per tracer per Hour (m/hr)
16 mm	1	26	1	25.3	62.4	2.47
22.6 mm	1	26	0			
32 mm	2	23	2	34	63.7	1.87
45 mm	2	17	0			

**Table 4.16** Missing/found tracers for event #6 January 29, 2013.

Grain Size	Number of Tracers Lost	Number of Tracers still Missing	Number of Missing Tracers Found	Hours above Critical Discharge (H)	Distance Tracers Traveled	Average Distance Traveled per tracer per Hour (m/H)
16 mm	29	25	2	63.5	34.1	0.54
22.6 mm	18	23	4	122.8	188.2	1.53
32 mm	18	22	3	72	110.7	1.54
45 mm	11	15	4	67.5	225.4	3.34

**Effect of Channel Location on Transport.** Using initial movement of tracers within the three channel locations (pool, glide, and riffle) and deployment points (left, center, and right) the percentage of initial movement could be compared (Tables 4.17 through 4.21). For this study, initial movement is defined as the first time a tracer moves from deployment site. From the four flow events (excluding the bankfull event where all areas had 100% movement), the riffle cross-section had the largest initial tracer movement in the September 1 and September 7 flow events. These two events both had a recurrence interval of less than one year. The pool cross-section had the largest initial tracer movement in the September 15 and January 29 flow events; these two events had a recurrence interval of 1.3 and 1.2 years.

The center deployment points within each cross-section had the largest percent (53%) of initial tracer movement, with the right sites in all but one flow event having the lowest initial

tracer movement (35%) and the left having 40% (except during the September 15, 2012 event) (Table 4.17 to 4.21). No initial tracer movements was calculated for the October 23 event due to all tracers moving off of the deployment sites during the bankfull flow event previous to the October 23 event and no new tracers being deployed.

In flow events with a recurrence interval over one year, initial movement does not consistently favor one cross-section or deployment point within each cross-section a tracer is placed over another. A tracer is more likely to show movement from a center deployment point during events with a recurrence interval less than one year (Tables 4.17 to 4.21).

**Table 4.17** Initial movement at cross-sections for September 1, 2012 event, RI <1.

	Left Deployment Point (L)	Center Deployment Point (C)	Right Deployment Point (R)	Cross-Section Tracer Movement Totals
Riffle (40 m)	25%	100%	8%	<b>44%</b>
Pool (60 m)	8%	33%	15%	<b>19%</b>
Glide (85 m)	0%	100%	0%	<b>33%</b>
L/C/R Tracer Movement Totals	<b>11%</b>	<b>78%</b>	<b>8%</b>	

**Table 4.18** Initial movement at cross-sections for September 7, 2012 event, RI <1.

	Left Deployment Point (L)	Center Deployment Point (C)	Right Deployment Point (R)	Cross-Section Tracer Movement Totals
Riffle (40 m)	33%	0%	9%	<b>14%</b>
Pool (60 m)	18%	25%	0%	<b>14%</b>
Glide (85 m)	0%	0%	8%	<b>3%</b>
L/C/R Tracer Movement Totals	<b>17%</b>	<b>8%</b>	<b>6%</b>	

**Table 4.19** Initial movement at cross-sections for September 15, 2012 event, RI 1.3.

	Left Deployment Point (L)	Center Deployment Point (C)	Right Deployment Point (R)	Cross-Section Tracer Movement Totals
Riffle (40 m)	50%	0%	30%	<b>27%</b>
Pool (60 m)	33%	100%	55%	<b>63%</b>
Glide (85 m)	42%	0%	64%	<b>35%</b>
L/C/R Tracer Movement Totals	<b>42%</b>	<b>33%</b>	<b>50%</b>	

**Table 4.20** Initial movement at cross-sections for October 14, 2012 event, RI 6.7.

	Left Deployment Point (L)	Center Deployment Point (C)	Right Deployment Point (R)	Cross-Section Tracer Movement Totals
Riffle (40 m)	100%	100%	100%	<b>100%</b>
Pool (60 m)	100%	100%	100%	<b>100%</b>
Glide (85 m)	100%	100%	100%	<b>100%</b>
L/C/R Tracer Movement Totals	<b>100%</b>	<b>100%</b>	<b>100%</b>	

**Table 4.21** Initial movement at cross-sections for January 29, 2013 event, RI 1.2.

	Left Deployment Point (L)	Center Deployment Point (C)	Right Deployment Point (R)	Cross-Section Tracer Movement Totals
Riffle (40 m)	82%	100%	100%	<b>94%</b>
Pool (60 m)	91%	96%	100%	<b>96%</b>
Glide (85 m)	100%	83%	25%	<b>69%</b>
L/C/R Tracer Movement Totals	<b>91%</b>	<b>93%</b>	<b>75%</b>	

**Tracer Transport at Discharges Above Bankfull.** Only one above-bankfull flow event occurred during the study period which was event 4 on October 14, 2012. During this event all tracer sizes traveled a longer average distance per hour above critical discharge than during less than bankfull events (Table 4.22, Figure 4.11 and 4.12). The D<sub>90</sub> traveled the farthest of all the tracers sizes during the bankfull event, followed by the D<sub>84</sub>, D<sub>75</sub> and D<sub>50</sub> (Figure 4.12). This

could be due to the larger tracers sizes having more surface area for the water to push against, and too large to hide in boundary layer. The largest average distance traveled during bankfull was by the D<sub>50</sub>, then the D<sub>84</sub>, D<sub>75</sub>, and D<sub>90</sub>. Maximum distance traveled for all sizes was higher during the bankfull event (Table 4.23, Figure 4.13 and 4.14). Recovery rates were much lower during the bankfull event, making accurate data collection difficult (Table 4.24, Figure 4.15). Low recovery rates of tracers make it difficult to calculate true transport distances. Tracers that showed no movement during flow events where other tracers of the same size did show movement also make calculating true transport distances difficult. One factor may be when placing tracers on the deployment sites some tracers may have been covered by others and only the top tracers were able to move when the flow duration was less than 30 hours. All three channel units and deployment sites within the channel units showed 100 percent initial movement during the bankfull event. Less than bankfull events had a much lower percentage of initial movement with the channel units and deployment sites (Table 4.25 and 4.26).

**Annual Transport Distances.** Using the information available through the USGS water data site, the percent flow exceedance for critical shear stress values correlating to the four tracer sizes were calculated for the study period of October 1, 2011 thru May 21, 2013 totaling 598 days or 14,352 hr with 1,616.5 hr (67.4 days) of discharge or storm runoff recorded (11% of the time).

Flow exceedance was found by calculating the discharge, which equaled or exceeded the critical shear stress for each grain size using the 14,352 hours within the study period. Flow exceedance calculated for each tracer size during the entire study period is as follows: 16 mm is



**Table 4.22** Comparison of distance traveled between events with a R.I. of >1 to 1.3 years and a bankfull event with a R.I. of 6.7 years.

Grain Size (mm)	Average Distance Traveled (m) Only Tracers w/Mvmt in Events With a R.I. of < 1 - 1.3 (years)	Average Distance Traveled (m) Only Tracers w/Mvmt in Bankfull Event (R.I. of 6.7 years)	Average Distance Traveled per Hour above Critical Discharge (m/H) Only Tracers w/Mvmt in Events With a R.I. of < 1 - 1.3 (years)	Average Distance Traveled per Hour above Critical Discharge (m/H) Only Tracers w/Mvmt in Bankfull Event (R.I. of 6.7 years)
16	1.8	63.6	0.2	3.9
22.6	1.4	42.8	0.5	3.2
32	1.6	60.3	0.3	5.6
45	0.9	35.1	0.3	4.1

**Table 4.23** Comparison of maximum distance traveled between an event with a R.I. of >1 to 1.3 years and a bankfull event with a R.I. of 6.7 years.

Grain Size (mm)	Maximum Distance Traveled (m) in an Event With a R.I. of < 1 - 1.3 (years)	Maximum Distance Traveled (m) for Bankfull Event (R.I. of 6.7 years)
16	9.77	81
22.6	22.02	82.58
32	23.25	94.6
45	7.5	108.55

**Table 4.24** Comparison of recovery rate between events with a R.I. of >1 to 1.3 years and a bankfull event with a R.I. of 6.7 years.

Grain Size (mm)	Recovery Rate (%) in Events With a R.I. of < 1 - 1.3 (years)	Recovery Rate (%) for Bankfull Event (R.I. of 6.7 years)
16	77.2	25
22.6	85.8	20
32	87.2	24
45	92.6	49

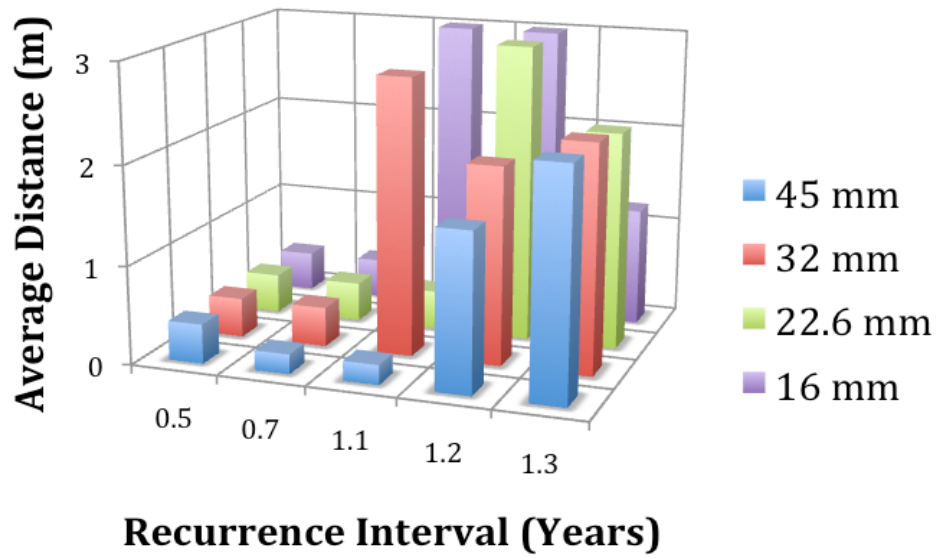


**Figure 4.11** Average travel distance vs recurrence interval (Recurrence intervals of 0.5-1.3 years).

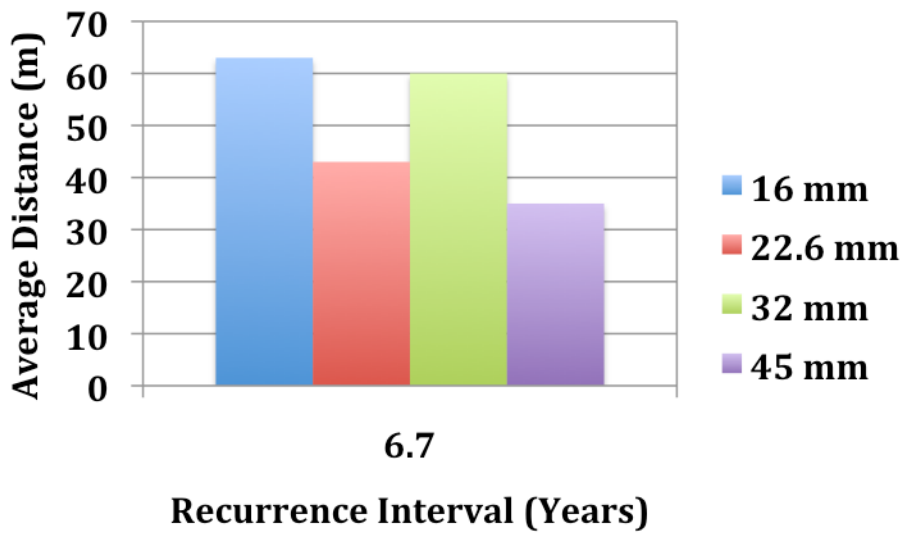


**Figure 4.12** Average travel distance vs recurrence interval (Recurrence interval of 6.7 years only).

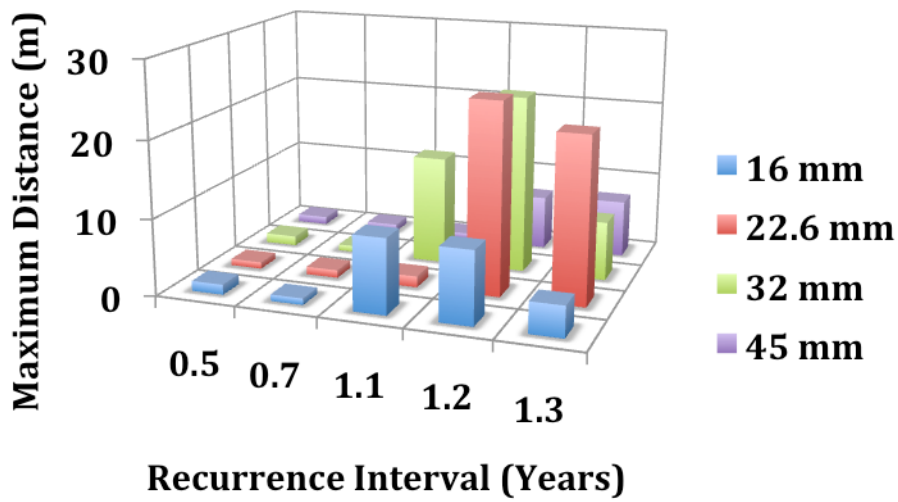


**Figure 4.13** Maximum distance traveled vs recurrence interval (Recurrence intervals of 0.5-1.3 years).

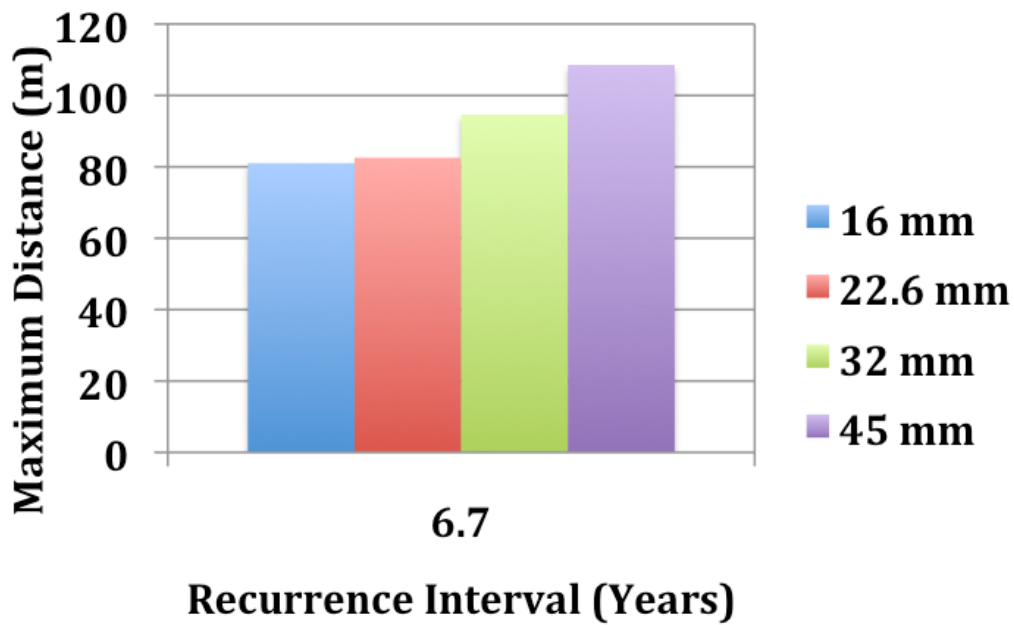


**Figure 4.14** Maximum distance traveled vs recurrence interval (Recurrence interval of 6.7 years only).

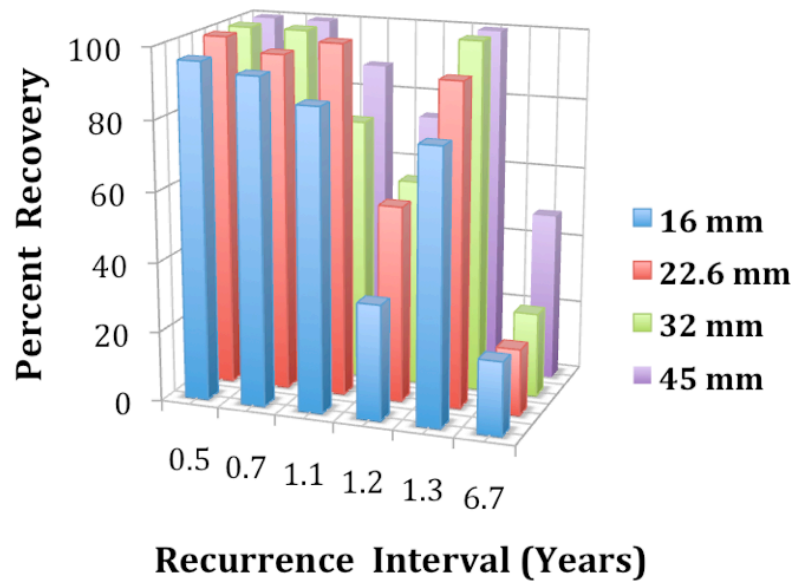


**Figure 4.15** Average percent recovered vs recurrence interval.

**Table 4.25** Comparison of initial movement within channel units between events with a R.I. of >1 to 1.3 years and a bankfull event with a R.I. of 6.7 years.

	Average Initial Movement (%) in Events With a R.I. of < 1 - 1.3 (years)	Initial Movement (%) in Bankfull Event (R.I. of 6.7 years)
Riffle	45	100
Pool	48	100
Glide	35	100

**Table 4.26** Comparison of initial movement within deployment sites between events with a R.I. of >1 to 1.3 years and a bankfull event with a R.I. of 6.7 years.

	Average Initial Movement (%) in Events With a R.I. of < 1 - 1.3 (years)	Initial Movement (%) in Bankfull Event (R.I. of 6.7 years)
Left	40	100
Center	53	100
Right	35	100

2.8%, 22.6 mm 1.9%, 32 mm 1.0%, and 45 mm 0.4%. During discharge (run off) periods, using only the 1,616.5 hours, discharge equaled or exceeded the critical shear stress 25.1% of the time for 16 mm, 17.2% for 22.6 mm, 8.8% for 32 mm, and 4.0% for 45 mm (Table 4.27).

The study period was then converted to one year 365 day (8760 hours). Multiplying the 8760 hr by the 11.3% water discharge, the hours of discharge during one year was calculated to be 980 hr. To calculate the time (hrs) each tracer size was above its critical shear stress for a one year period, flow exceedance for each tracer found using the 1,616.5 of discharge time was multiplied by the 980 hr of water discharge calculated for one year. Flow time for each tracer size is as follows: 16 mm is 246 hr (10.4 days), 22.6 mm is 169 hr (7.0 days), 32 mm is 86 hr (3.6 days), and 45 mm is 39 hr (1.6 days).

Using all six flow events, both the average distance traveled per hour above critical discharge and the maximum distance traveled per grain size above critical discharge (Table 4.9 and 4.10) were averaged (Table 4.27). These two averages did not include tracers with no movement. These final averages were then multiplied by the hours above critical shear stress for each tracer size for one year to calculate the average, and maximum distance each grain size would travel during a one year period with 11.3% runoff conditions (Table 4.28).

**Table 4.27** Average/Maximum distance traveled above critical shear stress.

<b>Tracer Size (mm)</b>	<b>Average Distance Traveled above Critical Shear Stress (m/hr)</b>	<b>Maximum Distance Traveled above Critical Shear Stress (m/hr)</b>
16	0.82	1.2
22.6	0.9	1.8
32	1.25	2.7
45	1.2	3.9

The 16 mm (D<sub>50</sub>) tracers were found to travel an average of 202 m/year with the longest distance observed at 295 m/year, 22.6 mm (D<sub>75</sub>) tracers traveled an average of 152 m/year with the longest distance possible at 304 m/year, 32 mm (D<sub>84</sub>) tracers traveled an average of 107.5 m/year with the longest distance possible at 232 m/year, and 45 mm (D<sub>90</sub>) tracers were found to travel an average distance of 46.8 m/year with the longest distance possible at 152.1 m/year (Table 4.28).

These averages did not take into consideration the tracers that went missing and were never recovered. Some, but not all missing tracers reappeared after a later flow event farther down stream, which indicates movement from deployment sites. Tracers found that had previously been missing were not included into the distances traveled, so it can be assumed that the average distance would increase if more time and effort was put into finding and tracking tracers over time.

**Table 4.28** Tracer transport in a year with 11.3% run off.

Grain Size (mm)	Total Time Above Critical Discharge (hr)	Time Above Critical Discharge During Runoff (%)	Average Distance Grain Size Would Travel A Year (m)	Longest Distance Grain Size Would Travel A Year (m)
16	246	25.1	202	295
22.6	169	17.2	152	306
32	86	8.8	107.5	232
45	39	4.0	46.8	152.1

## CONCLUSIONS

The purpose of this study was to: (i) determine downstream transport distances of painted tracers of different sizes over a range of flow conditions; (ii) evaluate the influence of channel morphology and thalweg location on transport; and (iii) compare field results to those predicted by mobility equations to understand travel time of gravel leading to a better understanding of bed load transport dynamics and gravel source/supply implications. The year 2013 was Missouri's 10<sup>th</sup> driest year in history, making rain and flow events few and far between. Nevertheless, this tracer study provided evidence that bed load material greater than median diameter is mobilized by most in-channel high flows or flood events with recurrence intervals greater than one year in South Creek. The following conclusions are based on the results of the release of 272 tracers in four sizes, deployed at nine locations in the channel per event, and during seven flow events over a seven-month period.

The larger the discharge and the longer the flow duration the farther the tracers traveled (Vazquez-Tarrio and Menendez-Duarte, 2014, Rainato *et al*, 2018). Transport distances for particles of a given size increase exponentially with increase shear stress (Hill, *et al*, 2010). In two of the six events the D<sub>90</sub> (largest size evaluated) traveled a longer average distance than the smaller tracers, a phenomenon termed reverse mobility (Hill *et al*, 2010). The overall average rate of transport above critical shear stress was 1.2 m/hr for the largest tracer (D<sub>90</sub>) and decreased to 0.82 m/hr for the smallest tracer (D<sub>50</sub>) (Table 4.27). Distance traveled for all four tracer sizes increased for events with a recurrence interval greater than one year (Table 4.22, Figure 4.12).

Tracer movement did not show dependence on channel unit or cross-bed location for high flows near and above bank-full stage with recurrence intervals greater than one year (Vazquez-Tarrio and Menendez-Duarte, 2014). However, in this study, a tracer was more likely to initiate

movement from a riffle and center (i.e., thalweg) deployment sites for in-channel flows with peak discharge recurrence intervals less than one year (Tables 4.17 & 4.21).

Recovery rates for tracer experiments are typically low (Hassan *et al*, 1984, Hassan and Church, 1992, and Vazquez-Tarrio and Menendez-Duarte, 2014). Recovery of tracers during less than bankfull events (RI of < 1 to 1.3 years) was 83%, while the recovery rate of the one bankfull event (RI of 6.7 years) was 31% (Figure 4.13). Several tracers (7% of total deployed) were not recovered during sampling events, but were later found exposed on the bed within the study area. This finding suggests that burial processes and residence times may affect bed-load transport rates even in flashy urban channels with scoured beds and only a thin mantle of sediment over bedrock .

Annual travel distances were calculated based on size-distance relationships and flow duration above critical shear stress. Runoff only occurred in South Creek at 11.3% of the time or about 41 days. As expected, the smaller the tracer size, the longer distance it traveled. The exception, for the longest distance traveled in a year, the 22.6 mm tracer was calculated to travel 11 meters longer than the 16 mm. The average distance traveled per year for tracers of given size was: 202 m for the 16 mm ( $D_{50}$ ); 152 m for the 22.6 mm ( $D_{75}$ ); 108 m for the 32 mm ( $D_{84}$ ); and 49 m for the 45 mm ( $D_{90}$ ) (Table 28). The longest distance traveled was: 295 m for the 16 mm ( $D_{50}$ ); 306 m for the 22.6 mm ( $D_{75}$ ); 232 m for the 32 mm ( $D_{84}$ ); and 152 m for the 45 mm ( $D_{90}$ ) (Table 28).

Bed mobility and transport characteristics influence thresholds of channel instability, patterns of sediment storage in channels, and recovery rates for disturbed river systems. Future studies on gravel transport in South Creek or other Ozark streams could be advanced with the use of radioactive, inserted magnets, or radio transmitter tracers to be able to locate buried tracers



(Vazques-Tarrio *et al*, 2019). The use of a Global Positioning System or Drone (UAV) technology could improve the accuracy of tracer movement measurements and related channel bedform interactions. Video documentation of first flush turbulence within during flow events would further an understanding of how turbulent water moves through an unsaturated channel at different discharges, sometimes with the result of upstream gravel displacement as observed several times in this study. Overall, the bed sediment transport distances described here can improve our understanding about how gravel bed streams in the Ozarks have responded to historical land disturbances and may respond to hydrological effects due to urbanization and climate change in the future.

## LITERATURE CITED

- Allan JD, Castillo MM. 2007. Chapter 2 and 3. In *Stream Ecology: Structures and function of running waters* 2<sup>nd</sup> ed. Springer, the Netherlands: 35-39.
- Bunte K, Ergenzinger P. 1989. New Tracer Techniques for Particles in Gravel Bed Rivers. *Bulletin de la Societe Geographique de Liege*. 85-90.
- Bunte K, Macdonald LH. 1995. Detecting change in sediment loads: where and how is it possible?. *Department of Earth Resources* **226**: 253-261.
- Carling PA, Orr HG. 2000. Morphology Of Riffle-Pool Sequences In The River Severn, England. *Earth Surface Processes and Landforms* **25**: 369-384.
- Charlton R. 2008. Chapter 7. In *Fundamentals of fluvial geomorphology* 1<sup>st</sup> ed. Routledge, New York: 103-104.
- Church M, Hassan MA. 1992. Size and distance of travel of unconstrained clasts on a streambed. *Water Resource Res* **28**: 299-303.
- Einstein HA. 1937. Bedload transport as a probability problem. *Sedimentation* **1972**: C.1-C.105.
- Emmett WW. 1981. Measurement of bed load in rivers. *IAHA Publication* **133**: 3-15.
- Hassan MA, Bradley DN. 2017. Geomorphic controls on tracer particle dispersion in gravel bed rivers. In *Gravel-Bed Rivers, Processes and Disasters*, Tsutsumi D, Laronne JB (ed): Wiley-Blackwell, UK: 439-466,
- Hassan MA, Church M, Ashworth PJ. 1992. Virtual rate and mean distance of travel of individual clasts in gravel-bed channels. *Earth Surface Processes and Landforms* **17**: 617-627.
- Hassan MA, Schick A, Laronne J. 1984. The recovery of flood-dispersed coarse sediment particles. *Catena Supplement* **5**: 153-162.
- Hassan MA, Ergenzinger P. 2003. Use of Tracers in Fluvial Geomorphology, In *Tools in fluvial geomorphology*, Kondaf GM, Piegay H. John Wiley and Sons Ltd (ed), South Gate Chichester, England: 397-423.
- Hill KM, DellAngelo L, Meerschaert MM. 2010. Heavy-tailed travel distance in gravel bed transport: An exploratory enquiry. *Journal of Geophysical Research* **115**: 1-13
- Intelisolve. 2013. ([Guideforums.autodesk.com/t5/civil-3d-forum/intelisolve-acquired-by-autodesk/td-p/2088605](http://Guideforums.autodesk.com/t5/civil-3d-forum/intelisolve-acquired-by-autodesk/td-p/2088605)).

- Horton J. 2003. Channel Geomorphology and Restoration Guidelines For Springfield Plateau Streams, South Dry Sac Watershed, Southwest Missouri. *Masters Thesis, Missouri State University*.
- Jacobson RB, Pugh AL. 1992. Effects of Land Use and Climate Shifts on Channel Instability, *Change on Hydrology and Water Resources at the Catchment Scale, Japan-US Committee of Hydrology, Water Resources and Global Climate Change, Public Works Research Inst., Tsukuba City*. 423-444.
- Jacobson RB, Bobbitt Gran KB. 1999. Gravel Sediment Routing From Widespread, Low-Intensity Landscape Disturbance, Current River Basin, Missouri. *Earth Surface Processes and Landforms* **24**: 897-917.
- Knapp DD. 2002. A “Smart” Instrument for Tracking Sediment Motion in Rivers, Research and Extension Regional Water Quality Conference. 1-3.
- Knighton D. 1998. Chapter 4 Fluvial Processes in *Fluvial Forms & Processes*. Oxford University Press Inc (ed) New York: 96-150.
- Koltun GF, Landers MN, Nolan KM, Parker RS. 1997. Sediment Transport and Geomorphology Issues in the Water Resources Division. *U. S. Geological Survey Sediment Workshop, February*: 1-7.
- Lane EW. 1955. The Importance of Fluvial morphology in Hydraulic Engineering. *Proceedings of the American Society of Civil Engineers* **81**: 745-761.
- Laronne JB, Duncan MJ 1989. Constraints on duration of sediment storage in a wide, gravel-bed river, New Zealand. *Sediment and the Environment* **184**: 165-172.
- Leopold LB. 1992. Sediment size that determines channel geometry, In *Dynamics of Gravel-Bed Rivers*. Chechester, New York: 297-311.
- Leopold LB, Emmett WW. 1976. Bedload measurements, East Fork River, Wyoming. *Proc. Natl. Acad. Sci.* **73 (4)**: 1000-1004.
- Leopold LB, Emmett WW, Myrick RM. 1966. Channel and Hillslope Processes in a Semi-arid Area, New Mexico. *US Geological Survey Professional Paper* **352G**: 193-253.
- Lisle TE, Nelson JM, Pitlick P, Madej MA, Barkett LB. 2000. Variability of bed mobility in natural, gravel-bed channels and adjustments to sediment load at local and reach scales. *Water Resources Research* **36**: 3743-3755.
- Martin DJ, Pavlowsky RT. 2011. Spatial Patterns of Channel Instability Along an Ozark River, Southwest Missouri. *Physical Geography* **32**: 445-468.

- Malmaeus JM, Hassan MA. 2002. Simulation of Individual Particle Movement in a Gravel Streambed. *Earth Surface Processes and Landforms* **27**: 81-97.
- McKenny R, Jacobson RB. 1996. Erosion and Deposition at the Riffle-Pool Scale in Gravel-Bed Streams, Ozark Plateaus, Missouri and Arkansas. *USGS Open File Report* **96-655A**: 1-28.
- McKenny R, Jacobson RB, Wertheimer RC. 1995. Woody vegetation and channel morphogenesis in low-gradient, gravel-bed streams in the Ozark Plateaus, Missouri and Arkansas. *Geomorphology* **13**: 175-198.
- Missouri Department of Conservation. 2013. (<http://mdc.mo.gov/>).
- National Weather Service Weather Forecast Office. 2012. ([Crh.noaa.gov/sgf/?=climate\\_2012annualsummary](http://crh.noaa.gov/sgf/?=climate_2012annualsummary)).
- [Odp.tamu.edu/publications/199\\_IR/chap\\_13/c13\\_10.htm](http://odp.tamu.edu/publications/199_IR/chap_13/c13_10.htm)
- Panfil MS, Jacobson RB. 2001. Relations among geology, physiography, land use, and stream habitat conditions in the Buffalo and Current River Systems, Missouri and Arkansas. *Biological Science Report* **5**.
- Pavlovsky RT, Lecce SA, Owen MR, Martin DJ. 2017. Legacy sediment, lead, and zinc storage in channel and floodplain deposits of the Big River, Old Lead Belt Mining District, Missouri, USA. *Geomorphology* **299**: 54-74.
- Phol M. 2004. Channel Bed Mobility Downstream from the Elwha Dams. *The Professional Geographer* **56(3)**: 422-431.
- Powers Index Chart. 2013. ([earthstudies.co.uk/Geography/Individual%20Research%20in%20Geography%20G3/Powers%20Scale%20of%20Roundness.html](http://earthstudies.co.uk/Geography/Individual%20Research%20in%20Geography%20G3/Powers%20Scale%20of%20Roundness.html)).
- Prothero D, Schwab F. 2004. Glossary. In *Sedimentary Geology An Introduction to Sedimentary Rocks and Stratigraphy* 2<sup>nd</sup> ed. W.H. Freeman and Company (ed): New York: 512.
- Rainato R, Mao L, Picco L. 2018. Near-bankfull floods in an Alpine stream: Effects on the sediment mobility and bedload magnitude. *International Journal of Sediment Research* **33(10)**: 27-34.
- Reynolds J, Johnson M, Kelly M, Morin P, Carter C. 2012. Chapter 16 Rivers and Streams. In *Exploring Geology* 2<sup>nd</sup> ed. McGraw Hill (ed): New York, NY: 466-499.
- Rosgen DL. 1994. A Classification of Natural Rivers. *Catena* **22**: 1409-1420.
- Shields A. 1936. Applications of Principles and Turbulence Research of Bed-Load Movement Translated from Anwendung der Ahnlichkeitsmechanik und der Turbulenz-forschung auf

- die Geschiebe -bewegung , " Mitteilungen der Preussischen  
Versuchsanstalt für Nassexbau und Schiffbau, by W. Ott and J. C. van Uchelen. Berlin.
- Sidle R.C. 1988. Bed Load Transport Regime of a Small Forest Stream. *Water Resources Research* **24**: 207-218.
- Takayama S. 1965. Bedload movement in torrential mountain streams. *Tokyo Geographical Paper* **9**: 169-188.
- TMDL for Wilson and Jordan creeks. 2011. ([dnr.mo.gov/env/wpp/tmdl/docs/2375-wilsons-3374-jordan-cks-tmdl.pdf](http://dnr.mo.gov/env/wpp/tmdl/docs/2375-wilsons-3374-jordan-cks-tmdl.pdf)).
- USDA Forest Service. 2012. ([stream.fs.fed.us/news/streamnt/apr96/apr96a1.htm](http://stream.fs.fed.us/news/streamnt/apr96/apr96a1.htm)).
- U.S. Department of Agriculture Methods for Streambed Mobility/Stability Analysis. 2008. ([http://www.fs.fed.us/eng/pubs/pdf/StreamSimulation/hi\\_res/%20FullDoc.pdf-E](http://www.fs.fed.us/eng/pubs/pdf/StreamSimulation/hi_res/%20FullDoc.pdf-E)).
- U.S. Geological Survey (USGS) Real-Time Water Data. 2013. (<https://waterdata.usgs.gov/nwis/rt>).
- U.S. Geological Survey (USGS) Water Resources of the United States. 2013. ([water.usgs.gov/software/PeakFQ](http://water.usgs.gov/software/PeakFQ)).
- van Rijn LC. 1984. Sediment Transport, Part I: Bed Load Transport. *Journal of Hydraulic Engineering* **110**: 1431-1456.
- Vazquez-Tarrio D, Menendez-Duarte R. 2014. Bedload transport rates for coarse-bed streams in an Atlantic region (Narcea River, NW Iberian Peninsula). *Geomorphology*. **217**: 1-14.
- Vazquez-Tarrio D, Recking A, Liebault F, Tal M, Menendez-Duarte R. 2019. Particle transport in gravel-bed rivers: Revisiting passive tracer data. *Earth Surface Processes and Landform* **44**: 112-128.
- Wilcock PR. 1997. Entrainment, Displacement, and Transport of Tracer Gravels. *Earth Surface Processes and Landforms* **22**: 1125-1138.
- Wildlife Supply Company. 2012. ([www.wildco.com/Gravelometer-aluminum-US-SAH-97-13.5in-x-11in-0.62-lbs.html](http://www.wildco.com/Gravelometer-aluminum-US-SAH-97-13.5in-x-11in-0.62-lbs.html)).
- Wolman MG. 1954. A method of sampling coarse river bed material. *Transactions of the American Geophysical Union (EOS)* **35**: 951-956.

## APPENDICES

### Appendix A-Individual Tracer Characteristics

Number	Size (mm)	Color	Weight (g)	Volume (ml <sup>3</sup> )	Density (g/ml <sup>3</sup> )	A axis (mm)	B axis (mm)	C axis (mm)	Smooth %	Rough %	Shape Index
1	16	Orange	5.7	2	2.85	26	21	9	60	40	SR
2	16	Orange	10.5	5	2.10	42	19	13	80	20	A
3	16	Orange	11.5	4.5	2.56	34	22	17	95	5	SA
4	16	Orange	19.5	9	2.17	45	30	19	95	5	A
5	16	Orange	10	4	2.50	26	25	16	20	80	SA
6	16	Orange	24.2	10	2.42	56	22	19	95	5	A
7	16	Orange	7.1	2.5	2.84	29	24	13	50	50	A
8	16	Orange	18.4	7	2.63	32	23	21	80	20	A
9	16	Orange	9.1	4	2.28	34	19	11	95	5	A
10	16	Orange	5.7	3	1.90	29	20	12	30	70	R
11	16	Orange	6.1	3	2.03	24	23	11	0	100	A
12	16	Orange	7.4	4	1.85	32	22	12	5	95	SR
13	16	Orange	9.3	4	2.33	32	20	18	95	5	A
14	16	Orange	11.1	6	1.85	30	25	16	30	70	SA
15	16	Orange	9.2	3.5	2.63	28	20	15	10	90	SR
16	16	Orange	15.7	6	2.62	43	22	15	20	80	A
17	16	Orange	13.7	5	2.74	40	20	14	20	80	SA
18	16	Orange	9	6.5	1.38	39	21	12	60	40	A
19	16	Orange	10	4	2.50	29	25	14	60	40	SA
20	16	Orange	10.4	4.5	2.31	38	30	10	95	5	A
21	16	Orange	10	4	2.50	29	21	17	20	80	SA
22	16	Orange	11.8	6.5	1.82	35	27	13	20	80	SA
23	16	Orange	7.2	3.5	2.06	30	27	10	5	95	A
24	16	Orange	6.5	3	2.17	25	20	15	70	30	A
25	16	Orange	6.4	3	2.13	22	19	15	70	30	SA
26	16	Orange	5.8	2	2.90	30	20	13	70	30	SA
27	16	Orange	13.7	5	2.74	35	20	15	70	30	A
28	16	Orange	17.9	8	2.24	44	24	15	95	5	SA
29	16	Orange	17.2	8	2.15	38	29	22	10	90	A
30	16	Orange	8.4	3.5	2.40	30	20	13	50	50	SA
31	16	Orange	9.1	3.5	2.60	25	23	17	5	95	A
32	16	Orange	17.6	8	2.20	48	24	21	50	50	SA
33	16	Orange	17.5	8	2.19	42	26	14	40	60	SA
34	16	Orange	11.1	5	2.22	30	18	16	95	5	SA
35	16	Orange	9.6	4	2.40	43	24	13	95	5	A
36	16	Orange	11.2	4	2.80	33	27	12	80	20	SA
37	16	Orange	13	5	2.60	39	27	9	95	5	SA
38	16	Orange	8.4	4.5	1.87	28	26	12	80	20	A
39	16	Orange	11.3	5	2.26	28	26	17	80	20	R
40	16	Orange	7.7	4	1.93	32	22	12	30	70	SR
41	16	Orange	8.5	3	2.83	37	26	12	90	10	SA
42	16	Orange	13.9	5	2.78	36	28	22	20	80	SA
43	16	Orange	13.3	5	2.66	48	24	11	60	40	A
44	16	Orange	11.5	4	2.88	35	27	10	90	10	SR

Number	Size (mm)	Color	Weight (g)	Volume (ml <sup>3</sup> )	Density (g/ml <sup>3</sup> )	A axis (mm)	B axis (mm)	C axis (mm)	Smooth %	Rough %	Shape Index
45	16	Orange	15.4	6	2.57	44	25	12	50	50	SR
46	16	Orange	5.8	3	1.93	25	19	13	5	95	SR
47	16	Orange	15.2	6.5	2.34	40	24	16	80	20	SA
48	16	Orange	10.1	5	2.02	24	24	17	70	30	A
49	16	Orange	23.5	10	2.35	37	21	19	5	95	SA
50	16	Orange	14.1	5	2.82	37	27	17	30	70	A
51	16	Orange	11.4	5	2.28	31	20	18	40	60	A
52	16	Orange	10.4	6	1.73	38	26	12	50	50	SR
53	16	Orange	10.5	7	1.50	34	31	12	40	60	SR
54	16	Orange	5.1	3	1.70	24	19	14	30	70	SR
55	16	Orange	19.5	9	2.17	46	22	20	30	70	SR
56	16	Orange	17.8	7	2.54	47	25	16	30	70	A
57	16	Orange	9.2	5	1.84	32	27	18	70	30	SR
58	16	Orange	19.4	9	2.16	45	24	20	5	95	SA
59	16	Orange	12.3	5	2.46	39	26	13	20	80	SA
60	16	Orange	10.2	4	2.55	36	23	10	60	40	A
61	16	Orange	5.5	4	1.38	28	20	13	80	20	SR
62	16	Orange	11.2	6	1.87	38	21	15	50	50	SR
63	16	Orange	7.1	4	1.78	29	24	13	20	80	SR
64	16	Orange	9.2	4	2.30	29	23	12	40	60	SR
65	16	Orange	5.8	4	1.45	25	25	8	40	60	A
66	16	Orange	17.6	8	2.20	46	24	11	90	10	VA
67	16	Orange	8.3	3.5	2.37	27	24	11	70	30	SA
68	16	Orange	13.3	6	2.22	34	21	20	50	50	SA
69	16	Orange	11	5	2.20	37	26	15	40	60	SA
70	16	Orange	9.4	4	2.35	32	29	10	90	10	SA
71	16	Orange	7.1	4	1.78	30	23	14	60	40	R
72	16	Orange	12	7	1.71	34	23	20	60	40	SA
73	16	Orange	9	5	1.80	29	24	11	20	80	SA
74	16	Orange	9.5	4	2.38	24	22	15	5	95	SR
75	16	Orange	10.3	5	2.06	35	20	15	40	60	SA
76	16	Orange	10.2	4	2.55	30	22	12	80	20	A
77	16	Orange	16.3	7	2.33	44	28	14	5	95	A
78	16	Orange	7.1	3.5	2.03	31	22	9	15	85	SA
79	16	Orange	12.3	5.5	2.24	26	22	17	0	100	R
80	16	Orange	7.8	4	1.95	25	24	13	5	95	R
81	16	Orange	12.7	4.5	2.82	39	22	16	10	90	SR
82	16	Orange	14	5	2.8	40	28	14	20	80	SA
83	16	Orange	13.4	7	1.91	37	26	15	30	70	SR
84	16	Orange	11.9	4	2.98	44	23	15	90	10	SA
85	16	Orange	11	4	2.75	38	22	13	50	50	SR
86	16	Orange	4.2	3	1.40	23	20	12	20	80	R
87	16	Orange	9.7	7	1.39	38	20	18	5	95	SR
88	16	Orange	10.3	5	2.06	39	22	14	0	100	SA
89	16	Orange	5	2.5	2.00	28	16	11	5	95	SA
90	16	Orange	9.1	4	2.28	34	30	11	60	40	SA
91	16	Orange	13.2	5.5	2.40	37	19	15	30	70	SA
92	16	Orange	4.2	2	2.10	26	21	8	70	30	SA

Number	Size (mm)	Color	Weight (g)	Volume (ml <sup>3</sup> )	Density (g/ml <sup>3</sup> )	A axis (mm)	B axis (mm)	C axis (mm)	Smooth %	Rough %	Shape Index
93	16	Orange	8.6	4	2.15	29	20	16	95	5	SA
94	16	Orange	9.9	4	2.48	23	20	18	30	70	SA
95	16	Orange	10.2	6	1.70	28	24	17	80	20	R
96	16	Orange	6.9	2.5	2.76	25	18	15	80	20	A
97	16	Orange	12.3	4.5	2.73	27	22	16	10	90	SR
98	16	Orange	10.3	4	2.58	29	21	14	90	10	SR
99	16	Orange	6.3	3.5	1.80	30	23	10	20	80	SA
100	16	Orange	16.6	6.5	2.55	35	20	18	0	100	R
101	22.6	Green	15.3	6	2.55	45	35	10	100	0	VA
102	22.6	Green	20	10	2.00	34	33	23	10	90	SR
103	22.6	Green	35.2	19	1.85	73	35	25	60	40	A
104	22.6	Green	24	10.5	2.29	39	35	19	70	30	R
105	22.6	Green	30.8	11	2.8	44	34	16	0	100	SR
106	22.6	Green	30.2	17.5	1.73	49	33	22	70	30	A
107	22.6	Green	16.7	8	2.09	36	31	16	10	90	SA
108	22.6	Green	34.1	15	2.27	51	34	20	90	10	SA
109	22.6	Green	24.6	10.5	2.34	57	34	14	40	60	A
110	22.6	Green	31.9	14	2.28	42	33	24	10	90	SA
111	22.6	Green	29.9	19	1.57	46	33	26	10	90	R
112	22.6	Green	47.1	25	1.88	72	40	25	60	40	SA
113	22.6	Green	18.4	10	1.84	35	30	20	10	90	R
114	22.6	Green	27.4	14	1.96	47	29	16	60	40	SA
115	22.6	Green	42.1	20	2.11	56	35	21	10	90	SR
116	22.6	Green	31.4	15	2.09	65	30	18	75	25	A
117	22.6	Green	26.7	15	1.78	44	30	26	10	90	A
118	22.6	Green	23.2	10	2.32	57	30	21	50	50	A
119	22.6	Green	31.5	15	2.10	41	39	22	0	100	SA
120	22.6	Green	21.8	11	1.98	39	36	19	20	80	SR
121	22.6	Green	20.5	10	2.05	39	29	20	60	40	SA
122	22.6	Green	29.2	11	2.65	27	27	24	20	80	SA
123	22.6	Green	26.6	12	2.22	51	31	19	20	80	SA
124	22.6	Green	28.2	13	2.17	50	28	23	20	80	SA
125	22.6	Green	24.7	13	1.90	53	24	23	20	80	SA
126	22.6	Green	79	31	2.55	64	42	27	30	70	SA
127	22.6	Green	51.9	20	2.60	53	36	24	20	80	SA
128	22.6	Green	32.8	15	2.19	50	33	28	20	80	SA
129	22.6	Green	18.1	7	2.59	43	33	17	95	5	A
130	22.6	Green	26.9	10	2.69	50	30	16	5	95	SA
131	22.6	Green	14.1	7	2.01	33	21	21	10	90	SA
132	22.6	Green	14.5	9	1.61	40	30	16	10	90	SA
133	22.6	Green	16.2	7	2.31	34	24	18	15	85	SA
134	22.6	Green	41.6	20	2.08	52	25	25	10	90	SA
135	22.6	Green	33.1	13	2.55	46	34	16	30	70	SA
136	22.6	Green	13.4	6	2.23	35	29	12	90	10	A
137	22.6	Green	42.5	24.5	1.73	44	41	30	15	85	SA
138	22.6	Green	28.9	13.5	2.14	50	39	22	30	70	SA
139	22.6	Green	17.5	8	2.19	41	33	24	70	30	A
140	22.6	Green	40.8	21	1.94	67	36	20	20	80	SA



Number	Size (mm)	Color	Weight (g)	Volume (ml <sup>3</sup> )	Density (g/ml <sup>3</sup> )	A axis (mm)	B axis (mm)	C axis (mm)	Smooth %	Rough %	Shape Index
141	22.6	Green	17.5	10	1.75	30	28	26	5	95	SR
142	22.6	Green	25.4	12	2.12	54	32	23	70	30	A
143	22.6	Green	29.5	14.5	2.03	46	41	19	10	90	SA
144	22.6	Green	29.2	17	1.72	50	32	17	15	85	R
145	22.6	Green	14.4	7	2.06	34	29	15	10	90	SA
146	22.6	Green	25	11	2.27	42	39	19	50	50	A
147	22.6	Green	23.3	8	2.91	40	28	27	0	100	R
148	22.6	Green	32.4	24	1.35	64	34	16	30	70	A
149	22.6	Green	28.4	17	1.67	41	32	28	10	90	R
150	22.6	Green	17.3	11	1.57	38	32	16	10	90	SR
151	22.6	Green	35.3	19	1.86	49	32	29	40	60	SR
152	22.6	Green	25.7	13	1.98	56	23	19	60	40	A
153	22.6	Green	44.1	19	2.32	58	35	20	80	20	A
154	22.6	Green	37	14	2.64	50	40	20	50	50	A
155	22.6	Green	53.3	25	2.13	50	40	33	60	40	A
156	22.6	Green	48.1	20	2.41	50	32	22	95	5	VA
157	22.6	Green	71	33	2.15	95	28	23	50	50	VA
158	22.6	Green	21.9	11.5	1.90	47	31	30	50	50	SA
159	22.6	Green	22	9	2.44	46	27	19	95	5	A
160	22.6	Green	13.6	6.5	2.09	34	32	14	25	75	A
161	22.6	Green	55.9	19	2.94	64	22	19	5	95	SA
162	22.6	Green	29.7	12.5	2.38	57	39	12	90	10	A
163	22.6	Green	28.7	15	1.91	33	33	30	10	90	SA
164	22.6	Green	26	14	1.86	42	34	23	30	70	SA
165	22.6	Green	31	14	2.21	58	28	22	40	60	SA
166	22.6	Green	51	25	2.04	42	41	23	50	50	SA
167	22.6	Green	22.3	11	2.03	45	38	20	70	30	SA
168	22.6	Green	13.8	7	1.97	37	27	16	50	50	SA
169	22.6	Green	42.7	24	1.78	70	40	30	20	80	SA
170	22.6	Green	66.5	28	2.38	76	35	26	50	50	SA
171	22.6	Green	23.2	9	2.58	32	30	22	20	80	SA
172	22.6	Green	24.5	10	2.45	46	33	29	10	90	A
173	22.6	Green	21	9	2.33	30	29	24	90	10	SA
174	22.6	Green	30	13.5	2.22	48	33	16	60	40	SA
175	22.6	Green	33.7	12.5	2.70	57	28	18	25	75	SA
176	22.6	Green	24.4	13	1.88	55	31	16	20	80	SA
177	22.6	Green	20.7	10	2.07	52	36	15	80	20	A
178	22.6	Green	21.1	9	2.34	39	29	18	50	50	SR
179	22.6	Green	40	18	2.22	45	36	21	95	5	A
180	22.6	Green	23	10	2.30	46	32	16	70	30	R
181	22.6	Green	54.2	24	2.26	77	34	19	95	5	A
182	22.6	Green	12.5	5	2.50	37	23	17	90	10	SA
183	22.6	Green	32.1	15	2.14	51	36	16	90	10	SA
184	22.6	Green	19.1	10	1.91	58	30	18	60	40	SA
185	22.6	Green	126.3	55	2.30	80	50	35	0	100	SA
186	22.6	Green	31.9	18	1.77	52	37	15	50	50	SR
187	22.6	Green	22	10	2.20	48	36	14	70	30	SA
188	22.6	Green	40.3	19	2.12	56	30	30	60	40	SA

Number	Size (mm)	Color	Weight (g)	Volume (ml <sup>3</sup> )	Density (g/ml <sup>3</sup> )	A axis (mm)	B axis (mm)	C axis (mm)	Smooth %	Rough %	Shape Index
189	22.6	Green	17.9	9	1.99	39	38	15	50	50	SA
190	22.6	Green	21.7	10	2.17	50	38	14	75	25	SA
191	22.6	Green	16.3	7	2.33	35	32	16	60	40	SA
192	22.6	Green	17.9	10	1.79	38	34	13	50	50	SR
193	22.6	Green	12.8	6	2.13	31	23	21	50	50	SR
194	22.6	Green	14.3	9	1.59	32	31	19	60	40	R
195	22.6	Green	24.7	11	2.25	52	32	19	70	30	A
196	22.6	Green	23.1	11	2.10	49	31	20	90	10	SA
197	22.6	Green	12	4.5	2.66	30	28	13	80	20	SA
198	22.6	Green	12.1	5	2.42	30	30	15	50	50	SA
199	22.6	Green	39.4	18	2.19	55	33	28	95	5	A
200	22.6	Green	21.9	8	2.74	36	29	19	60	40	SA
201	32	Yellow	74.7	32	2.33	59	40	31	90	10	VR
202	32	Yellow	108.4	43	2.52	89	47	24	10	90	A
203	32	Yellow	59.5	24	2.48	49	44	29	5	95	SA
204	32	Yellow	82.2	36	2.28	59	58	26	80	20	A
205	32	Yellow	52.7	20	2.64	54	37	33	85	15	A
206	32	Yellow	63.2	23	2.75	60	47	22	30	70	SR
207	32	Yellow	45.3	20	2.27	47	46	26	15	85	SA
208	32	Yellow	92.7	31	2.99	68	39	35	70	30	SA
209	32	Yellow	118.5	50	2.37	75	43	29	50	50	A
210	32	Yellow	86.5	40	2.16	60	46	30	30	70	SA
211	32	Yellow	78.8	38	2.07	56	52	36	60	40	A
212	32	Yellow	67.9	24	2.83	81	54	13	50	50	A
213	32	Yellow	140.3	60	2.34	98	43	41	20	80	SA
214	32	Yellow	36.4	20	1.82	54	45	14	25	75	SR
215	32	Yellow	75.7	30	2.52	69	48	23	30	70	SA
216	32	Yellow	43.8	20	2.19	42	34	28	20	80	SR
217	32	Yellow	152	55	2.76	120	47	36	15	85	A
218	32	Yellow	78.9	32	2.47	72	43	31	40	60	A
219	32	Yellow	102.6	40	2.57	56	40	31	15	85	SA
220	32	Yellow	50.4	21	2.40	60	58	16	70	30	SA
221	32	Yellow	87.2	40	2.18	80	43	24	30	70	SA
222	32	Yellow	67.8	38	1.78	51	50	36	10	90	SA
223	32	Yellow	57.8	35	1.65	59	50	27	5	95	SR
224	32	Yellow	119.4	41	2.91	60	51	40	40	60	SA
225	32	Yellow	141.2	56	2.52	79	45	37	30	70	SA
226	32	Yellow	53.6	22	2.44	57	45	24	70	30	A
227	32	Yellow	47.7	20	2.39	52	43	38	70	30	SA
228	32	Yellow	79.7	28	2.85	49	33	31	70	30	SR
229	32	Yellow	53.1	30	1.77	47	45	25	60	40	SA
230	32	Yellow	115.2	60	1.92	67	46	33	10	90	SA
231	32	Yellow	116.9	50	2.34	73	45	41	0	100	SA
232	32	Yellow	79.4	40	1.99	71	45	30	5	95	SA
233	32	Yellow	84.2	34	2.48	57	47	28	80	20	SR
234	32	Yellow	102	35	2.91	67	38	37	70	30	SA
235	32	Yellow	143.4	70	2.05	59	45	43	40	60	A
236	32	Yellow	80.2	35	2.29	62	49	30	10	90	SA

Number	Size (mm)	Color	Weight (g)	Volume (ml <sup>3</sup> )	Density (g/ml <sup>3</sup> )	A axis (mm)	B axis (mm)	C axis (mm)	Smooth %	Rough %	Shape Index
237	32	Yellow	72.8	40	1.82	55	42	28	15	85	SR
238	32	Yellow	40.7	20	2.04	53	35	23	70	30	SA
239	32	Yellow	36.9	15	2.46	45	37	27	50	50	SA
240	32	Yellow	30.5	18	1.69	44	37	21	5	95	R
241	32	Yellow	114.3	40	2.86	70	51	26	90	10	SR
242	32	Yellow	94.7	40	2.37	95	44	25	90	10	SA
243	32	Yellow	49.4	25	1.98	52	47	20	70	30	SR
244	32	Yellow	74.2	28	2.65	57	46	29	10	90	SR
245	32	Yellow	49.1	20	2.46	59	52	24	90	10	A
246	32	Yellow	201.3	85	2.37	72	44	43	90	10	SA
247	32	Yellow	90.2	33	2.73	62	42	31	95	5	A
248	32	Yellow	84.2	40	2.11	73	52	32	50	50	SA
249	32	Yellow	42	18	2.33	49	40	25	40	60	SA
250	32	Yellow	38.4	20	1.92	47	32	28	20	80	SR
251	32	Yellow	49	20	2.45	60	50	20	80	20	SA
252	32	Yellow	66.1	25	2.64	78	45	22	60	40	A
253	32	Yellow	75.8	38	1.99	73	59	18	70	30	SR
254	32	Yellow	46.9	22	2.13	52	38	22	60	40	SA
255	32	Yellow	54.4	20	2.72	56	42	21	95	5	A
256	32	Yellow	59.3	28	2.12	52	37	31	40	60	SA
257	32	Yellow	86.9	32	2.72	49	40	38	80	20	SA
258	32	Yellow	92.8	40	2.32	63	40	30	10	90	SA
259	32	Yellow	54.6	20	2.73	57	45	33	70	30	SA
260	32	Yellow	55.7	25	2.23	64	37	28	60	40	SA
261	32	Yellow	45.5	24	1.90	51	40	28	50	50	SA
262	32	Yellow	148.5	60	2.48	91	58	25	0	100	A
263	32	Yellow	59.2	27	2.19	59	48	35	30	70	SA
264	32	Yellow	78.1	38	2.06	73	55	21	10	90	SA
265	32	Yellow	89.3	30	2.98	64	46	23	80	20	SR
267	32	Yellow	77.6	46	1.69	46	41	38	30	70	R
268	32	Yellow	112	52	2.15	67	44	40	20	80	SA
269	32	Yellow	65.8	30	2.19	53	43	39	85	15	SA
270	32	Yellow	66.5	27	2.46	51	38	34	50	50	SR
271	32	Yellow	152.6	58	2.63	88	40	32	50	50	R
272	32	Yellow	61	27	2.26	64	46	27	60	40	SA
273	32	Yellow	63.1	30	2.10	72	38	31	60	40	SA
274	32	Yellow	69.9	28	2.50	77	44	20	80	20	A
275	32	Yellow	53.6	20	2.68	63	60	15	90	10	A
276	32	Yellow	96.9	43	2.25	67	52	40	70	30	SA
277	32	Yellow	61.7	26	2.37	48	48	24	80	20	SR
278	32	Yellow	83.7	40	2.09	70	52	35	50	50	SR
279	32	Yellow	45	19	2.37	42	34	32	95	5	SA
280	32	Yellow	67.5	30	2.25	60	37	31	85	15	SA
281	32	Yellow	180.5	80	2.26	100	46	41	0	100	SA
282	32	Yellow	56.4	30	1.88	51	46	26	70	30	SA
283	32	Yellow	79.9	38	2.10	67	38	31	80	20	SR
284	32	Yellow	100.1	40	2.50	62	49	33	90	10	SA
285	32	Yellow	146.4	53	2.76	80	50	35	80	20	SR

Number	Size (mm)	Color	Weight (g)	Volume (ml <sup>3</sup> )	Density (g/ml <sup>3</sup> )	A axis (mm)	B axis (mm)	C axis (mm)	Smooth %	Rough %	Shape Index
286	32	Yellow	66.3	27	2.46	66	36	26	60	40	SA
287	32	Yellow	66.1	35	1.89	51	43	27	20	80	SR
288	32	Yellow	50.8	30	1.69	54	43	27	10	90	SR
289	32	Yellow	30.7	19	1.62	49	42	23	30	70	SA
290	32	Yellow	81.5	30	2.72	73	50	22	50	50	SA
291	32	Yellow	60.3	40	1.51	62	53	28	10	90	SA
292	32	Yellow	57.3	35	1.64	48	46	35	50	50	SA
293	32	Yellow	72.1	45	1.60	76	46	43	5	95	SR
294	32	Yellow	52	25	2.08	47	44	31	5	95	SA
295	32	Yellow	44.4	30	1.48	45	44	32	0	100	R
296	32	Yellow	78.3	40	1.96	67	47	25	20	80	SA
297	32	Yellow	43.2	18	2.40	38	35	34	50	50	SA
298	32	Yellow	71.9	37	1.94	56	45	37	60	40	SA
299	32	Yellow	67.3	25	2.69	60	51	26	30	70	SA
300	32	Yellow	60.3	30	2.01	58	46	28	70	30	A
301	45	Blue	250.1	100	2.50	79	58	46	100	0	A
302	45	Blue	234.9	90	2.61	85	49	40	5	95	SR
303	45	Blue	220.8	100	2.21	87	60	45	50	50	SA
304	45	Blue	351	125	2.81	118	58	47	90	10	SA
305	45	Blue	279	140	1.99	89	68	51	50	50	SR
306	45	Blue	145.8	60	2.43	92	46	45	70	30	A
307	45	Blue	306.7	125	2.45	82	64	52	60	40	A
308	45	Blue	280.6	120	2.34	126	60	36	30	70	SA
309	45	Blue	298.3	120	2.49	88	59	42	75	25	SA
310	45	Blue	147.3	53	2.78	73	62	31	95	5	A
311	45	Blue	197.1	100	1.97	76	66	47	0	100	A
312	45	Blue	212.3	100	2.12	76	55	56	80	20	A
313	45	Blue	123.7	50	2.47	70	56	30	95	5	A
314	45	Blue	208.3	90	2.31	94	69	40	70	30	A
315	45	Blue	214.1	87	2.46	77	63	40	95	5	SA
316	45	Blue	291.7	115	2.54	84	58	44	10	90	SA
317	45	Blue	99.5	60	1.66	77	70	30	5	95	SA
318	45	Blue	140.1	52	2.69	72	59	27	50	50	SA
319	45	Blue	193.6	73	2.65	68	64	41	80	20	SA
320	45	Blue	213.2	75	2.84	76	54	42	70	30	A
321	45	Blue	116.1	60	1.94	66	66	34	50	50	A
322	45	Blue	139.5	60	2.33	83	64	28	10	90	SA
323	45	Blue	224.3	90	2.49	84	66	47	50	50	A
324	45	Blue	97	44	2.20	68	52	30	70	30	A
325	45	Blue	173.9	70	2.48	76	49	32	20	80	SA
326	45	Blue	185.7	71	2.62	56	49	44	60	40	SR
327	45	Blue	350	140	2.50	65	60	56	80	20	A
328	45	Blue	194.2	87	2.23	68	68	33	0	100	SA
329	45	Blue	195.1	80	2.44	83	73	36	80	20	SA
330	45	Blue	228.9	85	2.69	78	71	34	50	50	SA
331	45	Blue	297.7	120	2.48	73	60	53	20	80	SA
332	45	Blue	153.4	70	2.19	74	66	40	60	40	SA
333	45	Blue	93.4	50	1.87	73	49	31	25	75	SR

Number	Size (mm)	Color	Weight (g)	Volume (ml <sup>3</sup> )	Density (g/ml <sup>3</sup> )	A axis (mm)	B axis (mm)	C axis (mm)	Smooth %	Rough %	Shape Index
334	45	Blue	216.8	90	2.41	82	69	43	90	10	A
335	45	Blue	203.9	85	2.40	59	54	52	50	50	SA
336	45	Blue	116.3	60	1.94	70	55	35	60	40	SR
337	45	Blue	135.1	70	1.93	74	50	46	10	90	SA
338	45	Blue	207.8	107	1.94	92	66	39	50	50	SR
339	45	Blue	225.2	120	1.88	79	66	54	40	60	SR
340	45	Blue	249.5	95	2.63	97	90	47	50	50	SA
341	45	Blue	221.8	100	2.22	103	60	35	5	95	SA
342	45	Blue	144.2	60	2.40	72	52	31	90	10	SR
343	45	Blue	224.9	100	2.25	86	57	44	25	75	SA
344	45	Blue	415	150	2.77	83	72	56	85	15	A
345	45	Blue	249.6	100	2.50	73	64	36	40	60	SA
346	45	Blue	342	115	2.97	82	65	61	10	90	A
347	45	Blue	113.8	56	2.03	53	49	42	10	90	SA
348	45	Blue	164.2	68	2.41	83	63	40	70	30	SA
349	45	Blue	104.3	57	1.83	54	45	39	60	40	SA
350	45	Blue	143	80	1.79	80	62	43	50	50	SA
351	45	Blue	165.9	80	2.07	69	61	47	30	70	A
352	45	Blue	250.8	100	2.51	83	53	48	65	35	SA
353	45	Blue	223.5	105	2.13	57	63	53	60	40	SA
354	45	Blue	251.8	120	2.10	89	66	42	70	30	SA
355	45	Blue	253.9	100	2.54	87	52	46	10	90	SR
356	45	Blue	123.3	60	2.06	66	51	44	90	10	SA
357	45	Blue	173.2	80	2.17	78	61	46	5	95	SA
358	45	Blue	196.3	85	2.31	71	56	53	80	20	SA
359	45	Blue	267.5	125	2.14	110	49	42	60	40	SA
360	45	Blue	169.1	75	2.25	82	80	27	60	40	SR
361	45	Blue	187.3	105	1.78	90	45	41	5	95	SA
362	45	Blue	240.9	95	2.54	89	53	36	100	0	SA
363	45	Blue	206.5	97	2.13	103	48	41	50	50	SA
364	45	Blue	103.4	48	2.15	61	49	34	80	20	VA
365	45	Blue	225.3	87	2.59	82	49	39	10	90	SR
366	45	Blue	118.9	45	2.64	75	49	44	95	5	A
367	45	Blue	134.5	65	2.07	62	57	37	60	40	SA
368	45	Blue	117.8	60	1.96	58	57	30	70	30	SA
369	45	Blue	132.2	68	1.94	80	53	39	0	100	SA
370	45	Blue	125.9	65	1.94	96	66	33	40	60	SA
371	45	Blue	189	84	2.25	88	56	41	15	85	SA
372	45	Blue	166.1	60	2.77	61	47	45	80	20	SA
373	45	Blue	304.8	110	2.77	117	65	51	50	50	SA
374	45	Blue	192.9	80	2.41	104	66	41	95	5	A
375	45	Blue	113	53	2.13	77	62	30	0	100	SA
376	45	Blue	272.7	125	2.18	94	66	52	60	40	SR
377	45	Blue	229.7	90	2.55	73	62	35	50	50	SR
378	45	Blue	182.7	105	1.74	82	75	30	20	80	SR
379	45	Blue	121.1	60	2.02	72	47	39	50	50	SA

## Appendix B-Deployment Times

August 25, 2012	September 16, 2012	January 29, 2013
28-16mm (D <sub>50</sub> )	6-16mm (D <sub>50</sub> )	36-16mm (D <sub>50</sub> )
27-22.6mm (D <sub>75</sub> )	6-22.6mm (D <sub>75</sub> )	36-22.6mm (D <sub>75</sub> )
27-32mm (D <sub>84</sub> )	6-32mm (D <sub>84</sub> )	36-32mm (D <sub>84</sub> )
27-45mm (D <sub>90</sub> )	6-45mm (D <sub>90</sub> )	35-45mm (D <sub>90</sub> )
Total-109 Tracers	Total-24	Total-143
Site 40L		Site 40L
3-16mm		3-16mm
3-22.6mm		3-22.6mm
3-32mm		3-32mm
3-45mm		2-45mm
Site 40C	Site 40C	Site 40C
3-16mm	2-16mm	6-16mm
3-22.6mm	2-22.6mm	6-22.6mm
3-32mm	2-32mm	6-32mm
3-45mm	2-45mm	6-45mm
Site 40R		Site 40R
3-16mm		3-16mm
3-22.6mm		3-22.6mm
3-32mm		3-32mm
3-45mm		3-45mm
Site 60L		Site 60L
3-16mm		3-16mm
3-22.6mm		3-22.6mm
3-32mm		3-32mm
3-45mm		3-45mm
Site 60C	Site 60C	Site 60C
3-16mm	2-16mm	6-16mm
3-22.6mm	2-22.6mm	6-22.6mm
3-32mm	2-32mm	6-32mm
3-45mm	2-45mm	6-45mm
Site 60R		Site 60R
4-16mm		3-16mm
3-22.6mm		3-22.6mm
3-32mm		3-32mm
3-45mm		3-45mm
Site 85L		Site 85L
3-16mm		3-16mm
3-22.6mm		3-22.6mm
3-32mm		3-32mm
3-45mm		3-45mm
Site 85C	Site 60C	Site 85C
3-16mm	2-16mm	6-16mm
3-22.6mm	2-22.6mm	6-22.6mm
3-32mm	2-32mm	6-32mm
3-45mm	2-45mm	6-45mm
Site 85R		Site 85R
3-16mm		3-16mm
3-22.6mm		3-22.6mm
3-32mm		3-32mm
3-45mm		3-45mm
Total to Date: 109	Total to Date: 133	Total to Date: 276

Appendix C-Tracer Movement (First date indicates location and date of initial release)

Location on tapeline on given date (meters)

Tracer Number	Aug 25, 2012	Sept 3, 2012	Sept 9, 2012	Sept 16, 2012	Oct 17, 2012	Oct 25, 2012	Jan 11, 2013	Jan 28, 2013	Feb 2, 2013	March 3, 2013
1								85C	missing	85
2								60L	60.23	missing
3								40C	missing	missing
4								60R	missing	missing
5								60C	65.33	66.7
6								85L	90.9	96.6
7								85C	missing	missing
8	60R	60.63	61.95	65.99	missing	missing	missing	missing	missing	missing
9								85R	missing	85
10	40L	40	40.23	missing	missing	missing	missing	missing	missing	missing
11	60L	60	60	60	missing	missing	missing	missing	missing	missing
12	60R	60	60	60	141	141.1	141.1	141.1	141.05	141
13	85L	85	85	85	missing	missing	missing	missing	missing	missing
14	85R	85	85	85.93	missing	missing	missing	missing	missing	missing
15	60C	60.13	60.44	61.2	missing	missing	missing	missing	missing	missing
16	85C	85.2	86.05	86.4	missing	missing	missing	missing	missing	missing
17	40R	missing	missing	missing	missing	missing	missing	missing	missing	missing
18	40C	40.28	40.6	42.59	97.43	107.2	107.2	missing	missing	missing
19	40L	40.05	40.1	40.86	missing	missing	missing	missing	missing	missing
20	85C	85.85	85.86	86.02	missing	missing	missing	missing	missing	missing
21	40C	40.1	40.1	missing	missing	missing	missing	missing	missing	missing
22	85L	85	85	missing	missing	missing	missing	missing	missing	missing
23	85R	85	85	86.13	missing	missing	missing	missing	118.95	119.1
24	40R	40	40.3	42.7	missing	105.05	105.05	105.05	missing	missing
25	85C	85.65	85.99	missing	missing	missing	missing	missing	missing	missing
26	85R	85	85	85	missing	missing	missing	missing	missing	missing
27	85L	85	85	missing	missing	missing	missing	missing	missing	missing
28	40C	40.27	missing	45.4	missing	missing	missing	missing	missing	missing
29	40R	40	40	40.85	missing	missing	missing	missing	missing	missing
30	60R	60	60	60.4	missing	missing	missing	missing	missing	missing
31	60R	60	60	61.6	missing	missing	missing	missing	missing	missing
32	40L	40	40.22	40.63	missing	missing	missing	missing	missing	missing
33	60C	60	60	61.52	119.44	119.5	119.5	119.5	missing	missing
34	60L	60	60.36	60.87	missing	missing	missing	missing	missing	missing
35	60C	60	60	62.86	133.55	133.85	133.85	133.85	missing	missing
36	60L	60	60.57	61.05	114.2	114.1	114.1	114.1	missing	missing
37				85C	missing	missing	missing	missing	missing	missing
38				60C	135.2	missing	missing	missing	136.45	missing
39				40C	missing	missing	missing	missing	missing	missing
40				85C	missing	missing	missing	missing	missing	missing
41								40R	missing	missing
42				40C	missing	missing	missing	missing	missing	missing

Tracer Number	Aug 25, 2012	Sept 3, 2012	Sept 9, 2012	Sept 16, 2012	Oct 17, 2012	Oct 25, 2012	Jan 11, 2013	Jan 28, 2013	Feb 2, 2013	March 3, 2013
43								40C	missing	missing
44				60C	112.15 hole	112.15	112.15	112.15	112.15	112.15
45								40L	missing	moved
46								85C	91.9	92.4
47								40L	40.27	moved
48	ND									
49								60C	missing	61.6
50								85C	85.8	missing
51								40C	missing	missing
52								85R	missing	missing
53								40C	missing	missing
54								60C	missing	missing
55								60L	missing	missing
56								60C	63.15	moved
57								60R	missing	missing
58								60C	64.07	65.5
59								40R	missing	missing
60								85L	94.5	94.7
61								60L	missing	missing
62								85L	missing	missing
63								85C	missing	missing
64								85R	85	missing
65								40C	missing	missing
66								40C	missing	missing
67								40L	40	moved
68								60C	65.82	moved
69								40R	missing	missing
70								85C	missing	85
71								60R	missing	missing
72	ND									
73	ND									
74	ND									
75	ND									
76	ND									
77	ND									
78	ND									
79	ND									
80	ND									
81	ND									
82	ND									
83	ND									
84	ND									
85	ND									
86	ND									
87	ND									
88	ND									
89	ND									



Tracer Number	Aug 25, 2012	Sept 3, 2012	Sept 9, 2012	Sept 16, 2012	Oct 17, 2012	Oct 25, 2012	Jan 11, 2013	Jan 28, 2013	Feb 2, 2013	March 3, 2013
90	ND									
91	ND									
92	ND									
93	ND									
94	ND									
95	ND									
96	ND									
97	ND									
98	ND									
99	ND									
100	ND									
101								85C	85	85
102								60C	missing	63.1
103								40C	missing	missing
104								60R	60.34	moved
105								85C	85.03	missing
106								85L	missing	missing
107								85R	85	85.3
108								60L	60.2	moved
109								60C	60.65	67.7
110	40C	40.22	missing	43.3	missing	missing	missing	missing	missing	missing
111	40L	40	40.44	41.33	missing	missing	missing	missing	missing	missing
112	60R	60	60	60.55	missing	missing	missing	missing	122.85	missing
113	85C	85.2	85.58	87.15	missing	missing	missing	missing	missing	missing
114	40R	40	40	40	missing	missing	missing	missing	missing	missing
115	60L	60	60	60	missing	missing	missing	missing	125.9	126.2
116	60R	60	60	62.64	missing	missing	missing	missing	missing	missing
117	85R	85	85	85	missing	missing	missing	missing	missing	missing
118	85L	85	85	85	missing	missing	missing	missing	missing	131.4
119	85R	85	85	85.94	118.48	118.9	118.9	118.9	119.1	119.2
120	85C	85.2	86.22	86.12	missing	missing	missing	missing	missing	missing
121	85C	85.27	85.45	86.89	missing	missing	missing	missing	missing	missing
122	40C	40.45	41.31	missing	missing	missing	missing	missing	missing	missing
123	85L	85	85	85.81	missing	missing	missing	missing	missing	missing
124	40R	40	40	40.62	103.7	105.15	105.15	105.15	missing	missing
125	40L	40	40	41.49	missing	missing	missing	missing	missing	missing
126	85R	85	85	85.39	88.04	87.8	87.8	87.8	87.8	missing
127	85L	85	85	85	missing	missing	missing	missing	missing	missing
128	60R	60.18	60.18	63.02	145.6	146.5	146.5	146.5	missing	missing
129	60R	60	60	62.05	missing	missing	missing	missing	missing	missing
130	60R	60	60	60.17	moved	missing	missing	missing	missing	missing
131	60L	60	60	61.61	missing	missing	missing	missing	missing	missing
132	60R	60.63	60.63	82.35	missing	missing	missing	missing	missing	missing
133	40C	41.01	41.05	45.01	missing	missing	missing	missing	missing	missing
134	40L	40.1	40.16	40.5	missing	missing	missing	missing	98.9	99.2
135	60L	60	60	missing	101.8	missing	missing	missing	103.3	103.5
136	40R	40	40	40C	missing	missing	missing	missing	missing	missing

Tracer Number	Aug 25, 2012	Sept 3, 2012	Sept 9, 2012	Sept 16, 2012	Oct 17, 2012	Oct 25, 2012	Jan 11, 2013	Jan 28, 2013	Feb 2, 2013	March 3, 2013
137				60C	missing	missing	missing	missing	missing	missing
138				85C	missing	missing	missing	missing	missing	missing
139				60C	missing	missing	missing	missing	missing	missing
140								40L	40.13	41
141								40R	63.1	missing
142				40C	103.25	103.9	103.9	103.9	missing	missing
143				40C	missing	missing	missing	missing	missing	missing
144				85C	97.65	97.2	97.2	97.2	97.6	missing
145								40C	missing	missing
146								85L	96	96.1
147								40R	missing	81
148								85C	85	85
149								40C	missing	missing
150								60C	73.64	85.4
151								85R	missing	85.3
152								85C	86.25	85.3
153								60C	85.02	missing
154								40L	40.2	moved
155								60R	60.34	moved
156								60L	missing	missing
157								40C	missing	missing
158	ND									
159								60C	missing	moved
160								85C	missing	85.3
161								85L	86.3	missing
162								40R	missing	missing
163								60C	60.13	moved
164								85C	missing	missing
165								40C	missing	missing
166								40C	missing	missing
167								40L	40	41
168	ND									
169	ND							85R	85	85.25
170	ND									
171								60R	60.03	missing
172	ND									
173	ND									
174	ND									
175	ND									
176	ND									
177	ND									
178	ND									
179	ND									
180	ND									
181	ND									
182	ND									

Tracer Number	Aug 25, 2012	Sept 3, 2012	Sept 9, 2012	Sept 16, 2012	Oct 17, 2012	Oct 25, 2012	Jan 11, 2013	Jan 28, 2013	Feb 2, 2013	March 3, 2013
183	ND									
184	ND									
185	ND									
186	ND									
187	ND									
188	ND									
189	ND									
190	ND									
191	ND									
192	ND									
193	ND									
194	ND									
195	ND									
196	ND									
197	ND									
198	ND									
199	ND									
200	ND									
201								60R	62.8	moved
202								60C	missing	missing
203								85C	86.65	85.9
204								85C	85.05	85.3
205								40C	missing	missing
206								85L	85.9	missing
207								60C	missing	missing
208								85R	85	85.2
209								60L	60.45	moved
210	60C	60	60.68	60.68	115.1	missing	missing	missing	missing	missing
211	85C	85.8	85.85	85.7	missing	missing	missing	missing	missing	missing
212	40L	40	40	40	missing	missing	missing	missing	missing	missing
213	60L	60	60	61.3	missing	missing	missing	missing	missing	missing
214	40R	40	40	40	missing	missing	missing	missing	missing	missing
215	85L	85	85	85	missing	missing	missing	missing	missing	missing
216	60R	60	60	65.1	missing	missing	missing	missing	missing	missing
217	85R	85	85	85	missing	missing	missing	missing	missing	missing
218	40C	40.17	40.33	42.57	missing	missing	missing	missing	missing	missing
219	40C	40.3	40.33	48.06	missing	missing	missing	missing	missing	86.5
220	85L	85	85	85.44	missing	missing	missing	missing	missing	missing
221	40L	40	40	41	missing	missing	missing	missing	42.9	43.9
222	85R	85	85	86.42	missing	missing	missing	missing	missing	missing
223	85C	85.29	86.54	86.54	123.1	124.7	124.7	124.7	missing	missing
224	85C	85.3	86	86.48	missing	86.9	86.9	86.9	86.65	87
225	40R	40	40	40	91	90.8	90.8	90.8	90.8	missing
226	85L	85	85	85	missing	missing	missing	missing	missing	missing
227	85R	85	85	85.71	missing	missing	missing	missing	missing	missing
228	60L	60	60	60	missing	missing	missing	missing	missing	missing
229	60C	60	60	62.39	missing	missing	missing	missing	157.8	missing

Tracer Number	Aug 25, 2012	Sept 3, 2012	Sept 9, 2012	Sept 16, 2012	Oct 17, 2012	Oct 25, 2012	Jan 11, 2013	Jan 28, 2013	Feb 2, 2013	March 3, 2013
230	40L	40	40	41.95	missing	missing	missing	missing	55.3	missing
231	60C	60.2	60.21	62.15	missing	125.45	125.45	125.45	missing	missing
232	40C	40.53	41.2	46.45	112.15	missing	missing	missing	missing	missing
233	40R	40	40	40	95.03	94.65	94.65	94.65	96.1	95.1
234	60L	60	60	60	126.08	127.75	127.75	1267.75	128.4	missing
235	60R	60	60	60	missing	missing	missing	missing	missing	missing
236	60R	60	60	60	118.8	118.9	118.9	118.9	116.9	moved
237				40C	missing	missing	missing	missing	missing	missing
238								40C	missing	missing
239				60C	missing	missing	missing	missing	missing	missing
240				40C	134.6	148.8	148.8	148.8	missing	missing
241				85C	missing	missing	missing	missing	missing	missing
242				60C	missing	missing	missing	missing	missing	missing
243								40L	40.08	moved
244								40R	missing	missing
245				85C	missing	missing	missing	missing	missing	missing
246								85L	92.1	93.7
247								40C	missing	missing
248								60R	61.5	moved
249								40R	missing	missing
250								60L	60.45	moved
251								60C	missing	missing
252								40C	missing	missing
253								85C	87	missing
254								40L	40.2	missing
255								85C	85.05	85.7
256								60C	missing	missing
257								85R	85	85.3
258								85R	85	85.3
259								40L	40.44	moved
260								85C	missing	missing
261								85L	108.25	110.1
262								60R	62.85	moved
263								40R	missing	missing
264								40C	missing	missing
265								85C	85.06	85.4
267								60C	61.95	missing
268								40C	missing	missing
269								60L	67.07	missing
270	ND									
271								60C	missing	missing
272	ND									
273	ND									
274	ND									
275	ND									
276	ND									
277	ND									

Tracer Number	Aug 25, 2012	Sept 3, 2012	Sept 9, 2012	Sept 16, 2012	Oct 17, 2012	Oct 25, 2012	Jan 11, 2013	Jan 28, 2013	Feb 2, 2013	March 3, 2013
278	ND									
279	ND									
280	ND									
281	ND									
282	ND									
283	ND									
284	ND									
285	ND									
286	ND									
287	ND									
287	ND									
288	ND									
289	ND									
290	ND									
291	ND									
292	ND									
293	ND									
294	ND									
295	ND									
296	ND									
297	ND									
298	ND									
299	ND									
300	ND									
301								60L	60	missing
302								85L	85.75	missing
303								85C	85	85
304								60C	60	moved
305								60R	64.17	moved
306								60C	66.17	moved
307								85R	85	85.4
308								40C	missing	missing
309								85C	85	85
310	85R	85	85	85	86.8	86.7	86.7	86.7	86.65	87
311	60C	60	60	61.65	missing	missing	missing	missing	missing	missing
312	40R	40	40	40	missing	missing	missing	missing	missing	missing
313	60R	60	60	60.61	147.6	147.75	147.75	147.75	148.4	148.6
314	85C	85.35	85.73	86.55	127.15	127.1	127.1	127.1	128.3	missing
315	85L	85	85	85	125.66	125.7	127.7	127.7	125.35	moved
316	60L	60	60	60	missing	missing	missing	missing	missing	missing
317	40C	40.99	40.99	40.95	149.5	150.3	150.3	150.3	151.5	151.3
318	40L	40	40	40	48.23	missing	missing	missing	48.44	missing
319	40R	40	40	40	missing	missing	missing	missing	missing	missing
320	85C	85.11	86.14	86.16	missing	missing	missing	missing	missing	missing
321	40C	40.25	40.37	45.8	missing	missing	missing	missing	missing	missing
322	85L	85	85	85	missing	missing	missing	missing	117.1	117.4

Tracer Number	Aug 25, 2012	Sept 3, 2012	Sept 9, 2012	Sept 16, 2012	Oct 17, 2012	Oct 25, 2012	Jan 11, 2013	Jan 28, 2013	Feb 2, 2013	March 3, 2013
323	85C	85.25	85.63	87.04	missing	missing	missing	missing	missing	missing
324	40L	40.15	40.24	40.5	56.4	missing	missing	missing	missing	81.4
325	85L	85	85	85.84	102.8	102.6	102.6	102.6	102.3	missing
326	85R	85	85	85.4	88	87.75	87.75	87.75	87.75	90.9
327	85R	85	84.87	84.87	87.57	87.5	87.5	87.5	87.3	87.6
328	60R	60	60	60	missing	missing	missing	missing	150.7	151.7
329	40L	40	40	40	104.73	105.3	105.3	105.3	missing	missing
330	60R	60	60	60	60.34	60.34	60.34	60.34	60.34	moved
331	40R	40	40	43.1	missing	missing	missing	missing	missing	166.9
332	60L	60	60	60	118	118.6	118.6	118.6	missing	missing
333	60C	60	60	67.07	111.6	111.8	111.8	111.8	missing	missing
334	40C	40.34	40.3	47.8	missing	missing	missing	missing	missing	missing
335	60C	60	60.2	61.72	missing	missing	missing	missing	164.1	missing
336	60L	60	60	60	missing	missing	missing	missing	missing	missing
337								40L	40.9	moved
338				85C	91.65	91.45	91.45	91.45	91.4	92
339								40C	missing	missing
340				40C	missing	missing	missing	missing	missing	missing
341				85C	missing	missing	missing	missing	missing	missing
342								40R	missing	missing
343				60C	123.2	123.15	123.15	123.15	120	missing
344				40C	missing	missing	missing	missing	missing	missing
345				60C	missing	missing	missing	missing	missing	missing
346								85L	87	missing
347								60L	67.07	moved
348								60R	60.01	moved
349								85C	86.86	87.3
350	ND									
351								60C	62.83	missing
352								40C	missing	missing
353								60C	65.74	moved
354								40R	missing	missing
355								60C	60.65	moved
356								85R	85	missing
357								85C	87.8	85.35
358								40L	40.62	moved
359								60L	61.95	moved
360								85R	85	85.3
361								85C	88	missing
362								60C	61.87	moved
363								40C	missing	missing
364								40C	missing	missing
365								40R	missing	missing
366								85L	88.1	missing
367								85C	85.85	86.2
368	ND									
369	ND									

\* ND = Not Deployed

## Appendix D-Percent of Tracer Movement per Event

Event #1-September 1, 2012 maximum discharge 2.1 m<sup>3</sup>/s.

Data calculated for all 9 deployment sites.

Amount of Movement No Movement or Missing Tracers per Event	Tracer Size (mm)	Total # of Tracers Deployed	Percent of Size that Moved	Number of Tracers	Average Distance Traveled w/Missing & No Movement Tracers (m)	Average Distance Traveled Including Tracers w/No Movement (m)	Average Distance Traveled Of Only Tracers with Movement (m)	Longest Distance Traveled (m)
29% Movement	16	28	32%	9	0.11	0.12	0.35	0.85
	22.6	27	33%	9	NA	0.12	0.36	1.01
	32	27	26%	7	NA	0.10	0.37	0.8
	45	27	26%	7	NA	0.09	0.35	0.99
70% No Movement	16	28	64%	18	x	x	x	x
	22.6	27	67%	18	x	x	x	x
	32	27	74%	20	x	x	x	x
	45	27	74%	20	x	x	x	x
1% Missing	16	28	4%	1	x	x	x	x
	22.6	27	0%	0	x	x	x	x
	32	27	0%	0	x	x	x	x
	45	27	0%	0	x	x	x	x

Data calculated for individual sites.

Site	Percent Movement	Percent No Movement	Percent Missing
40L	25%	75%	0%
40C	100%	0%	0%
40R	0%	92%	8%
60L	0%	100%	0%
60C	25%	75%	0%
60R	15%	85%	0%
85L	0%	100%	0%
85C	100%	0%	0%
85R	0%	100%	0%



Event #2-September 7, 2012 maximum discharge 2.5 m<sup>3</sup>/s.

Data calculated for all 9 deployment sites.

Amount of Movement No Movement or Missing Tracers per Event	Tracer Size (mm)	Total # of Tracers Deployed	Percent of Size that Moved	Number of Tracers	Average Distance Traveled w/Missing & No Movement Tracers (m)	Average Distance Traveled Including Tracers w/No Movement (m)	Average Distance Traveled Of Only Tracers with Movement (m)	Longest Distance Traveled (m)
32% Movement	16	28	43%	12	0.15	0.16	0.35	1.32
	22.6	27	26%	7	0.11	0.11	0.41	1.02
	32	27	30%	8	NA	0.13	0.44	1.25
	45	27	30%	7	NA	0.04	0.17	1.03
66% No Movement	16	28	50%	14	x	x	x	x
	22.6	27	70%	19	x	x	x	x
	32	27	70%	19	x	x	x	x
	45	27	70%	20	x	x	x	x
2% Missing	16	28	7%	2	x	x	x	x
	22.6	27	4%	1	x	x	x	x
	32	27	0%	0	x	x	x	x
	45	27	0%	0	x	x	x	x

Data calculated for individual sites.

Site	Percent Movement	Percent No Movement	Percent Missing
40L	50%	50%	0%
40C	58%	25%	17%
40R	9%	91%	0%
60L	17%	83%	0%
60C	25%	75%	0%
60R	8%	92%	0%
85L	0%	100%	0%
85C	100%	0%	0%
85R	8%	92%	0%

Event #3-September 15, 2012 maximum discharge 12.5 m<sup>3</sup>/s.

Data calculated for all 9 deployment sites.

Amount of Movement No Movement or Missing Tracers per Event	Tracer Size (mm)	Total # of Tracers Deployed	Percent of Size that Moved	Number of Tracers	Average Distance Traveled w/Missing & No Movement Tracers (m)	Average Distance Traveled Including Tracers w/No Movement (m)	Average Distance Traveled Of Only Tracers with Movement (m)	Longest Distance Traveled (m)
57% Movement	16	27	63%	17	0.78	0.91	1.23	4.04
	22.6	26	69%	18	1.54	1.67	2.22	21.72
	32	27	52%	14	NA	1.18	2.27	7.73
	45	27	48%	13	NA	1.15	2.31	7.51
36% No Movement	16	27	15%	4	x	x	x	x
	22.6	26	23%	6	x	x	x	x
	32	27	48%	13	x	x	x	x
	45	27	52%	14	x	x	x	x
7% Missing	16	27	22%	6	x	x	x	x
	22.6	26	8%	2	x	x	x	x
	32	27	0%	0	x	x	x	x
	45	27	0%	0	x	x	x	x

Data calculated for individual sites.

Site	Movement	No Movement	Missing
40L	67%	25%	8%
40C	80%	0%	20%
40R	36%	64%	0%
60L	42%	50%	8%
60C	92%	8%	0%
60R	62%	38%	0%
85L	25%	58%	17%
85C	84%	8%	8%
85R	58%	42%	0%

Event #4-October 14, 2012 maximum discharge 43.1 m<sup>3</sup>/s.

Data calculated for all 9 deployment sites.

Amount of Movement No Movement or Missing Tracers per Event	Tracer Size (mm)	Total # of Tracers Deployed	Percent of Size that Moved	Number of Tracers	Average Distance Traveled w/Missing & No Movement Tracers (m)	Average Distance Traveled Including Tracers w/No Movement (m)	Average Distance Traveled Of Only Tracers with Movement (m)	Longest Distance Traveled (m)
30% Movement	16	34	21%	7	13.10	NA	63.58	81.1
	22.6	31	19%	6	8.28	NA	42.79	82.58
	32	33	24%	6	14.61	NA	60.27	94.6
	45	33	48%	16	17.04	NA	35.14	108.55
0% No Movement	16	34	0%	0	x	x	x	x
	22.6	31	0%	0	x	x	x	x
	32	33	0%	0	x	x	x	x
	45	33	0%	0	x	x	x	x
70% Missing	16	34	79%	27	x	x	x	x
	22.6	31	81%	25	x	x	x	x
	32	33	76%	25	x	x	x	x
	45	33	52%	17	x	x	x	x

Data calculated for individual sites.

Site	Percent Movement	Percent No Movement	Percent Missing
40L	27%	0%	73%
40C	28%	0%	72%
40R	27%	0%	73%
60L	27%	0%	73%
60C	40%	0%	60%
60R	33%	0%	67%
85L	20%	0%	80%
85C	21%	0%	79%
85R	42%	0%	58%

Event #5 -October 23, 2012 maximum discharge 9.5 m<sup>3</sup>/s.

Data calculated for all 9 deployment sites.

Amount of Movement No Movement or Missing Tracers per Event	Tracer Size (mm)	Total # of Tracers Deployed	Percent of Size that Moved	Number of Tracers	Average Distance Traveled w/Missing & No Movement Tracers (m)	Average Distance Traveled Including Tracers w/No Movement (m)	Average Distance Traveled Of Only Tracers with Movement (m)	Longest Distance Traveled (m)
81% Movement	16	7	43%	3	1.45	1.69	3.37	9.77
	22.6	10	60%	6	0.22	NA	0.37	1.45
	32	8	75%	6	2.15	NA	2.83	14.2
	45	17	59%	10	0.13	0.14	0.22	0.80
5% No Movement	16	7	14%	1	x	x	x	x
	22.6	10	0%	0	x	x	x	x
	32	8	0%	0	x	x	x	x
14% Missing	45	16	29%	5	x	x	x	x
	16	7	14%	1	x	x	x	x
	22.6	10	0%	0	x	x	x	x
	32	8	25%	2	x	x	x	x
	45	16	12%	2	x	x	x	x

Data calculated for individual sites.

Site	Percent Movement	Percent No Movement	Percent Missing
40L	33%	0%	67%
40C	80%	0%	20%
40R	100%	0%	0%
60L	75%	0%	25%
60C	50%	25%	25%
60R	50%	50%	0%
85L	50%	50%	0%
85C	75%	25%	0%
85R	80%	20%	0%

January 11, 2013 maximum discharge 0.04 m<sup>3</sup>/s.

This flow event did not move any tracers.

Event #6-January 29, 2013 maximum discharge 10.6 m<sup>3</sup>/s.

Data calculated for all 9 deployment sites.

Amount of Movement No Movement or Missing Tracers per Event	Tracer Size (mm)	Total # of Tracers Deployed	Percent of Size that Moved	Number of Tracers	Average Distance Traveled w/Missing & No Movement Tracers (m)	Average Distance Traveled Including Tracers w/No Movement (m)	Average Distance Traveled Of Only Tracers with Movement (m)	Longest Distance Traveled (m)
44% Movement	16	43	26%	11	0.97	2.99	3.81	9.5
	22.6	41	41%	17	1.41	2.52	3.41	25.02
	32	44	50%	22	1.01	1.71	2.02	23.25
	45	42	50%	21	0.78	1.06	1.56	6.17
12% No Movement	16	43	7%	3	x	x	x	x
	22.6	41	15%	6	x	x	x	x
	32	44	9%	4	x	x	x	x
44% Missing	45	42	24%	10	x	x	x	x
	16	43	67%	29	x	x	x	x
	22.6	41	44%	18	x	x	x	x
	32	44	41%	18	x	x	x	x
	45	42	26%	11	x	x	x	x

Data calculated for individual sites.

Site	Percent Movement	Percent No Movement	Percent Missing
40L	66%	17%	17%
40C	4%	0%	96%
40R	19%	81%	0%
60L	64%	0%	36%
60C	47%	6%	47%
60R	69%	12%	19%
85L	86%	0%	14%
85C	55%	17%	28%
85R	6%	76%	18%

## Appendix E-Data for Cross-Sections and Boundary Shear Stress vs. Water Depth and Discharge

Data for the riffle cross-section, at 40 m.

Stage (m)	Discharge (m <sup>3</sup> /s)	Area (m <sup>2</sup> )	Wetted Perimeter (m)	Hydraulic Radius (m)	Boundary Shear Stress (N/m <sup>2</sup> )
0.25	0.79	1.36	6.86	0.20	6.04
0.50	2.74	2.98	7.75	0.38	11.68
0.75	5.5	4.90	8.71	0.56	17.11
1.00	8.63	6.74	10.24	0.66	20.02
1.25	12.81	8.86	11.52	0.77	23.40
1.50	17.87	11.19	12.80	0.87	26.60
1.75	23.85	13.89	14.13	0.98	29.89
2.00	29.9	16.84	16.23	1.04	31.55
2.25	36.24	20.31	19.22	1.06	32.12

Data for the pool cross-section, at 60 m.

Stage (m)	Discharge (m <sup>3</sup> /s)	Area (m <sup>2</sup> )	Wetted Perimeter (m)	Hydraulic Radius (m)	Boundary Shear Stress (N/m <sup>2</sup> )
0.25	0.04	0.12	1.37	0.09	2.68
0.50	0.62	1.35	10.13	0.13	4.04
0.75	3.33	4.10	11.25	0.36	11.07
1.00	7.00	6.58	12.12	0.54	16.52
1.25	11.57	9.16	12.98	0.71	21.45
1.5	15.79	11.92	15.73	0.76	23.03

Data for the glide cross-section, at 85 m.

Stage (m)	Discharge (m <sup>3</sup> /s)	Area (m <sup>2</sup> )	Wetted Perimeter (m)	Hydraulic Radius (m)	Boundary Shear Stress (N/m <sup>2</sup> )
0.25	0.43	0.86	4.79	0.18	5.45
0.50	1.80	2.15	6.11	0.35	10.69
0.75	4.02	3.88	7.12	0.55	16.58
1.00	6.66	5.90	9.70	0.61	18.49
1.25	10.98	8.26	10.78	0.77	23.29
1.50	15.88	10.90	12.63	0.86	26.23
1.75	22.25	14.80	14.52	0.98	29.69
2.00	30.13	17.87	16.03	1.11	33.89

## Appendix F-Longitudinal Profile and Cross-Section Data

### Longitudinal Profile April 17, 2012

Distance (m)	"Relative" Elevation (m)	Location Description	Distance (m)	"Relative" Elevation (m)	Location Description
-30	1	Upstream	58	0.25	
-28	0.87		60	0.27	
-26	0.74		62	0.23	
-24	0.71		65	0.2	
-22	0.62		66.8	0.19	
-20	0.62		70	0.29	
-18	0.57		73	0.3	
-16	0.51		76	0.33	
-14	0.56		78	0.3	
-12	0.61		80	0.32	
-10	0.68		81.5	0.28	
-8	0.77		83.3	0.23	
-6	0.92		85	0.22	
-4.5	1.29		88	0.32	
-1.4	1.29		91	0.43	
0	1.29	Downstream edge of low water bridge	95	0.36	
1.5	0.34		97.5	0.38	
3	0.19		99	0.37	
5	0.24		101	0.39	
7	0.23		102.2	0.22	
9	0.3		105	0.38	
10.5	0.41		107	0.35	
12	0.5		109	0.25	
14	0.5		111	0.3	
16	0.59		113	0.22	
18	0.63		114.7	0.17	
20	0.72		117	0	
23	0.76		118.5	0.08	
25	0.57		120	0.05	
27	0.58		122	0.23	
29	0.53		123.7	0.21	
30	0.34		125	0.12	
31	0.22		127	0.09	
32	0.25		129	0.08	
33	0.34		132	0.03	Downstream
35	0.53				
37	0.5				
40	0.43				
42	0.44				
46	0.33				
49	0.29				
52	0.25				
55	0.23				

**Longitudinal Profile March 7, 2012**

Distance (m)	"Relative" Elevation (m)	Location Description	Distance (m)	"Relative" Elevation	Location Description
-12	0.71	Upstream	78	0.47	
-10	0.7		80	0.44	
-8	0.92		82	0.44	
-6	1.02		85	0.46	
-5.2	1.06		87	0.49	
-4.5	1.36		91	0.57	
-1.2	1.34		95	0.56	
-0.6	1.06		98.6	0.4	
0	0.54	Downstream edge of low water bridge	100	0.34	
2	0.38		102	0.37	
3.6	0.13		104.5	0.4	
4.6	0.36		106.3	0.39	
6	0.56		108	0.39	
8	0.54		109.8	0.4	
10	0.77		111.3	0.32	
11.5	1.12		114	0.18	
13	0.93		117	0.07	
15	0.62		118.7	0.27	
17.3	0.66		121	0.37	
18.4	0.78		122.8	0.22	
20.3	0.84		124.5	0.22	
23	0.81		126	0.19	
25	0.81		129	0.11	
28	0.8		132	0.24	
30.2	0.71		135	0.46	
31.5	0.53		139	0.26	
33.5	0.55		142	0.49	
36	0.56		144	0.25	
38	0.46		145.8	0.27	
39.8	0.56		148	0.4	
40	0.6		151	0.43	
42	0.51		155	0.37	
45	0.45		158	0.22	
46.4	0.4		161.5	0.14	
48	0.35		164	0.02	
50	0.35		169	0	
52	0.35		172	0.11	
54	0.39		175	0.2	
56	0.37		178	0.27	
59	0.37		182	0.22	Downstream
59.9	0.36				
62	0.39				
65	0.39				
67	0.38				
71	0.4				
74	0.45				

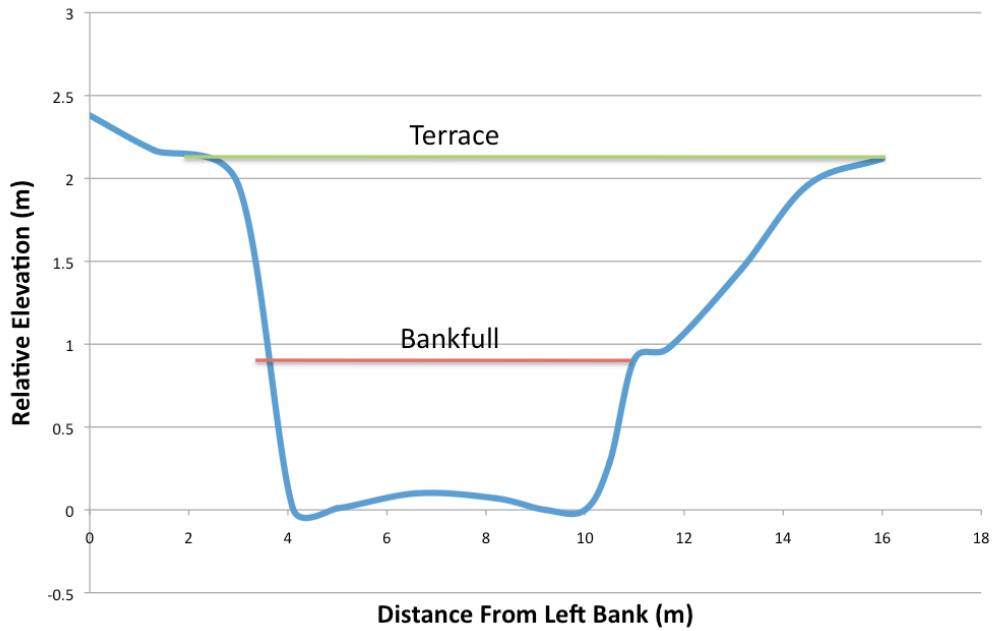


**Riffle Cross-Section (Recorded at 40 m on tapeline)**

Distance (m)	“Relative” Elevation (m)	Location Description
0	2.38	Left Bank
1.3	2.17	
3	1.96	
4.1	0.01	
5	0.01	
6.6	0.1	
8.2	0.07	
9.2	0	
10	0	
10.5	0.29	
11	0.91	
11.7	0.98	
13.15	1.45	
14.5	1.96	
16	2.12	Right Bank

Riffle cross-section data

	Mean Depth (m)	Q (m <sup>3</sup> /s)	Area (m <sup>2</sup> )	Velocity (m/s)	Wetted Perimeter (m)	Top Width (m)	Hydraulic Radius (m)	Recurrence Interval
Bankfull	0.95	7.97	6.25	1.27	8.73	7.82	0.72	1.07 Year
Terrace	2.19	34.32	19.39	1.77	16.58	14.9	1.17	4 Year



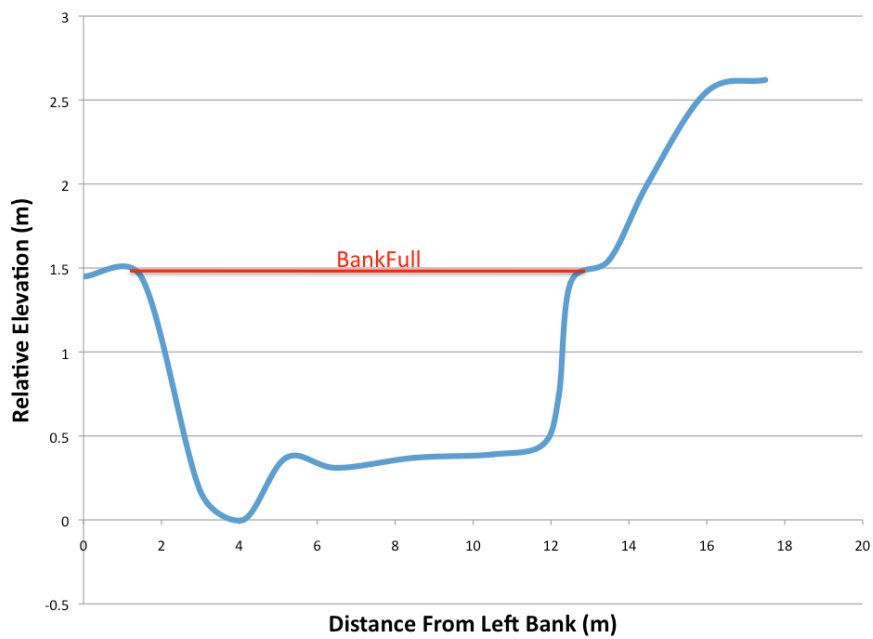
Riffle cross-section

**Pool Cross-Section (Recorded at 60 m on tapeline)**

Distance (m)	“Relative” Elevation (m)	Location Description
0	1.45	Left Bank
1.5	1.44	
3	0.17	
4.1	0	
5.2	0.37	
6.5	0.31	
8.5	0.37	
10.5	0.39	
11.8	0.45	
12.2	0.74	
12.5	1.41	
13.5	1.55	
14.5	2.01	
16	2.55	
17.5	2.62	Right Bank

Pool cross-section data

	Mean Depth (m)	Q (m <sup>3</sup> /s)	Area (m <sup>2</sup> )	Velocity (m/s)	Wetted Perimeter (m)	Top Width (m)	Hydraulic Radius (m)	Recurrence Interval
Bankfull	1.46	17.68	11.65	1.52	12.53	11.47	0.93	1.6



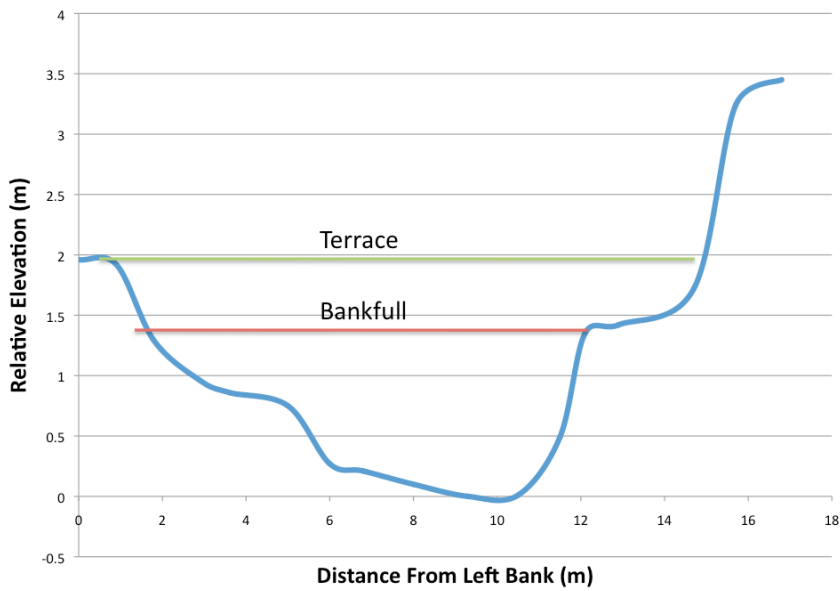
Pool cross-section

**Glide Cross-Section (Recorded at 85 m on tapeline)**

Distance (m)	"Relative" Elevation (m)	Location Description
0	1.96	Left Bank
0.9	1.92	
1.8	1.29	
2.9	0.96	
3.6	0.86	
5	0.75	
6	0.27	
6.8	0.21	
8	0.1	
9.3	0	
10.5	0.01	
11.5	0.49	
12.1	1.35	
12.9	1.42	
14.7	1.72	
15.7	3.24	
16.8	3.45	Right Bank

Glide cross-section data

	Mean Depth (m)	Q (m <sup>3</sup> /s)	Area (m <sup>2</sup> )	Velocity (m/s)	Wetted Perimeter (m)	Top Width (m)	Hydraulic Radius (m)	Recurrence Interval
Bankfull	1.4	13.91	9.85	1.41	11.81	11.03	0.83	1.35 Years
Terrace	1.95	28.17	16.96	1.66	15.96	14.85	1.06	3 Years



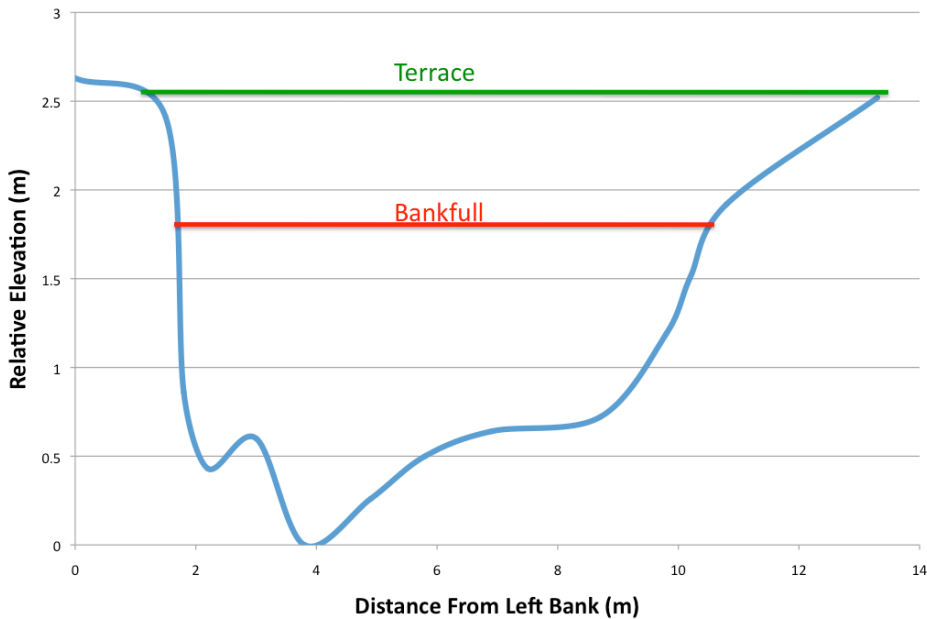
Glide cross-section

**Gage Cross-Section (Recorded at 80 m upstream of downstream edge of low water bridge)**

Distance (m)	“Relative” Elevation (m)	Location Description
0	2.63	Left Bank
1.5	2.41	
1.8	0.86	
2.2	0.43	
3	0.6	
3.8	0	
4.9	0.26	
5.8	0.5	
6.9	0.64	
8.7	0.72	
9.8	1.19	
10.2	1.51	
10.8	1.92	
13.3	2.52	

Gage cross-section

	Mean Depth (m)	Q (m <sup>3</sup> /s)	Area (m <sup>2</sup> )	Velocity (m/s)	Wetted Perimeter (m)	Top Width (m)	Hydraulic Radius (m)	Recurrence Interval
Bankfull	1.9	19.12	11.55	1.66	10.90	9.21	1.06	1.8 Year
Terrace	2.56	33.5	18.39	1.82	15.05	12.88	1.22	3.6 Year



Gage cross-section

## Appendix G-Pebble Count Data

Entire Reach Pebble Count - Sample point locations were from the left bank toe

Cross Section Number	Distance (m)	Width (m)	0 m	0.5 m	1.0 m	1.5 m	2 m	2.5 m	3.0 m	3.5 m	4 m	4.5 m	5.0 m	5.5 m	6.0 m	6.5 m
1	18	5	f	9	8	20	40	18	21	10	10	8	18			
2	21	5	f	24	R	11	16	32	48	28	12	50	8			
3	24	5.6	f	120	45	18	25	13	180	45	90	16	80	24		
4	27	5.7	f	2	30	42	40	30	16	90	20	150	30	50		
5	30	5.9	f	f	58	180	20	18	32	20	10	7	11	8		
6	33	5.5	20	f	R	18	30	24	30	64	50	90	28	18		
7	36	5.9	f	12	200	10	34	9	13	19	16	14	9	26		
8	39	6	f	2	f	16	6	4	8	30	32	22	20	35	f	
9	42	5.7	f	20	12	22	20	38	15	10	35	2	8	16		
10	45	5.9	f	16	15	16	28	50	25	12	16	100	20	f		
11	48	6	f	40	35	10	25	22	80	15	f	300	20	f	f	
12	51	6	f	24	48	30	9	20	40	2	20	4	6	f	f	
13	54	6	6	4	7	8	30	40	20	40	32	150	20	100	240	
14	57	6	Br	9	45	60	35	18	28	25	12	40	6	7	65	
15	60	6.5	f	9	10	60	7	16	10	20	16	30	20	8	2	f
16	63	6.5	f	28	6	20	12	20	150	25	20	22	20	20	10	200
17	66	6.5	f	18	20	23	32	30	17	20	22	12	8	f	35	f
18	69	6.7	f	6	45	15	25	4	14	25	15	60	30	10	15	f
19	72	6	f	18	13	30	10	12	10	30	35	f	25	26	f	
20	75	6.2	f	14	28	18	60	20	20	70	15	f	8	f	f	
21	78	6.5	14	10	8	10	16	25	16	18	16	22	22	22	20	5
22	81	5.8	f	20	20	150	22	10	14	Br	45	Br	45	20		
23	84	5.5	f	25	20	14	50	10	Br	18	30	Br	70	Br		
24	87	5.5	10	70	22	20	50	46	42	20	30	35	32	35		
25	90	6.1	10	22	10	75	14	8	20	100	80	15	22	25	6	
26	93	5.8	f	10	14	6	12	34	25	22	10	32	f	40		
27	96	5.8	f	100	f	Br	Br	18	Br	18	50	Br	Br	32		
28	99	5.6	22	26	Br	13	Br	240	18	70	60	Br	Br	20		

Study Reach Pebble Count – Modified Rosgen pebble count for entire study reach from tapeline 0 m to 99m

Size-Diameter of B axis (mm)	Number	Percent
2	9	3.1
5.6	24	8.2
8	32	10.9
11	44	15
16	65	22.2
22.6	51	17.4
32	24	8.2
45	16	5.5
64	12	4.1
90	5	1.7
128	6	2
>200	5	1.7

Riffle Pebble Count (40 m on tapeline)

Size-Diameter of B Axis (mm)	Number	Percent
0	3	10
2	1	3
4	1	3
5.6	2	7
8	5	17
11	4	13
16	5	17
22.6	2	7
32	6	20
45	1	3

Glide Pebble Count (60 m on tapeline)

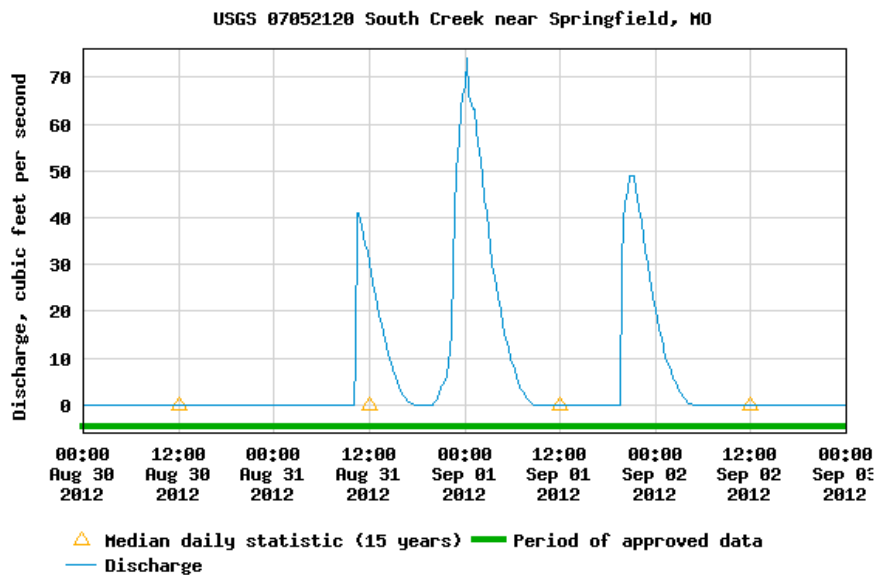
Size-Diameter of B Axis (mm)	Number	Percent
0	2	7
2	1	3
2.8	2	7
4	2	7
5.6	7	22
8	3	10
11	2	7
16	5	17
22.6	2	7
32	3	10
45	1	3

Pool Pebble Count (85 m on tapeline)

Size-Diameter of B Axis (mm)	Number	Percent
0	3	10
2	3	10
4	5	16
5.6	2	6
6.4	1	3
8	3	10
11	3	10
16	5	16
22.6	2	6
32	1	3
45	1	3
64	2	6

# Appendix H-Flow Event Data from Gage #07052120 South Creek near Springfield, MO

## Event #1-September 1, 2012 Event

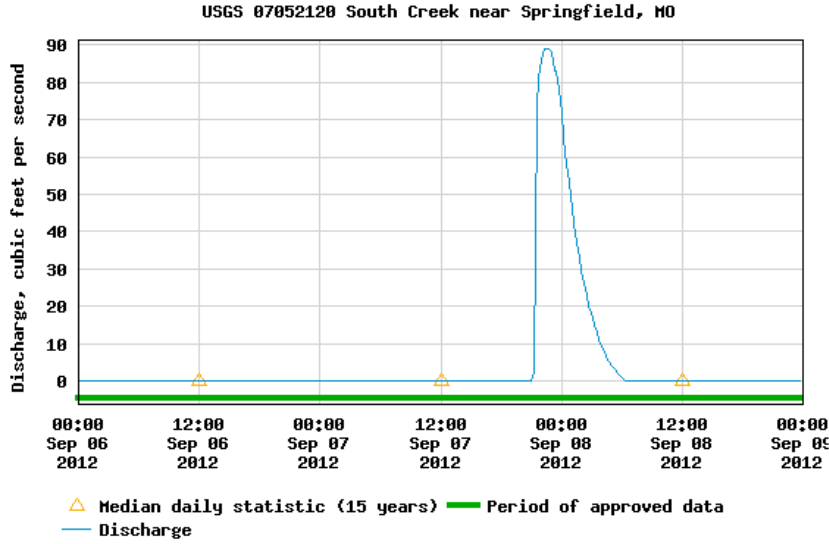


Date and Time	Discharge (m <sup>3</sup> /s)
08/31/2012 20:15 CDT	0.01
08/31/2012 20:30 CDT	0.0
08/31/2012 20:45 CDT	0.07
08/31/2012 21:00 CDT	0.10
08/31/2012 21:15 CDT	0.12
08/31/2012 21:30 CDT	0.14
08/31/2012 21:45 CDT	0.18
08/31/2012 22:00 CDT	0.25
08/31/2012 22:15 CDT	0.43
08/31/2012 22:30 CDT	0.85
08/31/2012 22:45 CDT	1.16
08/31/2012 23:00 CDT	1.42
08/31/2012 23:15 CDT	1.61
08/31/2012 23:30 CDT	1.78
08/31/2012 23:45 CDT	1.87
09/01/2012 00:00 CDT	1.92
09/01/2012 00:15 CDT	2.09
09/01/2012 00:30 CDT	1.87
09/01/2012 00:45 CDT	1.84
09/01/2012 01:00 CDT	1.78
09/01/2012 01:15 CDT	1.78
09/01/2012 01:30 CDT	1.67
09/01/2012 01:45 CDT	1.59
09/01/2012 02:00 CDT	1.47
09/01/2012 02:15 CDT	1.39
09/01/2012 02:30 CDT	1.25
09/01/2012 02:45 CDT	1.16

<b>Date and Time</b>	<b>Discharge (m<sup>3</sup>/s)</b>
09/01/2012 03:00 CDT	1.05
09/01/2012 03:15 CDT	0.96
09/01/2012 03:30 CDT	0.85
09/01/2012 03:45 CDT	0.76
09/01/2012 04:00 CDT	0.71
09/01/2012 04:15 CDT	0.65
09/01/2012 04:30 CDT	0.57
09/01/2012 04:45 CDT	0.48
09/01/2012 05:00 CDT	0.43
09/01/2012 05:15 CDT	0.40
09/01/2012 05:30 CDT	0.34
09/01/2012 05:45 CDT	0.283
09/01/2012 06:00 CDT	0.25
09/01/2012 06:15 CDT	0.21
09/01/2012 06:30 CDT	0.17
09/01/2012 06:45 CDT	0.14
09/01/2012 07:00 CDT	0.11
09/01/2012 07:15 CDT	0.09
09/01/2012 07:30 CDT	0.06
09/01/2012 07:45 CDT	0.04
09/01/2012 08:00 CDT	0.03
09/01/2012 08:15 CDT	0.02
09/01/2012 08:30 CDT	0.01



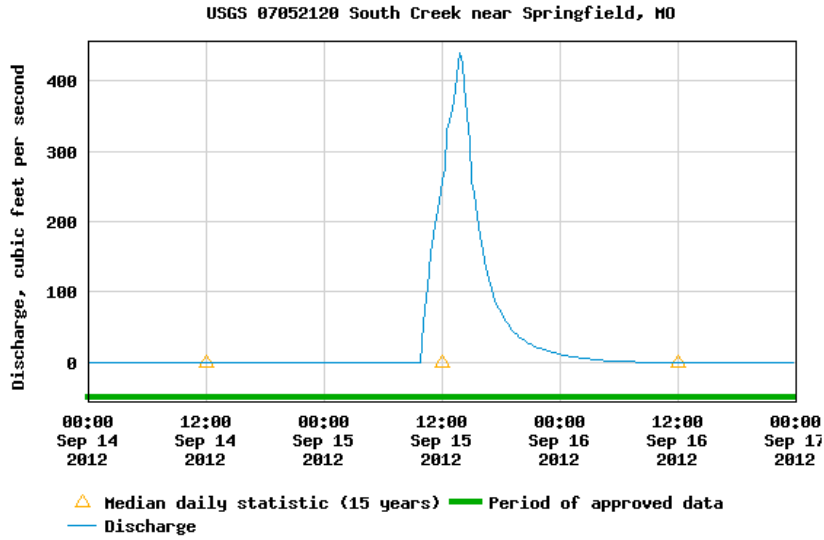
Event #2-September 7, 2012 Event



Date and Time	Discharge (m <sup>3</sup> /s)
09/07/2012 21:15 CDT	0.07
09/07/2012 21:30 CDT	2.07
09/07/2012 21:45 CDT	2.29
09/07/2012 22:00 CDT	2.43
09/07/2012 22:15 CDT	2.52
09/07/2012 22:30 CDT	2.52
09/07/2012 22:45 CDT	2.52
09/07/2012 23:00 CDT	2.49
09/07/2012 23:15 CDT	2.35
09/07/2012 23:30 CDT	2.35
09/07/2012 23:45 CDT	2.21
09/08/2012 00:00 CDT	2.04
09/08/2012 00:15 CDT	1.84
09/08/2012 00:30 CDT	1.64
09/08/2012 00:45 CDT	1.50
09/08/2012 01:00 CDT	1.30
09/08/2012 01:15 CDT	1.19
09/08/2012 01:30 CDT	1.05
09/08/2012 01:45 CDT	0.93
09/08/2012 02:00 CDT	0.82
09/08/2012 02:15 CDT	0.74
09/08/2012 02:30 CDT	0.65
09/08/2012 02:45 CDT	0.57
09/08/2012 03:00 CDT	0.51
09/08/2012 03:15 CDT	0.43
09/08/2012 03:30 CDT	0.37
09/08/2012 03:45 CDT	0.31
09/08/2012 04:00 CDT	0.26
09/08/2012 04:15 CDT	0.22
09/08/2012 04:30 CDT	0.18
09/08/2012 04:45 CDT	0.14
09/08/2012 05:00 CDT	0.11

<b>Date and Time</b>	<b>Discharge (m<sup>3</sup>/s)</b>
09/08/2012 05:15 CDT	0.09
09/08/2012 05:30 CDT	0.06
09/08/2012 05:45 CDT	0.04
09/08/2012 06:00 CDT	0.03
09/08/2012 06:15 CDT	0.02
09/08/2012 06:30 CDT	0.01

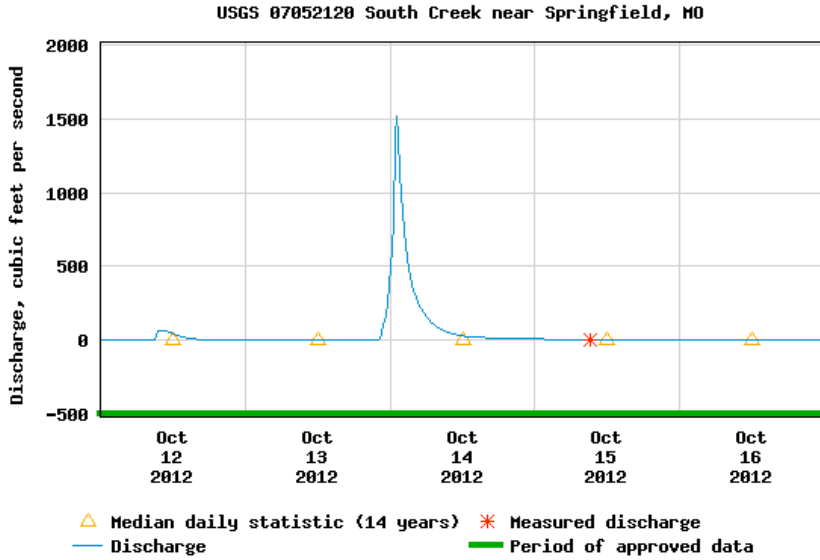
Event #3-September 15, 2012 Event



Date and Time	Discharge (m <sup>3</sup> /s)
09/15/2012 10:00 CDT	1.56
09/15/2012 10:15 CDT	2.09
09/15/2012 10:30 CDT	3.03
09/15/2012 10:45 CDT	4.36
09/15/2012 11:00 CDT	4.79
09/15/2012 11:15 CDT	5.55
09/15/2012 11:30 CDT	6.11
09/15/2012 11:45 CDT	6.45
09/15/2012 12:00 CDT	7.30
09/15/2012 12:15 CDT	7.75
09/15/2012 12:30 CDT	9.34
09/15/2012 12:45 CDT	9.71
09/15/2012 13:00 CDT	10.24
09/15/2012 13:15 CDT	10.53
09/15/2012 13:30 CDT	11.49
09/15/2012 13:45 CDT	12.45
09/15/2012 14:00 CDT	12.06
09/15/2012 14:15 CDT	11.15
09/15/2012 14:30 CDT	9.93
09/15/2012 14:45 CDT	8.86
09/15/2012 15:00 CDT	7.30
09/15/2012 15:15 CDT	6.76
09/15/2012 15:30 CDT	5.89
09/15/2012 15:45 CDT	5.43
09/15/2012 16:00 CDT	4.78
09/15/2012 16:15 CDT	4.10
09/15/2012 16:30 CDT	3.79
09/15/2012 16:45 CDT	3.31
09/15/2012 17:00 CDT	2.97
09/15/2012 17:15 CDT	2.66
09/15/2012 17:30 CDT	2.35
09/15/2012 17:45 CDT	2.12
09/15/2012 18:00 CDT	1.92
09/15/2012 18:15 CDT	1.81

<b>Date and Time</b>	<b>Discharge (m<sup>3</sup>/s)</b>
09/15/2012 18:30 CDT	1.64
09/15/2012 18:45 CDT	1.50
09/15/2012 19:00 CDT	1.33
09/15/2012 19:15 CDT	1.22
09/15/2012 19:30 CDT	1.13
09/15/2012 19:45 CDT	1.02
09/15/2012 20:00 CDT	0.96
09/15/2012 20:15 CDT	0.91
09/15/2012 20:30 CDT	0.85
09/15/2012 20:45 CDT	0.76
09/15/2012 21:00 CDT	0.74
09/15/2012 21:15 CDT	0.71
09/15/2012 21:30 CDT	0.65
09/15/2012 21:45 CDT	0.59
09/15/2012 22:00 CDT	0.57
09/15/2012 22:15 CDT	0.54
09/15/2012 22:30 CDT	0.45
09/15/2012 22:45 CDT	0.45
09/15/2012 23:00 CDT	0.40
09/15/2012 23:15 CDT	0.40
09/15/2012 23:30 CDT	0.37
09/15/2012 23:45 CDT	0.34
09/16/2012 00:00 CDT	0.34
09/16/2012 00:15 CDT	0.28
09/16/2012 00:30 CDT	0.28
09/16/2012 00:45 CDT	0.26
09/16/2012 01:00 CDT	0.24
09/16/2012 01:15 CDT	0.23
09/16/2012 01:30 CDT	0.21
09/16/2012 01:45 CDT	0.20
09/16/2012 02:00 CDT	0.18
09/16/2012 02:15 CDT	0.17
09/16/2012 02:30 CDT	0.15
09/16/2012 02:45 CDT	0.14
09/16/2012 03:00 CDT	0.14
09/16/2012 03:15 CDT	0.12
09/16/2012 03:30 CDT	0.11
09/16/2012 03:45 CDT	0.10
09/16/2012 04:00 CDT	0.09
09/16/2012 04:15 CDT	0.08
09/16/2012 04:30 CDT	0.07
09/16/2012 04:45 CDT	0.07
09/16/2012 05:00 CDT	0.06
09/16/2012 05:15 CDT	0.06
09/16/2012 05:30 CDT	0.05
09/16/2012 05:45 CDT	0.05
09/16/2012 06:00 CDT	0.04
09/16/2012 06:15 CDT	0.03
09/16/2012 06:30 CDT	0.03
09/16/2012 06:45 CDT	0.03
09/16/2012 07:00 CDT	0.02
09/16/2012 07:15 CDT	0.02
09/16/2012 07:30 CDT	0.02
09/16/2012 07:45 CDT	0.01
09/16/2012 08:00 CDT	0.01
09/16/2012 08:15 CDT	0.01
09/16/2012 08:30 CDT	0.01

Event #4-October 14, 2012 Event



Date and Time	Discharge (m <sup>3</sup> /s)
10/13/2012 22:15 CDT	0.23
10/13/2012 22:30 CDT	1.08
10/13/2012 22:45 CDT	2.86
10/13/2012 23:00 CDT	3.65
10/13/2012 23:15 CDT	5.01
10/13/2012 23:30 CDT	6.71
10/13/2012 23:45 CDT	10.92
10/14/2012 00:00 CDT	13.30
10/14/2012 00:15 CDT	18.17
10/14/2012 00:30 CDT	22.44
10/14/2012 00:45 CDT	39.05
10/14/2012 01:00 CDT	43.02
10/14/2012 01:15 CDT	39.34
10/14/2012 01:30 CDT	31.98
10/14/2012 01:45 CDT	28.30
10/14/2012 02:00 CDT	24.28
10/14/2012 02:15 CDT	20.97
10/14/2012 02:30 CDT	18.17
10/14/2012 02:45 CDT	15.65
10/14/2012 03:00 CDT	13.30
10/14/2012 03:15 CDT	12.45
10/14/2012 03:30 CDT	10.47
10/14/2012 03:45 CDT	9.65
10/14/2012 04:00 CDT	8.72
10/14/2012 04:15 CDT	8.04
10/14/2012 04:30 CDT	7.13
10/14/2012 04:45 CDT	6.51
10/14/2012 05:00 CDT	6.06
10/14/2012 05:15 CDT	5.55
10/14/2012 05:30 CDT	5.15
10/14/2012 05:45 CDT	4.75
10/14/2012 06:00 CDT	4.30

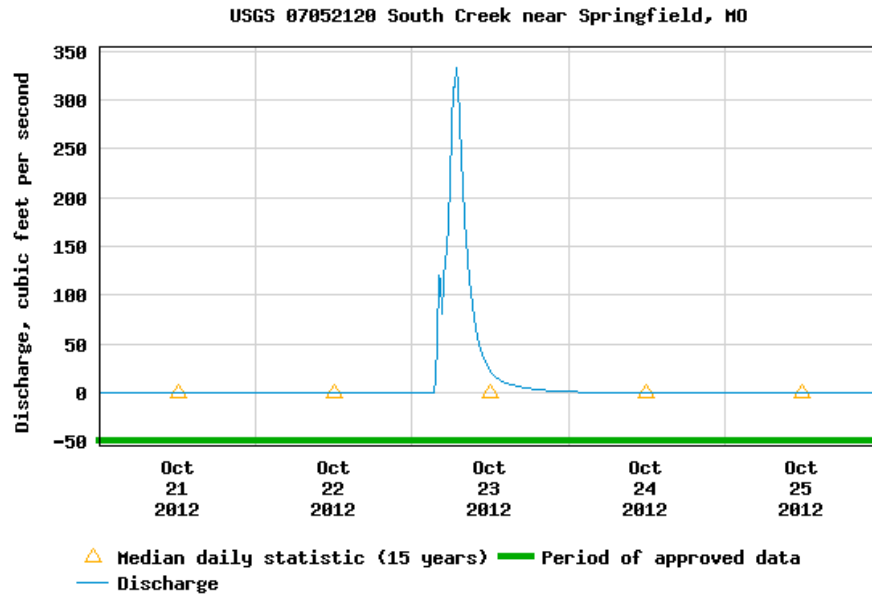
<b>Date and Time</b>	<b>Discharge (m<sup>3</sup>/s)</b>
10/14/2012 06:15 CDT	3.96
10/14/2012 06:30 CDT	3.65
10/14/2012 06:45 CDT	3.31
10/14/2012 07:00 CDT	3.11
10/14/2012 07:15 CDT	2.86
10/14/2012 07:30 CDT	2.63
10/14/2012 07:45 CDT	2.43
10/14/2012 08:00 CDT	2.29
10/14/2012 08:15 CDT	2.12
10/14/2012 08:30 CDT	1.98
10/14/2012 08:45 CDT	1.84
10/14/2012 09:00 CDT	1.73
10/14/2012 09:15 CDT	1.58
10/14/2012 09:30 CDT	1.50
10/14/2012 09:45 CDT	1.42
10/14/2012 10:00 CDT	1.3
10/14/2012 10:15 CDT	1.22
10/14/2012 10:30 CDT	1.16
10/14/2012 10:45 CDT	1.08
10/14/2012 11:00 CDT	1.02
10/14/2012 11:15 CDT	0.93
10/14/2012 11:30 CDT	0.91
10/14/2012 11:45 CDT	0.85
10/14/2012 12:00 CDT	0.82
10/14/2012 12:15 CDT	0.76
10/14/2012 12:30 CDT	0.74
10/14/2012 12:45 CDT	0.71
10/14/2012 13:00 CDT	0.65
10/14/2012 13:15 CDT	0.65
10/14/2012 13:30 CDT	0.59
10/14/2012 13:45 CDT	0.59
10/14/2012 14:00 CDT	0.57
10/14/2012 14:15 CDT	0.57
10/14/2012 14:30 CDT	0.51
10/14/2012 14:45 CDT	0.51
10/14/2012 15:00 CDT	0.51
10/14/2012 15:15 CDT	0.48
10/14/2012 15:30 CDT	0.48
10/14/2012 15:45 CDT	0.48
10/14/2012 16:00 CDT	0.45
10/14/2012 16:15 CDT	0.45
10/14/2012 16:30 CDT	0.45
10/14/2012 16:45 CDT	0.42
10/14/2012 17:00 CDT	0.42
10/14/2012 17:15 CDT	0.42
10/14/2012 17:30 CDT	0.40
10/14/2012 17:45 CDT	0.40
10/14/2012 18:00 CDT	0.40
10/14/2012 18:15 CDT	0.37
10/14/2012 18:30 CDT	0.37
10/14/2012 18:45 CDT	0.37
10/14/2012 19:00 CDT	0.34
10/14/2012 19:15 CDT	0.34
10/14/2012 19:30 CDT	0.34
10/14/2012 19:45 CDT	0.31
10/14/2012 20:00 CDT	0.31
10/14/2012 20:15 CDT	0.31
10/14/2012 20:30 CDT	0.28
10/14/2012 20:45 CDT	0.28
10/14/2012 21:00 CDT	0.28
10/14/2012 21:15 CDT	0.27
10/14/2012 21:30 CDT	0.27
10/14/2012 21:45 CDT	0.26
10/14/2012 22:00 CDT	0.26
10/14/2012 22:15 CDT	0.25
10/14/2012 22:30 CDT	0.25
10/14/2012 22:45 CDT	0.24
10/14/2012 23:00 CDT	0.24
10/14/2012 23:15 CDT	0.23

<b>Date and Time</b>	<b>Discharge (m<sup>3</sup>/s)</b>
10/14/2012 23:30 CDT	0.22
10/14/2012 23:45 CDT	0.22
10/15/2012 00:00 CDT	0.21
10/15/2012 00:15 CDT	0.21
10/15/2012 00:30 CDT	0.21
10/15/2012 00:45 CDT	0.20
10/15/2012 01:00 CDT	0.19
10/15/2012 01:15 CDT	0.19
10/15/2012 01:30 CDT	0.19
10/15/2012 01:45 CDT	0.18
10/15/2012 02:00 CDT	0.18
10/15/2012 02:15 CDT	0.17
10/15/2012 02:30 CDT	0.17
10/15/2012 02:45 CDT	0.16
10/15/2012 03:00 CDT	0.16
10/15/2012 03:15 CDT	0.15
10/15/2012 03:30 CDT	0.15
10/15/2012 03:45 CDT	0.16
10/15/2012 04:00 CDT	0.15
10/15/2012 04:15 CDT	0.15
10/15/2012 04:30 CDT	0.14
10/15/2012 04:45 CDT	0.14
10/15/2012 05:00 CDT	0.14
10/15/2012 05:15 CDT	0.14
10/15/2012 05:30 CDT	0.13
10/15/2012 05:45 CDT	0.13
10/15/2012 06:00 CDT	0.12
10/15/2012 06:15 CDT	0.11
10/15/2012 06:30 CDT	0.11
10/15/2012 06:45 CDT	0.10
10/15/2012 07:00 CDT	0.10
10/15/2012 07:15 CDT	0.09
10/15/2012 07:30 CDT	0.08
10/15/2012 07:45 CDT	0.08
10/15/2012 08:00 CDT	0.08
10/15/2012 08:15 CDT	0.07
10/15/2012 08:30 CDT	0.07
10/15/2012 08:45 CDT	0.07
10/15/2012 09:00 CDT	0.06
10/15/2012 09:15 CDT	0.06
10/15/2012 09:30 CDT	0.06
10/15/2012 09:45 CDT	0.05
10/15/2012 10:00 CDT	0.05
10/15/2012 10:15 CDT	0.05
10/15/2012 10:30 CDT	0.05
10/15/2012 10:45 CDT	0.05
10/15/2012 11:00 CDT	0.04
10/15/2012 11:15 CDT	0.04
10/15/2012 11:30 CDT	0.04
10/15/2012 11:45 CDT	0.04
10/15/2012 12:00 CDT	0.03
10/15/2012 12:15 CDT	0.03
10/15/2012 12:30 CDT	0.03
10/15/2012 12:45 CDT	0.03
10/15/2012 13:00 CDT	0.03
10/15/2012 13:15 CDT	0.03
10/15/2012 13:30 CDT	0.02
10/15/2012 13:45 CDT	0.02
10/15/2012 14:00 CDT	0.02
10/15/2012 14:15 CDT	0.02
10/15/2012 14:30 CDT	0.02
10/15/2012 14:45 CDT	0.02
10/15/2012 15:00 CDT	0.02
10/15/2012 15:15 CDT	0.02
10/15/2012 15:30 CDT	0.02
10/15/2012 15:45 CDT	0.02
10/15/2012 16:00 CDT	0.02
10/15/2012 16:15 CDT	0.03
10/15/2012 16:30 CDT	0.03

<b>Date and Time</b>	<b>Discharge (m<sup>3</sup>/s)</b>
10/15/2012 16:45 CDT	0.03
10/15/2012 17:00 CDT	0.03
10/15/2012 17:15 CDT	0.02
10/15/2012 17:30 CDT	0.02
10/15/2012 17:45 CDT	0.02
10/15/2012 18:00 CDT	0.02
10/15/2012 18:15 CDT	0.02
10/15/2012 18:30 CDT	0.02
10/15/2012 18:45 CDT	0.02
10/15/2012 19:00 CDT	0.02
10/15/2012 19:15 CDT	0.02
10/15/2012 19:30 CDT	0.01
10/15/2012 19:45 CDT	0.01
10/15/2012 20:00 CDT	0.01
10/15/2012 20:15 CDT	0.01
10/15/2012 20:30 CDT	0.01
10/15/2012 20:45 CDT	0.01
10/15/2012 21:00 CDT	0.01



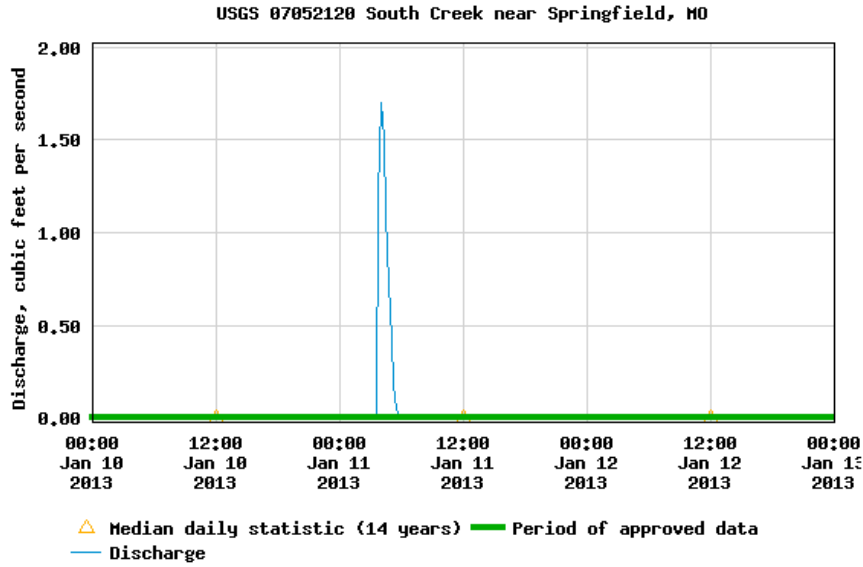
Event #5-October 23, 2012



Date and Time	Discharge (m <sup>3</sup> /s)
10/23/2013 3:30 CDT	0.40
10/23/2013 3:45 CDT	1.56
10/23/2013 4:00 CDT	3.46
10/23/2013 4:15 CDT	3.26
10/23/2013 4:30 CDT	2.32
10/23/2013 4:45 CDT	3.26
10/23/2013 5:00 CDT	3.92
10/23/2013 5:15 CDT	4.12
10/23/2013 5:30 CDT	5.06
10/23/2013 5:45 CDT	6.12
10/23/2013 6:00 CDT	7.78
10/23/2013 6:15 CDT	8.95
10/23/2013 6:30 CDT	8.95
10/23/2013 6:45 CDT	9.52
10/23/2013 7:00 CDT	9.01
10/23/2013 7:15 CDT	8.04
10/23/2013 7:30 CDT	6.84
10/23/2013 7:45 CDT	6.12
10/23/2013 8:00 CDT	5.06
10/23/2013 8:15 CDT	4.49
10/23/2013 8:30 CDT	3.92
10/23/2013 8:45 CDT	3.29
10/23/2013 9:00 CDT	2.97
10/23/2013 9:15 CDT	2.52
10/23/2013 9:30 CDT	2.20
10/23/2013 9:45 CDT	1.89
10/23/2013 10:00 CDT	1.66
10/23/2013 10:15 CDT	1.43
10/23/2013 10:30 CDT	1.26
10/23/2013 10:45 CDT	1.09
10/23/2013 11:00 CDT	0.97
10/23/2013 11:15 CDT	0.89

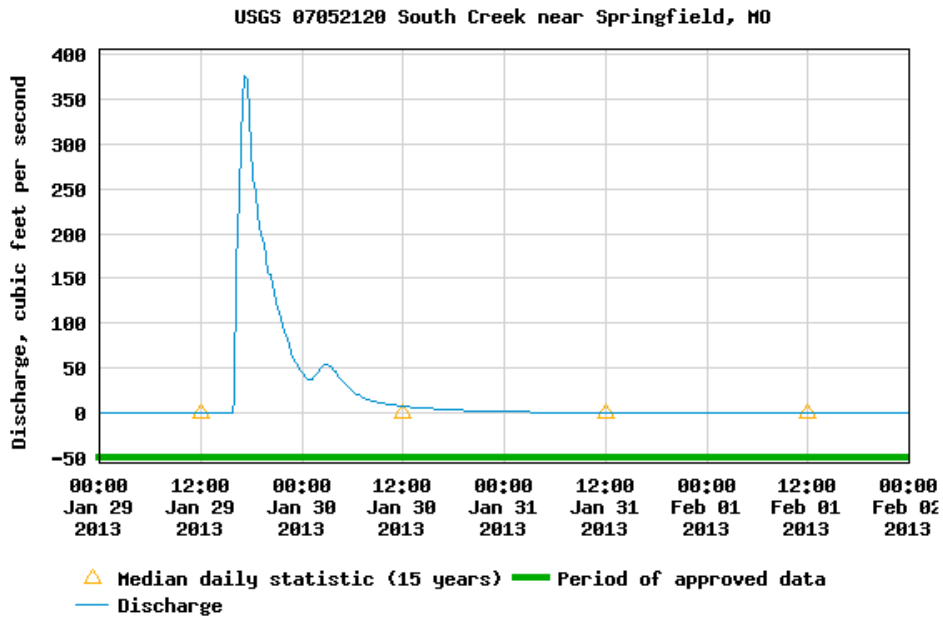
<b>Date and Time</b>	<b>Discharge (m<sup>3</sup>/s)</b>
10/23/2013 11:30 CDT	0.77
10/23/2013 11:45 CDT	0.72
10/23/2013 12:00 CDT	0.63
10/23/2013 12:15 CDT	0.57
10/23/2013 12:30 CDT	0.51
10/23/2013 12:45 CDT	0.49
10/23/2013 13:00 CDT	0.43
10/23/2013 13:15 CDT	0.40
10/23/2013 13:30 CDT	0.37
10/23/2013 13:45 CDT	0.34
10/23/2013 14:00 CDT	0.31
10/23/2013 14:15 CDT	0.29
10/23/2013 14:30 CDT	0.27
10/23/2013 14:45 CDT	0.26
10/23/2013 15:00 CDT	0.24
10/23/2013 15:15 CDT	0.23
10/23/2013 15:30 CDT	0.22
10/23/2013 15:45 CDT	0.21
10/23/2013 16:00 CDT	0.19
10/23/2013 16:15 CDT	0.18
10/23/2013 16:30 CDT	0.17
10/23/2013 16:45 CDT	0.16
10/23/2013 17:00 CDT	0.15
10/23/2013 17:15 CDT	0.15
10/23/2013 17:30 CDT	0.14
10/23/2013 17:45 CDT	0.13
10/23/2013 18:00 CDT	0.11
10/23/2013 18:15 CDT	0.11
10/23/2013 18:30 CDT	0.11
10/23/2013 18:45 CDT	0.11
10/23/2013 19:00 CDT	0.10
10/23/2013 19:15 CDT	0.09
10/23/2013 19:30 CDT	0.09
10/23/2013 19:45 CDT	0.08
10/23/2013 20:00 CDT	0.08
10/23/2013 20:15 CDT	0.07
10/23/2013 20:30 CDT	0.07
10/23/2013 20:45 CDT	0.06
10/23/2013 21:00 CDT	0.06
10/23/2013 21:15 CDT	0.06
10/23/2013 21:30 CDT	0.05
10/23/2013 21:45 CDT	0.05
10/23/2013 22:00 CDT	0.05
10/23/2013 22:15 CDT	0.04
10/23/2013 22:30 CDT	0.04
10/23/2013 22:45 CDT	0.04
10/23/2013 23:00 CDT	0.04
10/23/2013 23:15 CDT	0.03
10/23/2013 23:30 CDT	0.03
10/23/2013 23:45 CDT	0.03

Event #6-January 11, 2013 Event



Date and Time	Discharge (m <sup>3</sup> /s)
01/11/2013 03:45 CST	0.03
01/11/2013 04:00 CST	0.05
01/11/2013 04:15 CST	0.04
01/11/2013 04:30 CST	0.03
01/11/2013 04:45 CST	0.02
01/11/2013 05:00 CST	0.01

Event # 7-January 29, 2013 Event

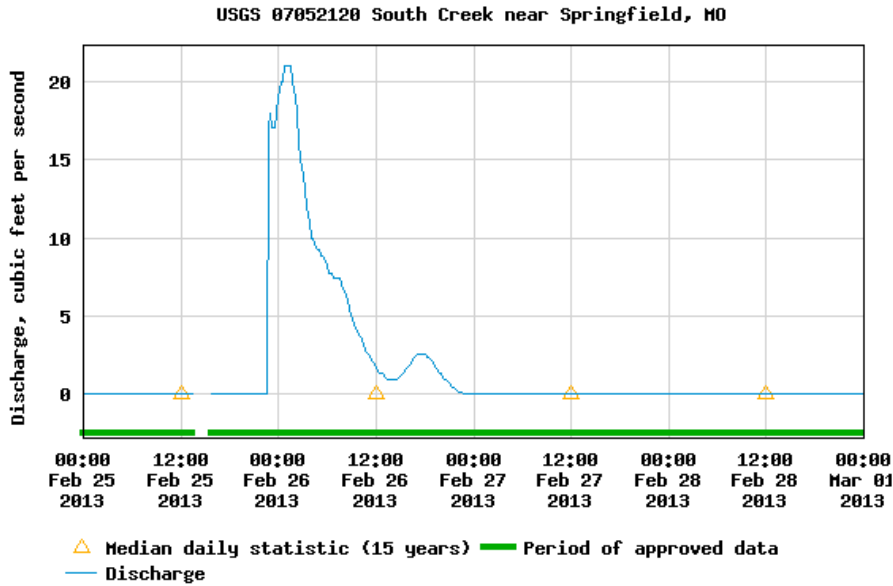


Date and Time	Discharge (m <sup>3</sup> /s)
01/29/2013 16:00 CST	0.42
01/29/2013 16:15 CST	4.64
01/29/2013 16:30 CST	6.82
01/29/2013 16:45 CST	8.57
01/29/2013 17:00 CST	9.79
01/29/2013 17:15 CST	10.61
01/29/2013 17:30 CST	10.53
01/29/2013 17:45 CST	9.34
01/29/2013 18:00 CST	8.43
01/29/2013 18:15 CST	7.44
01/29/2013 18:30 CST	6.93
01/29/2013 18:45 CST	6.28
01/29/2013 19:00 CST	5.83
01/29/2013 19:15 CST	5.66
01/29/2013 19:30 CST	5.32
01/29/2013 19:45 CST	4.90
01/29/2013 20:00 CST	4.44
01/29/2013 20:15 CST	4.39
01/29/2013 20:30 CST	4.02
01/29/2013 20:45 CST	3.79
01/29/2013 21:00 CST	3.48
01/29/2013 21:15 CST	3.17
01/29/2013 21:30 CST	2.94
01/29/2013 21:45 CST	2.77
01/29/2013 22:00 CST	2.55
01/29/2013 22:15 CST	2.35
01/29/2013 22:30 CST	2.12
01/29/2013 22:45 CST	1.90
01/29/2013 23:00 CST	1.75
01/29/2013 23:15 CST	1.58

<b>Date and Time</b>	<b>Discharge (m<sup>3</sup>/s)</b>
01/29/2013 23:30 CST	1.47
01/29/2013 23:45 CST	1.39
01/30/2013 00:00 CST	1.27
01/30/2013 00:15 CST	1.19
01/30/2013 00:30 CST	1.13
01/30/2013 00:45 CST	1.08
01/30/2013 01:00 CST	1.08
01/30/2013 01:15 CST	1.08
01/30/2013 01:30 CST	1.16
01/30/2013 01:45 CST	1.22
01/30/2013 02:00 CST	1.33
01/30/2013 02:15 CST	1.42
01/30/2013 02:30 CST	1.47
01/30/2013 02:45 CST	1.53
01/30/2013 03:00 CST	1.53
01/30/2013 03:15 CST	1.50
01/30/2013 03:30 CST	1.50
01/30/2013 03:45 CST	1.39
01/30/2013 04:00 CST	1.30
01/30/2013 04:15 CST	1.19
01/30/2013 04:30 CST	1.13
01/30/2013 04:45 CST	1.02
01/30/2013 05:00 CST	0.93
01/30/2013 05:15 CST	0.91
01/30/2013 05:30 CST	0.85
01/30/2013 05:45 CST	0.76
01/30/2013 06:00 CST	0.71
01/30/2013 06:15 CST	0.65
01/30/2013 06:30 CST	0.59
01/30/2013 06:45 CST	0.57
01/30/2013 07:00 CST	0.54
01/30/2013 07:15 CST	0.48
01/30/2013 07:30 CST	0.48
01/30/2013 07:45 CST	0.45
01/30/2013 08:00 CST	0.42
01/30/2013 08:15 CST	0.40
01/30/2013 08:30 CST	0.37
01/30/2013 08:45 CST	0.37
01/30/2013 09:00 CST	0.34
01/30/2013 09:15 CST	0.34
01/30/2013 09:30 CST	0.31
01/30/2013 09:45 CST	0.31
01/30/2013 10:00 CST	0.28
01/30/2013 10:15 CST	0.28
01/30/2013 10:30 CST	0.27
01/30/2013 10:45 CST	0.26
01/30/2013 11:00 CST	0.25
01/30/2013 11:15 CST	0.25
01/30/2013 11:30 CST	0.24
01/30/2013 11:45 CST	0.23
01/30/2013 12:00 CST	0.22
01/30/2013 12:15 CST	0.21
01/30/2013 12:30 CST	0.21
01/30/2013 12:45 CST	0.20
01/30/2013 13:00 CST	0.19
01/30/2013 13:15 CST	0.19
01/30/2013 13:30 CST	0.18
01/30/2013 13:45 CST	0.18
01/30/2013 14:00 CST	0.17
01/30/2013 14:15 CST	0.16
01/30/2013 14:30 CST	0.16
01/30/2013 14:45 CST	0.15
01/30/2013 15:00 CST	0.15
01/30/2013 15:15 CST	0.14
01/30/2013 15:30 CST	0.14
01/30/2013 15:45 CST	0.14
01/30/2013 16:00 CST	0.13
01/30/2013 16:15 CST	0.13
01/30/2013 16:30 CST	0.13

<b>Date and Time</b>	<b>Discharge (m<sup>3</sup>/s)</b>
01/30/2013 16:45 CST	0.12
01/30/2013 17:00 CST	0.12
01/30/2013 17:15 CST	0.11
01/30/2013 17:30 CST	0.11
01/30/2013 17:45 CST	0.10
01/30/2013 18:00 CST	0.10
01/30/2013 18:15 CST	0.10
01/30/2013 18:30 CST	0.10
01/30/2013 18:45 CST	0.09
01/30/2013 19:00 CST	0.09
01/30/2013 19:15 CST	0.08
01/30/2013 19:30 CST	0.08
01/30/2013 19:45 CST	0.08
01/30/2013 20:00 CST	0.08
01/30/2013 20:15 CST	0.08
01/30/2013 20:30 CST	0.07
01/30/2013 20:45 CST	0.07
01/30/2013 21:00 CST	0.07
01/30/2013 21:15 CST	0.07
01/30/2013 21:30 CST	0.06
01/30/2013 21:45 CST	0.06
01/30/2013 22:00 CST	0.06
01/30/2013 22:15 CST	0.06
01/30/2013 22:30 CST	0.06
01/30/2013 22:45 CST	0.05
01/30/2013 23:00 CST	0.05
01/30/2013 23:15 CST	0.05
01/30/2013 23:30 CST	0.05
01/30/2013 23:45 CST	0.05
01/31/2013 00:00 CST	0.05
01/31/2013 00:15 CST	0.04
01/31/2013 00:30 CST	0.04
01/31/2013 00:45 CST	0.04
01/31/2013 01:00 CST	0.04
01/31/2013 01:15 CST	0.04
01/31/2013 01:30 CST	0.04
01/31/2013 01:45 CST	0.04
01/31/2013 02:00 CST	0.04
01/31/2013 02:15 CST	0.03
01/31/2013 02:30 CST	0.03
01/31/2013 02:45 CST	0.03
01/31/2013 03:00 CST	0.03
01/31/2013 03:15 CST	0.03
01/31/2013 03:30 CST	0.03
01/31/2013 03:45 CST	0.03
01/31/2013 04:00 CST	0.03
01/31/2013 04:15 CST	0.03
01/31/2013 04:30 CST	0.03
01/31/2013 04:45 CST	0.02
01/31/2013 05:00 CST	0.02
01/31/2013 05:15 CST	0.02
01/31/2013 05:30 CST	0.02
01/31/2013 05:45 CST	0.02
01/31/2013 06:00 CST	0.02
01/31/2013 06:15 CST	0.01
01/31/2013 06:30 CST	0.01
01/31/2013 06:45 CST	0.01
01/31/2013 07:00 CST	0.01
01/31/2013 07:15 CST	0.01
01/31/2013 07:30 CST	0.01
01/31/2013 07:45 CST	0.01
01/31/2013 08:00 CST	0.01
01/31/2013 08:15 CST	0.01
01/31/2013 08:30 CST	0.01
01/31/2013 08:45 CST	0.01
01/31/2013 09:00 CST	0.01
01/31/2013 09:15 CST	0.01
01/31/2013 09:30 CST	0.01
01/31/2013 09:45 CST	0.01

Event #8-February 25, 2013 Event



Date and Time	Discharge (m <sup>3</sup> /s)
02/25/2013 22:45 CST	0.48
02/25/2013 23:00 CST	0.51
02/25/2013 23:15 CST	0.48
02/25/2013 23:30 CST	0.48
02/25/2013 23:45 CST	0.51
02/26/2013 00:00 CST	0.54
02/26/2013 00:15 CST	0.57
02/26/2013 00:30 CST	0.57
02/26/2013 00:45 CST	0.59
02/26/2013 01:00 CST	0.59
02/26/2013 01:15 CST	0.59
02/26/2013 01:30 CST	0.59
02/26/2013 01:45 CST	0.57
02/26/2013 02:00 CST	0.54
02/26/2013 02:15 CST	0.51
02/26/2013 02:30 CST	0.45
02/26/2013 02:45 CST	0.42
02/26/2013 03:00 CST	0.40
02/26/2013 03:15 CST	0.37
02/26/2013 03:30 CST	0.34
02/26/2013 03:45 CST	0.31
02/26/2013 04:00 CST	0.28
02/26/2013 04:15 CST	0.28
02/26/2013 04:30 CST	0.27
02/26/2013 04:45 CST	0.26
02/26/2013 05:00 CST	0.26
02/26/2013 05:15 CST	0.25
02/26/2013 05:30 CST	0.25
02/26/2013 05:45 CST	0.24
02/26/2013 06:00 CST	0.23
02/26/2013 06:15 CST	0.22
02/26/2013 06:30 CST	0.22
02/26/2013 06:45 CST	0.21
02/26/2013 07:00 CST	0.21

<b>Date and Time</b>	<b>Discharge (m<sup>3</sup>/s)</b>
02/26/2013 07:15 CST	0.21
02/26/2013 07:30 CST	0.21
02/26/2013 07:45 CST	0.20
02/26/2013 08:00 CST	0.19
02/26/2013 08:15 CST	0.18
02/26/2013 08:30 CST	0.17
02/26/2013 08:45 CST	0.15
02/26/2013 09:00 CST	0.14
02/26/2013 09:15 CST	0.13
02/26/2013 09:30 CST	0.12
02/26/2013 09:45 CST	0.11
02/26/2013 10:00 CST	0.10
02/26/2013 10:15 CST	0.10
02/26/2013 10:30 CST	0.09
02/26/2013 10:45 CST	0.08
02/26/2013 11:00 CST	0.07
02/26/2013 11:15 CST	0.07
02/26/2013 11:30 CST	0.06
02/26/2013 11:45 CST	0.06
02/26/2013 12:00 CST	0.05
02/26/2013 12:15 CST	0.04
02/26/2013 12:30 CST	0.04
02/26/2013 12:45 CST	0.04
02/26/2013 13:00 CST	0.03
02/26/2013 13:15 CST	0.03
02/26/2013 13:30 CST	0.03
02/26/2013 13:45 CST	0.03
02/26/2013 14:00 CST	0.03
02/26/2013 14:15 CST	0.03
02/26/2013 14:30 CST	0.03
02/26/2013 14:45 CST	0.03
02/26/2013 15:00 CST	0.03
02/26/2013 15:15 CST	0.04
02/26/2013 15:30 CST	0.04
02/26/2013 15:45 CST	0.05
02/26/2013 16:00 CST	0.05
02/26/2013 16:15 CST	0.06
02/26/2013 16:30 CST	0.06
02/26/2013 16:45 CST	0.07
02/26/2013 17:00 CST	0.07
02/26/2013 17:15 CST	0.07
02/26/2013 17:30 CST	0.07
02/26/2013 17:45 CST	0.07
02/26/2013 18:00 CST	0.07
02/26/2013 18:15 CST	0.07
02/26/2013 18:30 CST	0.07
02/26/2013 18:45 CST	0.06
02/26/2013 19:00 CST	0.06
02/26/2013 19:15 CST	0.05
02/26/2013 19:30 CST	0.05
02/26/2013 19:45 CST	0.04
02/26/2013 20:00 CST	0.04
02/26/2013 20:15 CST	0.03
02/26/2013 20:30 CST	0.03
02/26/2013 20:45 CST	0.02
02/26/2013 21:00 CST	0.02
02/26/2013 21:15 CST	0.01
02/26/2013 21:30 CST	0.01
02/26/2013 21:45 CST	0.01
02/26/2013 22:00 CST	0.01



